The role of RAD4/XPC and RAD7 homologues in Arabidopsis UV tolerance

By

Triparna Lahari

A thesis submitted to the Faculty of Graduate Studies of the University of Manitoba in partial fulfillment of the requirements of the degree of

Doctor of Philosophy

Department of Biological Sciences

University of Manitoba

Winnipeg

Copyright © 2018 by Triparna Lahari

Abstract

Plants need sunlight for photosynthesis and survival. However, frequent exposure to solar ultraviolet (UV) rays can damage DNA by inducing dipyrimidine photolesions such as cyclobutane pyrimidine dimers (CPDs) and 6,4 pyrimidine-pyrimidone photoproducts (6-4PPs). These lesions interrupt DNA replication and transcription, leading to mutation and cell death; thus DNA repair is essential. Plants have two mechanisms to repair UV-damaged DNA, one utilizes light (Photoreactivation) and the other does not (Nucleotide Excision Repair (NER)). The plant NER pathway is similar to those in mammals and yeast. In humans, defective or deficient NER causes serious consequences such as xeroderma pigmentosum, where UV-sensitive skin is prone to skin cancer. In mammals, the xeroderma pigmentosum complementation group C (XPC) protein recognizes DNA damage during whole genome NER (global genomic NER (GG-NER)). In this thesis I examine the role of RAD4, the plant homologue of mammalian XPC. RAD4 overexpression lines exhibited increased UV tolerance and YFP-tagged RAD4 localized to the nucleus. RAD4 interacted with RAD23B and the RAD23-like protein HEMERA (HMR) in yeast two hybrid assays and *hmr* mutants were found to exhibit increased UV sensitivity. In the yeast *S. cerevisiae,* GG-NER damage recognition is performed by the Rad7p/16p complex. In this study I identified three Arabidopsis RAD7 homologues, RAD7a, RAD7b, and RAD7c. Loss of function alleles in each of the three *RAD7* genes led to plants that exhibited increased UV sensitivity, while gain of function lines of *RAD7b* and *RAD7c* exhibited increased UV tolerance. YFP-tagged RAD7b and RAD7c localized to the nucleus, and this localization was not affected by UV treatment. Therefore, RAD4 and the three RAD7 homologues contribute to Arabidopsis UV tolerance.

Acknowledgements

I would like to express my deepest gratitude to my supervisor Dr. Dana Schroeder for accepting an international graduate student and her kind supervision during my graduate studies. It was such a great learning experience to work under her guidance. Dr. Schroeder is an excellent supervisor and professor. She always encouraged me and provided full support in every aspect. Dr. Schroeder supported me even while battling cancer. She corrected my thesis as well as provided me with direction for research work even though she was undergoing chemotherapy treatment.

I would like to express my sincere appreciation to my committee members Dr. Mark Belmonte, Dr. Deborah Court, and Dr. Claudio Stasolla for providing me with constructive feedback during my committee meetings as well as providing suggestions and guidance for my research.

I would like to thank the University of Manitoba for funding support including an International Graduate Student Entrance Scholarship, International Graduate Student Scholarship, Faculty of Science Scholarship, University of Manitoba Graduate Fellowship, and travel grants. I would like to thank the Department of Biological Sciences and all the excellent office staff for helping me. My sincere gratitude to our former Department head, Dr. Judy Anderson, for always being a great help in spite of her busy schedule.

I would also like to appreciate Dr. Court for guiding me for yeast work and providing me with the necessary laboratory set up as well as letting me use equipment from Department of Microbiology to successfully carry forward my experiments. I would like to thank the Department Microscope facility for letting me use the microscopes and Andre Dufresne for

instruction and helping me with microscope imaging. I am thankful for the use of the growth room facility to grow my plants and for the dark room to carry out my UV experiments.

The past and present members of Schroeder laboratory have always been friendly and approachable which made me feel comfortable and able to learn new things very quickly. I was fortunate enough to have Harvey and Ruth Thiessen as my welcome family who provided me every single support to settle down as an international student.

I am indebted to my parents (Mr. Sumanta Lahari and Mrs. Jayanti Lahari) for motivating me to keep my dream alive. I would be happy to accomplish my elder sister Rituparna's dream by completing my PhD degree. I could not thank enough my elder sister and brother in law Samya as they have supported my every accomplishment. I believe my little niece Madhura is my lucky charm to carve my way towards success. Thanks to my husband Subhankar for being my strength during the ups and downs as well as tolerating my mood swings for past years. Finally, my baby boy cooperated enough to finish my thesis work. My son Ronav's smile inspires me every day to move on in life positively as well as deal the tough times easily.

List of Abbreviations

6-4 PPs	pyrimidine 6-4 pyrimidone photoproducts
CEN	CENTRIN
Col	*Arabidopsis thaliana* ecotype Columbia
CPD	Cyclobutane Pyrimidine Dimers
CS	Cockayne Syndrome
CUL	Cullin family member
DDB	Damaged DNA Binding protein
DNA	Deoxyriboneuclic Acid
ELC	ELONGIN C
GG-NER	Global Genomic Nucleotide Excision Repair
HMR	HEMERA
NER	Nucleotide Excision Repair
PCNA	Proliferating cell nuclear antigen
PCR	Polymerase Chain Reaction
PR	Photoreactivation
RAD	Radiation sensitive
RPA	Recruitment protein A
TC-NER	Transcription Coupled Nucleotide Excision Repair
T-DNA	Transfer DNA
Ub	Ubiquitin
UV	Ultraviolet radiation

uvh	UV hypersensitive
Ws	*Arabidopsis thaliana* ecotype Wassilevskija
XP	Xeroderma pigmentosum
XPC	Xeroderma pigmentosum complementation group C

Table of Contents

Abstract I
Acknowledgements II
List of Abbreviations IV
Table of Contents VI
List of Figures VIII
List of Tables IX

1. Literature Review 1
    1.1 Ultraviolet radiation 1
    1.2 UV induced DNA damage 2
    1.3 UV damaged DNA repair 2
        1.3.1 Photoreactivation 3
        1.3.2 Nucleotide Excision Repair (NER) 4
            1.3.2.1 Ubiquitin–mediated degradation in NER 5
            1.3.2.2 Global Genomic-NER 7
                1.3.2.2.1 UV Damaged DNA Binding proteins (DDBs) 7
                1.3.2.2.2 XPC-CENTRIN-HR23B complex 10
                1.3.2.2.3 Rad7p/Rad16p complex 14
                1.3.2.2.4 Damage verification: TFIIH activity 15
                1.3.2.2.5 Endonuclease activity: the next step of damage verification 16
                1.3.2.2.6 Ligation and DNA synthesis 17
            1.3.2.3 TC-NER 18
2. RAD4 and RAD23/HMR contribute to Arabidopsis UV tolerance 24
    2.1 Abstract 24
    2.2 Introduction 24
    2.3 Materials and methods 26
        2.3.1 Plant material and growth conditions 27
        2.3.2 Generation of overexpression lines 27
        2.3.3 RNA extraction and qRT-PCR 28

2.3.4 UV sensitivity assays 28
2.3.5 Protein localization 29
2.3.6 Yeast two hybrid analysis 30
2.3.7 Statistical analysis 30
2.4 Results 30
2.5 Discussion 33
3. RAD7 homologues contribute to Arabidopsis UV tolerance 50
3.1. Abstract 50
3.2 Introduction 51
3.3 Materials and methods 52
3.3.1 Phylogenetic tree construction 52
3.3.2 Plant material and growth conditions 53
3.3.3 RNA extraction and RT-PCR 54
3.3.4 Generation of overexpression constructs 54
3.3.5 Developmental parameter measurement and analysis 55
3.3.6 UV sensitivity assays 55
3.3.7 Protein localization 56
3.3.8 Yeast two hybrid analysis 57
3.3.9 Statistical analysis 57
3.4 Results 57
3.5 Discussion 62
4. Discussion 93
4.1 General Discussion 93
4.2 Future directions 96
4.3 Conclusion 97
5. References 99

List of Figures

Fig. 1.1 Cyclobutane pyrimidine dimers (CPDs) and pyrimidine 6-4 pyrimidone photoproducts (6-4PPs) 3
Fig. 1.2 Photoreactivation/Photolysis/light-dependent repair..... 4
Fig. 1.3 Target protein ubiquitination with E1, E2, and E3 SCF ligase complex..... 6
Fig. 1.4 GG-NER in mammals (humans) and yeast (*Saccharomyces cerevisiae*)..... 8
Fig. 2.1 RAD4 and YFP-RAD4 overexpression results in increased UV tolerance..... 38
Fig. 2.2 YFP-RAD4 exhibits nuclear localization..... 39
Fig. 2.3 Yeast two hybrid analysis of RAD4 N-terminus and RAD23B interaction..... 40
Fig. 2.4 Yeast two hybrid analysis of RAD4-HMR interaction 41
Fig. 2.5 The mutant *hmr* exhibits increased UV sensitivity 42
Fig. 2.6 Mutants of *rad23* exhibit increased UV sensitivity..... 43
Fig. S2.1 RAD4 overexpression increases adult UV tolerance 44
Fig. S2.2 Yeast two hybrid analysis of RAD4 DDB2 interaction 45
Fig. S2.3 Yeast two hybrid analysis of RAD4 self-interaction..... 46
Fig. S2.4 Yeast two hybrid analysis of RAD4 RAD23B interaction..... 47
Fig. 3.1 Loss of function alleles of RAD7 homologues 66
Fig. 3.2 *rad7a* mutant seedlings exhibit increased UV sensitivity 67
Fig. 3.3 *rad7b* mutant seedlings exhibit increased UV sensitivity. 68
Fig. 3.4 *rad7c* mutant seedlings exhibit increased UV sensitivity. 69
Fig. 3.5 *rad7* mutant seedlings exhibit dark specific UV sensitivity..... 70
Fig. 3.6 *rad7a* and *rad7b* adults exhibit increased UV sensitivity 71
Fig. 3.7 RAD7b overexpression results in increased UV tolerance 72
Fig. 3.8 YFP-RAD7b overexpression results in increased UV tolerance..... 73
Fig. 3.9 RAD7c overexpression results in increased UV tolerance..... 74
Fig. 3.10 35S:YFP-RAD7c overexpression results in increased UV tolerance..... 75
Fig. 3.11 YFP-RAD7b localizes to nuclear speckles..... 76
Fig. 3.12 YFP-RAD7c exhibits nuclear localization 77
Fig. S3.1 Phylogenetic tree of RAD7 orthologues 81
Fig. S3.2 Alignment of RAD7 homologues 82
Fig. S3.3 *RAD7a* and *RAD7b* transcript level via AtGeneExpress..... 83
Fig. S3.4 Phenotypic analysis of *rad7a* and *rad7b* adults 84
Fig. S3.5 Phenotypic analysis of *rad7c* adults..... 85
Fig. S3.6 *rad7c-3* adults do not exhibit increased UV sensitivity 86
Fig. S3.7 Overexpression of RAD7b and RAD7c rescues seedling UV sensitivity..... 88
Fig. S3.8 Yeast two hybrid analysis of RAD7b RAD4 interaction 89
Fig. S3.9 Yeast two hybrid analysis of RAD7c RAD4 interaction 90
Fig. S3.10 Yeast two hybrid analysis of RAD7b RAD7c interaction 91
Fig. S3.11 Yeast two hybrid analysis of RAD7b/RAD7c ELC1 interaction..... 92

List of Tables

Table 1.1 NER factors in mammals, plants (*Arabidopsis thaliana*) and the yeast *Saccharomyces cerevisiae.* 11
Table S3.1 Primers used in this study (5' -> 3') 78
Table S3.2 Arabidopsis Interaction Viewer predictions of AtRAD4 (At5g16630) interacting proteins..... 79
Table S3.3 Results of WU-BLAST2.0 search of *S. cerevisiae* Rad7p versus TAIR10 proteins.. 80

1. Literature Review

1.1 Ultraviolet radiation

When living organisms are exposed to sunlight, there may be some harmful effects. The ultraviolet (UV) radiation present in sunlight can damage biological macromolecules such as proteins, lipids, and nucleic acids (Brash 1997). Sunlight in the visible spectrum ranges from 400 to 700 nm, while UV radiation consists of UV-A (315-400 nm), UV-B (280-315 nm), and UV-C (100-280 nm) (Kulandaivelu et al. 1997). Of these three types of UV radiation, UV-B causes the most cellular damage, because while a portion of UV-B is absorbed by the stratosphere during transmission, a significant amount of UV-B radiation still reaches the earth's surface. Therefore UV-B poses the most threat, even though it comprises only 1% of solar energy (Kerr and McElroy 1993; Ries et al. 2000). On the other hand, while UV-A is largely transmitted through the atmosphere, it has the longest wavelength and therefore lowest energy, and causes minimal damage at the cellular level. UV-C possesses the shortest wavelength, thus it should have the most deleterious effect. Fortunately, UV-C radiation is completely absorbed by the atmospheric ozone and oxygen layer (McKenzie et al. 2007; McKenzie et al. 2011).

The increase of air pollution and abundance of chloroflorocarbons has lead to depletion of the ozone layer (Coldiron 1992). This results in higher transmission of UV to earth and more damage at the cellular level (Bais et al. 2015; McKenzie et al. 2011). The UV radiation that reaches the earth's surface increased significantly from 1979 to 2008. UV is also believed to a factor in global warming. UV stimulates the release of volatile organic compounds from soil and plants, which leads to increased greenhouse gases and temperature (Ballaré et al. 2011; Bornman et al. 2015).

1.2 UV induced DNA damage

UV radiation damages DNA, directly affecting genome integrity. Both UV-B and UV-C can induce photoproducts, which arrest the replication and transcription processes. Ultimately, DNA is the primary target in all radiation-induced cutaneous carcinogenesis. In humans, both UV-A and UV-B induce human skin melanomas, including squamous cell carcinoma (SCC) and basal cell carcinoma (BCC) predominantly (Cadet et al. 1992; Cadet et al. 2015).

UV radiation causes two types of DNA lesions: i) cyclobutane pyrimidine dimers (CPDs), and ii) pyrimidine 6-4 pyrimidone photoproducts (6-4 PPs) (Franklin et al. 1985). CPDs were the first stable pyrimidine photoproduct to be discovered around 65 years ago. Since then they have been well studied in various fields of research like mutagenicity, photocarcinogenesis, DNA photochemistry, genotoxicity, and DNA repair. 6-4 PPs were the second major photoproduct described (Mitchell and Rosenstein 1987; Mitchell et al. 1989). CPDs form four member ring structures with c5 and c6 of the adjacent base. In 6-4 PPs a noncyclic bond is in between c4 at the 5' end and c6 at the 3' end. In both cases, the helical structure of DNA is distorted, forming bends of 7-9^{o} and 44^{o} respectively for CPDs and 6-4 PPs (Fig. 1.1). These bends in turn interrupt polymerase activity, arresting DNA replication and transcription, resulting in mutation, tumorigenesis, and apoptosis. Ultimately the repair of UV damaged DNA is essential (Cadet et al. 2015; Cadet et al. 2005).

1.3 UV damaged DNA repair

Repair of UV damaged DNA is absolutely required to maintain genomic integrity and avoid genotoxic stress. UV damaged DNA repair is mainly of two types: i) light dependent (Chen et al. 1994) and ii) light independent (Sancar 1996). Light dependent repair is known as

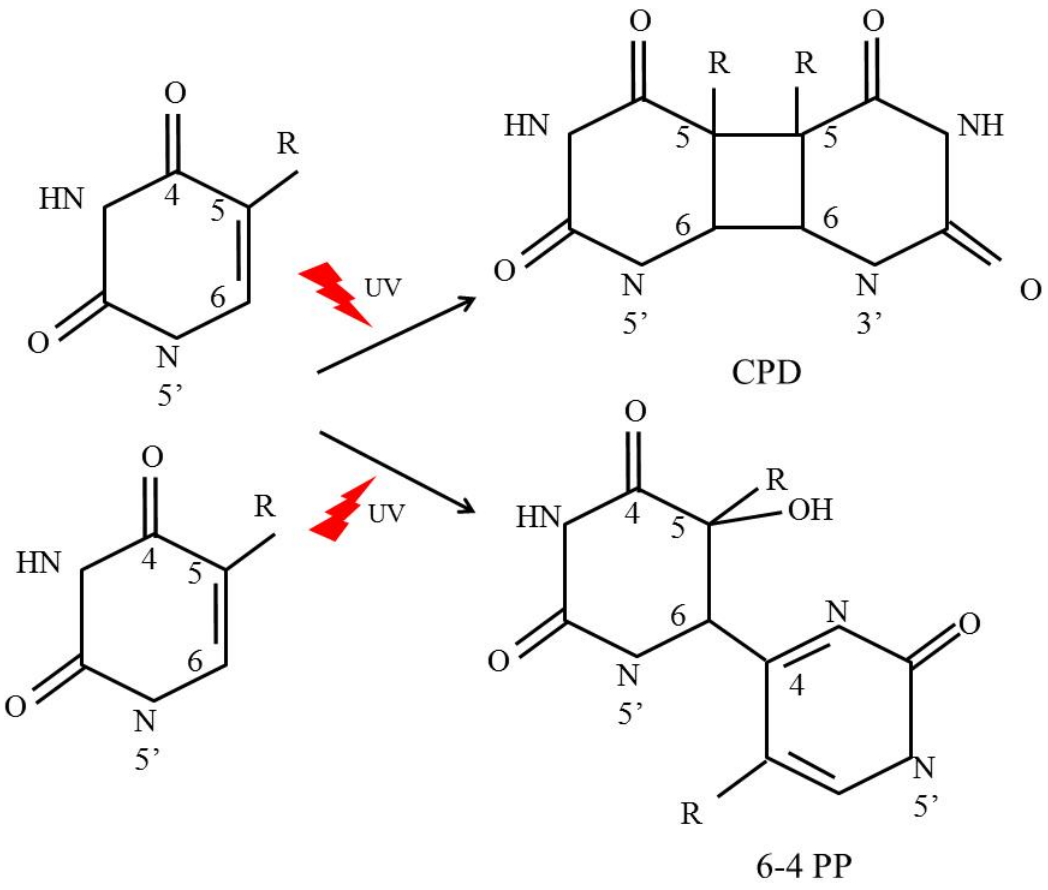

Fig. 1.1 Cyclobutane pyrimidine dimers (CPDs) and pyrimidine 6-4 pyrimidone photoproducts (6-4PPs)

Photoreactivation (PR) or photorepair. The light independent repair is called dark repair or nucleotide excision repair (Tuteja et al. 2009).

1.3.1 Photoreactivation

Photoreactivation (PR) or photorepair exists in a variety of prokaryotes and eukaryotes, such as *E. coli*, yeast, plants, and some animal systems (Sancar 1994). Photoreactivation is not universal however, since placental mammals lack PR (Li et al. 1993). Photoreactivation reverts pyrimidine dimers to their original structure. The substrate specific enzyme photolyase regulates PR. Photolyase directly recognizes the DNA dimer and binds to it. In a single step reaction, the

enzyme absorbs the energy from blue light (range 300-600 nm) to break the pyrimidine dimer into monomers, recovering the original DNA form (Fig. 1.2) (Liu et al. 2015). Photolyase enzymes are specific to the type of lesion, such as CPD photolyase and 6-4 PP photolyase. Photolyases are reduced Flavin dependent (FAD) enzymes with two factors, the photocatalyst and the light harvesting factor. The reduced FADH- transfers the energy to the CPD in the form of two electrons and breaks the dimer into monomers (Manova and Gruszka 2015).

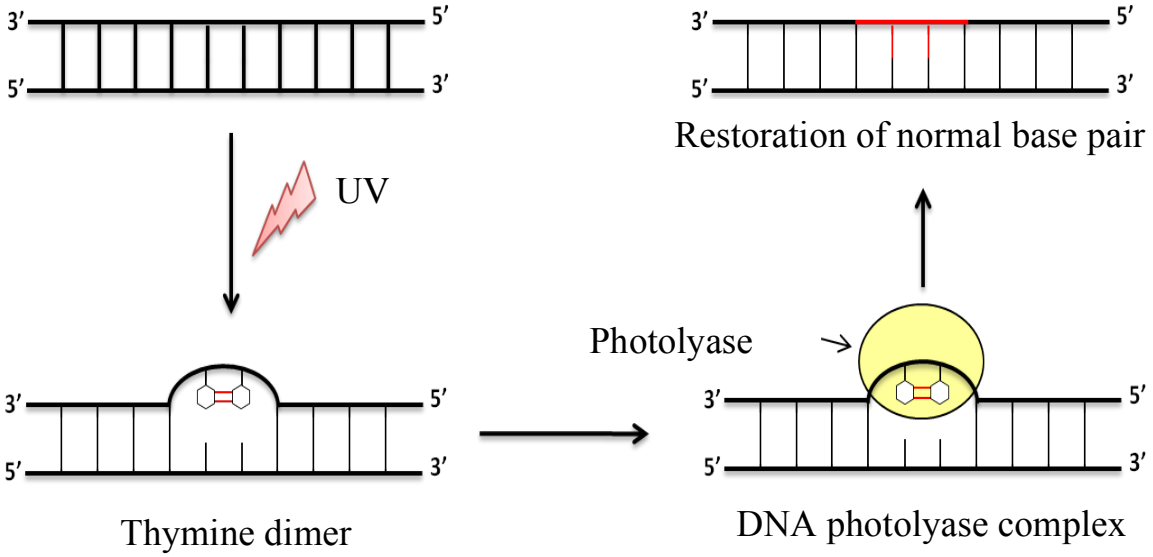

Fig. 1.2 Photoreactivation/Photolysis/light-dependent repair. UV-induced thymine dimer is repaired by photolyase in the presence of visible light. See text for details and references.

1.3.2 Nucleotide Excision Repair (NER)

The light independent excision and repair of DNA lesions, nucleotide excision repair (NER), is a complex process involving many proteins. The NER machinery recognizes and excises distorted DNA lesions induced by UV radiation and other mutagens. NER involves damaged lesion recognition, unwinding of the DNA double helix at the damaged site, double incision of the lesion, resynthesis of the native DNA strand, and ligation (Sancar 1996; Wood 1997). NER has been best characterized in mammals and the yeast *S. cerevisiae*. Lack of NER

leads to persistent damaged DNA, which results in humans in the diseases Xeroderma pigmentosum (XP), Cockayne syndrome (CS), and Trichothiodystrophy (TTD) (de Boer and Hoeijmakers 2000). Xeroderma pigmentosum increases the sensitivity of the skin to UV exposure, resulting in hyperpigmentation and increased probability of UV induced skin cancer (Sugasawa et al. 1998). XP patients also have an elevated risk of internal tumors, neurological symptoms, and premature aging due to accumulation of damaged DNA lesions. Cells derived from various XP patients were grouped into eight complementation groups. Cloning of the genes defective in these complementation groups identified proteins involved in NER (Manova and Gruszka 2015; Petruseva et al. 2014).

Nucleotide excision repair is subdivided into two sub types. Global genomic repair (GG-NER) repairs untranscribed DNA throughout the genome while transcription coupled repair (TC-NER) repairs damage in transcribed strands (Pani and Nudler 2017; Rüthemann et al. 2016). These two processes have distinct recognition mechanisms followed by a common repair process. GG-NER is a nonspecific, random, and slow process while TC-NER is a highly specific and fast process associated with RNA polymerase II transcription (Spivak 2015).

1.3.2.1 Ubiquitin–mediated degradation in NER

Ubiquitin mediated proteasomal degradation controls protein turnover in the cell. Ubiquitin (a 76 amino acid long conserved protein) is attached to a lysine rich sequence in order to identify the protein targets for degradation. Subsequently, the 26S proteasome carries out protein degradation. This process involves 3 enzymes, namely the E1 ubiquitin activating enzyme, the E2 ubiquitin conjugating enzyme, and the E3 ubiquitin ligating enzyme. The diverse group of E3 ligase complexes include HECT (homologous to E6-associated protein C-terminus), RING (Really Interesting New Gene), U-box (a modified RING motif without the full

complement of Zn-binding ligands), and Cullin Ring Ligase (CRL) types (Hershko 2005; Sharma et al. 2016). Cullin 1 interacts with the RBX1 RING protein and the SKP1 adaptor. SKP1 in turn interacts with F box proteins, which provide substrate specificity, to form SCF (SKP1-CUL1- F box) type E3 ligase complex (Fig. 1.3) (Ohta et al. 1999; Skowyra et al. 1997). In cullin 4 based E3 ligase complexes, DDB1 acts as the adapter, interacting with substrate specific DWD (DDB1-binding WD40) proteins (Groisman et al. 2003). CUL3 interacts directly with substrate specific BTB proteins (Furukawa et al. 2003). Several cullin-type E3 ubiquitin ligases are involved in NER. For example, the DDB2 DDB1 CUL4 complex initiates mammalian GG-NER, while a Rad7p-Rad16p Cul3p complex acts in yeast GG-NER, and a CSA DDB1 CUL4 complex functions in mammalian TC-NER. These will be discussed in more detail below.

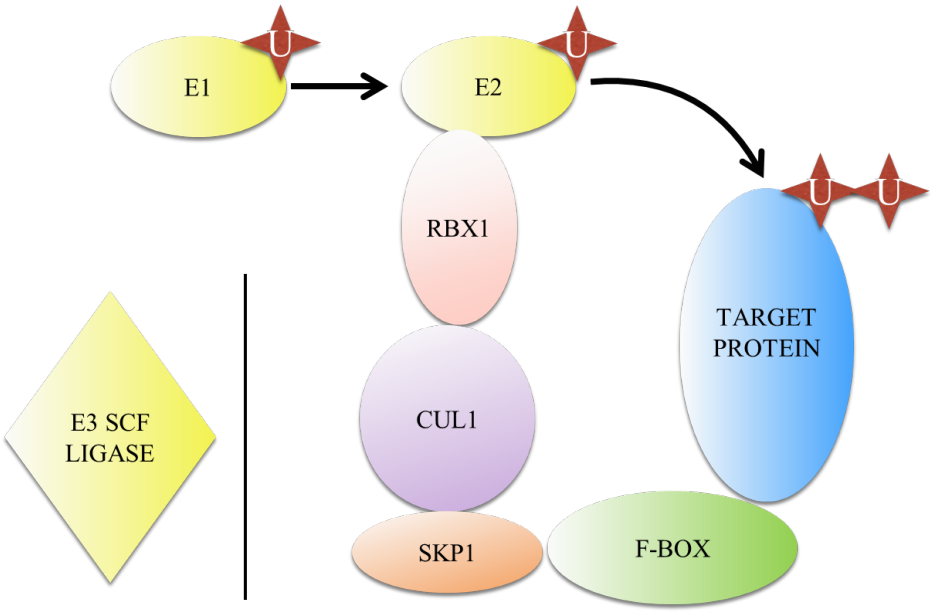

Fig. 1.3 Target protein ubiquitination with E1, E2, and E3 SCF ligase complex.
Ubiquitination (U) is carried out by three steps: activation by E1 enzyme, conjugation by E2 enzyme, and ligation by E3 enzyme. E2 interacts with RBX1 RING protein, Cullin 1, the SKP1 adaptor and an F box protein, which provides substrate specificity, to form an SCF (SKP1-CUL1- F box) type E3 ligase complex See text for details and references.

1.3.2.2 Global Genomic-NER

In mammalian GG-NER two major complexes, UV-DDB (UV Damaged DNA Binding protein) and XPC-RAD23b-CENTRIN2, are involved in damage detection (Sugasawa et al. 2005).

1.3.2.2.1 UV Damaged DNA Binding proteins (DDBs)

In mammalian GG-NER, UV damage recognition is facilitated by the UV-DDB complex. UV-DDB, a complex which includes DDB1 and DDB2 proteins, has high specificity for 6-4 PPs and also has a significant affinity for CPDs (Fig. 1.4) (Treiber et al. 1992). DDB1 is composed of three consecutive β-propeller domains and a C-terminal helical domain. DDB2 contains one WD40 domain and an N-terminal helix-loop-helix structure, responsible for interaction with DDB1 and DNA damage site binding, respectively. Human DDB2 is also known as XPE, so *xpe* patients lack DDB activity. Other factors bind to the DDB1-DDB2 heterodimer, such as E3 ubiquitin ligase components including cullin family member CUL4A and RBX/ROC1 (Sugasawa 2011). DDB2 is dispensable for NER in vitro, but stimulates XPC (Xeroderma pignemtosum group C) to attach to the UV damaged chromatin site or directly to lesions like CPDs in vivo. UV–DDB is recruited first to the damaged lesion before the XPC complex as a part of the Cullin-RING ubiquitin ligase complex CUL4A- DDB1-RBX1 (Higa et al. 2006; Scrima et al. 2011).

In mammals, CUL4-type E3 ubiquitin ligase complexes consist of a common backbone composed of DDB1-CUL4-RBX1. This backbone is linked to different WD40 repeat proteins, resulting in complex specificity (Higa et al. 2006; Sugasawa et al. 2005). In normal/non UV exposed cells, the UV-DDB complex is associated with the COP9 signalosome (CSN), which prevents the E3 ligase activity until UV exposure. Following UV exposure, the CSN separates

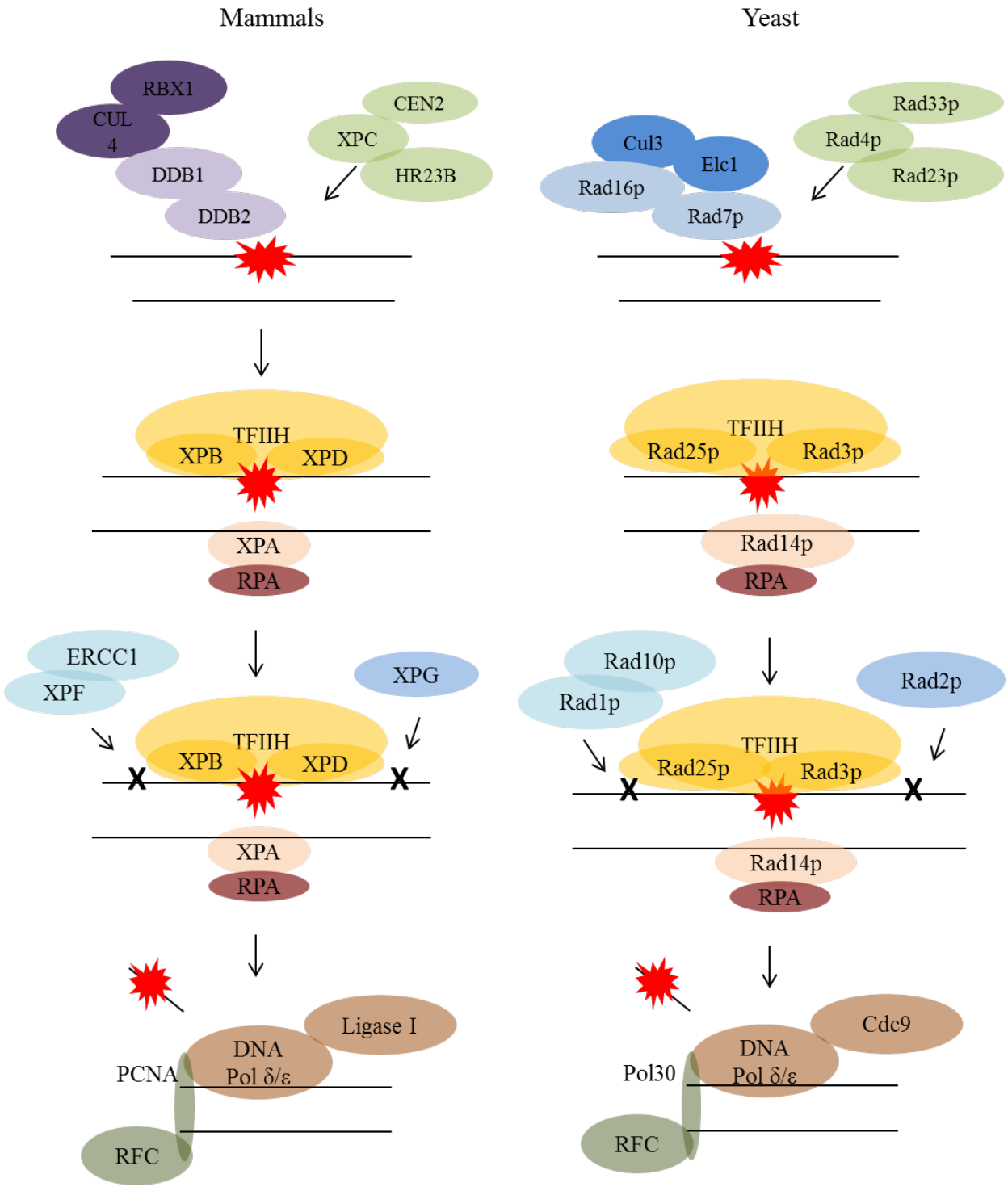

Fig. 1.4 GG-NER in mammals (humans) and yeast (*Saccharomyces cerevisiae*)

The first step is damage recognition in both systems. The second step is unwinding and incision of the damaged strand, followed by ligation and repair. Colour coding indicates homologous complexes. See text for details and references.

from the E3 ligase complex, activating the UV-DDB ubiquitin ligase, resulting in the ubiquitination of XPC and DDB2 itself (Hannss and Dubiel 2011). DDB2 is required to target DDB1 and CUL4A to the damaged DNA site and has strong affinity for UV lesions (CPD and 6-4 PP). In order to provide access to the damage repair site for subsequent NER factors, the degradation of the UV-DDB recognition complex takes place (Sugasawa et al. 2005). In addition, the CUL4 ubiquitin ligase targets the histones H2A, H3, and H4 for chromatin remodeling following UV irradiation, resulting in increased accessibility to the DNA damage by NER proteins (Alekseev and Coin 2015).

Brewers yeast (*Saccharomyces cerevisiae*) does not have DDB1 or DDB2 homologues, but utilizes another complex for DNA damage recognition, discussed below (Reed 2005). In plant systems, the roles of DDB1 and DDB2 have been studied in detail. In rice, *DDB2* is expressed more in proliferating cells like meristem but less in leaves, and is upregulated by UV-B. OsDDB2 overexpression results in increased UV tolerance (Ishibashi et al. 2006). In Arabidopsis, *DDB2* mutants and RNAi silenced plants showed sensitivity to UV and other mutagens (Koga et al. 2006; Molinier et al. 2008). In addition, *DDB2* mutants have recently been shown to exhibit DNA methylation defects throughout the genome (Schalk et al. 2016). Arabidopsis has two homologues of DDB1 - DDB1A and DDB1B (Schroeder et al. 2002). The *DDB1A* loss of function mutant showed UV sensitivity in roots and decreased photoproduct repair after UV treatment, while DDB1A overexpression resulted in increased UV resistance and photoproduct repair (Al Khateeb and Schroeder 2009; Molinier et al. 2008). Weak alleles of *ddb1b* did not exhibit UV sensitivity. *ddb1a ddb1b* double mutants are lethal, but plants homozygous for one allele and heterozygous for the other showed increased UV sensitivity relative to the single mutants, suggesting that both DDB1A and DDB1B contribute to UV

tolerance (Bernhardt et al. 2010; Ganpudi and Schroeder 2013). *CUL4* co-suppression lines also exhibit hypersensitivity to UV-C, indicating that the CUL4-DDB1A-DDB2 E3 ligase is involved in maintaining genome integrity via repair of UV damaged DNA in the Arabidopsis (Molinier et al. 2008). Arabidopsis CUL4 associates with DDB1, DDB2, and RBX1 and also has a role in development (Bernhardt et al. 2006) (Table 1.1).

1.3.2.2.2 XPC-CENTRIN-HR23B complex

In mammals, XPC is a 940 amino acid protein that was identified as a primary detector of DNA damage lesions and initiator of damage repair in GG-NER (Sugasawa et al. 1998). XPC interacts with the TFIIH complex, which has two helicases, XPD and XPB, for scanning the mismatch from 5'-3' and 3'-5' directions, along with ATPase activity. Stabilization of XPC is carried out by hHR23B, the human homologue of yeast Rad23B, as well as by CENTRIN2 (CEN2). The XPC-hHR23B-CEN2 complex initiates GG-NER in vitro (Araki et al. 2001). The bubble structure of the XPC complex binds to the damaged DNA site, but the repair process initiates only after validation of the lesions by TFIIH (Sugasawa et al. 2009) (Fig. 1.4).

Radiation sensitive 23 (RAD23) is involved in the stability of XPC and the formation of the XPC-RAD23-CENTRIN2 complex (Araki et al. 2001; Ng et al. 2003). RAD23 has four domains: Ubiquitin like domain (UBL), Ubiquitin associated domain 1 (UBA1), XPC/RAD4 binding domain, and Ubiquitin associated domain 2 (UBA2) (Dantuma et al. 2009). RAD23 interacts with and stabilizes XPC, facilitating recognition of DNA damage (Ortolan et al. 2004). RAD23 is an acceptor of ubiquitin and mediates the degradation of ubiquitinated proteins by the proteasome. Thus RAD23 is not only a damage repair protein but also regulates intercellular protein breakdown (Ng et al. 2003).

Table 1.1 NER factors in mammals, plants (*Arabidopsis thaliana*) and the yeast *Saccharomyces cerevisiae.* See text for details and references.

NER complex	Mammalian subunits	Plant homologue (Arabidopsis)	*S. cerevisiae* homologue	Function
UV-DDB CUL4	DDB1 DDB2	AtDDB1a AtDDB1b AtDDB2	Not Found Not Found	Damaged DNA recognition
	CUL4	AtCUL4	Not Found	Backbone of E3 ubiquitin ligase complex
XPC HR23B CEN2	XPC	AtRAD4	Rad4p	Damaged DNA recognition
	HR23B	AtRAD23A AtRAD23B AtRAD23C AtRAD23D	Rad23p	Damaged DNA recognition, binds to XPC
	CEN2	AtCEN2	Cen2	Damaged DNA recognition, stabilizes XPC complex
RAD7 RAD16 ABF1	Not found	RAD7a RAD7b RAD7c RAD16a RAD16b	Rad7p Rad16p	Damage recognition
	Not found	Not found	Abf1	DNA binding protein
TFIIH	XPB	AtXPB1 AtXPB2	Rad25p	3'to 5' helicase
	XPD/ERCC2	AtXPD/UVH6	Rad3p	5' to 3' helicase
	p62/GTF2H1	AtTFB1-1 AtTFB1-2	Tfb1	Core TFIIH subunits
	p52/GTF2H4	AtTFB2	Tfb2	
	p44/GTF2H2	Atp44	Ssl1	
	p34/GTF2H3	AtTFB4	Tfb4	
	p8/GTF2H5	AtTFB5-1 AtTFB5-2	Tfb5	
	CDK7	ATCDK D1;1 ATCDK D1;2 ATCDK D1;3	Kin28	CAK kinase complex
	MAT1	AtMAT1	Tfb3	
	Cyclin H	CYCH;1	Ccl1	
XPA	XPA	Not found	Rad14p	Binds to damaged DNA strand
RPA	RPA70 RPA32	AtRPA70A AtRPA70B AtRPA70C AtRPA70D AtRPA70E AtRPA32A AtRPA32B	Rfa1 Rfa2	Binding to single stranded DNA, dual incision and repair

	RPA14	AtRPA14A AtRPA14B	Rfa3	
XPF	ERCC1 XPF	AtERCC1/UVR7 AtXPF/UVH1	Rad10p Rad1p	5’ endonuclease activity, catalyzes break at 5’ ssDNA
XPG	XPG	AtXPG/UVH3	Rad2p	5’ endonuclease activity, catalyzes break at 3’ ssDNA
PCNA	PCNA	AtPCNA1 AtPCNA2	Pol30	DNA polymerase processing
RFC	RFC1 RFC2 RFC3 RFC4 RFC5	AtRFC1 AtRFC2 AtRFC3 AtRFC4 AtRFC5	Rfc1 Rfc2 Rfc3 Rfc4 Rfc5	ATP dependent DNA replication and repair
Ligase	Ligase I	AtLIG1 AT1G49250	Cdc9	ssDNA break ligation
TC-NER	CSA/ERCC8	AtCSA1A AtCSA1B	Rad28p	Ubiquitination, proteosomal degradation
	CSB/ERCC6	AtCSB/CHR8	Rad26p	Helicase activity, DNA binding, ATP binding, nucleic acid binding
	USP7	UBP12 UBP13	Ubp15	Ubiquitin specific protease activity
	XAB2	AtXAB2	Syf1	Pre mRNA splicing
	HMGN1	Not found	Not found	Chromatin conformation in transcribable genes
	TFIIS	TFIIS/RDO2	Dst1	RNA polymerase II transcript elongation factor
	UVSSA	At3g61800	Not found	Recruited to UV lesion

Mammalian XPC has homologues in yeast and plant systems named Rad4p. In the yeast *Saccharomyces cerevisiae,* Rad4p activity is similar to that in the mammal system. Rad4p identifies the UV damaged DNA lesion, along with Rad23p, by inserting a β-hairpin structure into the damaged DNA site (Min and Pavletich 2007). Yeast Rad4p and Rad23p form a stoichiometric complex called NER Factor 2 (NEF2). Another complex, called NEF4, which is formed by Rad7p and Rad16p, coordinates with the NEF2 complex for the recognition step. Rad4p is targeted for ubiquitination and degradation after UV damage recognition (Gillette et al. 2006). Rad23p also stabilizes cellular Rad4p in the absence of UV damage along with its role in

NER (Xie et al. 2004). Yeast Rad23p has an N terminal ubiquitin like (UBL) domain which interacts with the 26S proteasome (Krasikova et al. 2015).

In plant systems the role of XPC/Rad4p in DNA repair has yet to be studied in detail. However the role of CEN2 was studied in Arabidopsis (AtCEN2) and CEN2 was found to be involved in NER damage recognition, as well as homologous recombination repair. *CEN2* mutant and RNAi lines showed moderate UV-C sensitivity. Transcriptional profiling of the *cen2* mutant showed significant changes in NER factors as well as other DNA repair components (Molinier et al. 2004). In response to UV-C, AtCEN2 protein levels were found to increase and to localize to the nucleus. The CEN2 EF hand region, a Ca^{2+} binding domain, is required for interaction with AtRAD4 (Liang et al. 2006). The CEN2 binding site in the AtRAD4 C-terminus was recently defined (La Verde et al. 2018). The role of AtRAD4 in Arabidopsis UV tolerance will be a major focus of this thesis.

Homologues of RAD23 have been identified in plant systems such as Arabidopsis, rice, and *Daucus carrota* (Schultz and Quatrano 1997; Sturm and Lienhard 1998). In *Arabidopsis thaliana* the RAD23 family includes four isoforms, RAD23A, RAD23B, RAD23C and RAD23D, with UBA/UBL domains to bind to ubiquitinated proteins. While *rad23* single mutants exhibit no or mild phenotypes, higher order mutants are highly dwarfed and the quadrouple mutant showed reproductive lethality (Farmer et al. 2010). A *rad23D* mutant showed reduced rates of pollen grain germination and increased rates of seed abortion in response to UV-B (Li et al. 2012). Chen et al. (2010) identified a novel protein in the Arabidopsis phytochrome nuclear body, HEMERA (HMR), also known as pTAC12, which had previously been identified as part of a plastid complex involved in transcription. HEMERA was identified as an Arabidopsis seedling lethal mutant that has an abnormal phytochrome nuclear localization pattern. Phytochromes are red/far red photoreceptors which move from cytoplasm to

nucleus in response to light (Chen et al. 2010; Pfalz et al. 2006). Thus HEMERA has an role in phytochrome signaling in the nucleus in addition to its role in the plastid. Recent studies indicate that HMR is initially targeted to the plastid, where it is processed, then moves to the nucleus (Nevarez et al. 2017). HMR was found to be structurally similar to the multi-ubiquitin binding domain of RAD23 and partially complements the growth and UV sensitivity defects of *rad23* mutant yeast (Chen et al. 2010).

1.3.2.2.3 Rad7p/Rad16p complex

The damage recognition step in yeast (*Saccharomyces cerevisiae*) relies on the GG-NER specific Rad7p/Rad16p complex rather than UV-DDB as in mammals. Rad16p mutation results in radiation sensitivity in *Saccharomyces* (Prakash 1976). Rad16p is a SWI/SNF family protein. The SWI/SNF superfamily displays ATPase activity upon DNA or chromatin stimulation to initiate chromatin remodeling. The chromatin remodeling includes superhelical structural transformation of a linear DNA fragment by DNA translocase activity along with ATPase activity. The Rad7p/Rad16p complex also has DNA translocase activity. Rad7p and Rad16p form a stoichiometric complex, NEF4, to recognize the UV damaged DNA site (Guzder et al. 1997). Yeast GG-NER requires the Rad7p/Rad16p complex. Rad4p is subjected to ubiquitination and a cullin based E3 ligase is required for this process. Elongin C (Elc1p) interacts with the Rad7p/16p complex along with Cullin3 (Cul3p) for Rad4p degradation after UV (Fig. 1.4) (Gillette et al. 2006). Thus Rad7p is a component of the E3 ubiquitin ligase complex that degrades Rad4p after the DNA damage recognition step in yeast GG-NER. Rad7p and Rad16p are also accompanied by the DNA binding factor Abf1p (ARS-binding factor 1) in the GG-NER recognition complex. In the absence of UV, Abf1p forms a heterotrimetric complex along with Rad7p and Rad16p (Waters et al. 2015) (Fig. 1.4).

Homologs of the majority of these components of *S. cerevisiae* GG-NER exist in plants (Table 1.1). For example, Rad16p has two homologs in Arabidopsis (At1g05120, At1g02670) (Shaked et al. 2006). *Arabidopsis thaliana* also has 6 Cullin-like proteins including two CULLIN3 homologues: CULLIN3a (CUL3a: At1g25830), and CULLIN3b (CUL3b: At1g69670) (Weber et al. 2005). The Elc1p homologue in Arabidopsis (At5g59140) is a BTB/POZ domain protein (Risseeuw et al. 2003). We have identified homologues of yeast Rad7p in Arabidopsis and their analysis is a major part of this thesis.

1.3.2.2.4 Damage verification: TFIIH activity

The TFIIH complex is activated after UV damage recognition by the XPC/RAD4 complex. The main role of this complex in NER is to verify the damage followed by unwinding of the damaged DNA strand. The complex is composed of two helicase subunits, XPB and XPD, along with p38, p44, p52, p62, p8, and a kinase for CDK activation, CAK. The recruitment of TFIIH by XPC damage recognition depends on XPB and p62 subunit interaction. The uncoiling is done by the helicase activity of XPB (3'-5') and XPD (5'-3') to open up the damaged site to form a 27 nucleotide single stranded region, 22 nucleotides 5' of the damaged site and 5 nucleotides 3' of the damaged site. Uneven separated strands requires energy from ATP hydrolysis to proceed further (Petruseva et al. 2014) (Fig. 1.4).

Mammalian XPB has a yeast homolog, Rad25p, which is essential for viability in yeast (Park et al. 1992). The TFIIH complex is also involved in *Saccharomyces* NER with two main components, Rad3p (XPD homologue) and Rad25p, which both have DNA dependent ATPase/helicase activity. Yeast TFIIH is composed of two complexes that include 10 components in total. The core complex with 7 subunits (Rad25p, Rad3p, Tfb1p, Tfb2p, Ssl1p, Tfb4p, and Tfb5p) is involved in NER. The other

complex is the CAK kinase complex, which is composed of 3 subunits (Kin28p, Ccl1p, and Tfb3p) (Boiteux and Jinks-Robertson 2013) (Table 1.1).

Arabidopsis thaliana has duplicated XPB/Rad25p homologs, AtXPB1 and AtXPB2, which are 95% similar at the amino acid level (Table 1.1). They were studied for their role in DNA repair and transcription as well as plant development. The single loss of function mutant *xpb1* is not UV sensitive (Costa et al. 2001). However complementation assays with yeast *rad25* showed the helicase activity of AtXPB2 is conserved (Morgante et al. 2005). Arabidopsis XPD is homologous to human and yeast (56% and 60% amino acid identity respectively) XPD/Rad3p. The AtXPD mutant *uvh6* (*UV hypersensitive 6*) is sensitive to UV with yellow-green leaf coloration and growth defects (Liu et al. 2003). A p44 homologue is also present in Arabidopsis, is named ATGTF2H2, and interacts with AtXPD (Vonarx et al. 2006). Another plant component of TFIIH is rice OsREX1-S, homologous to TFB5. Transgenic Arabidopsis expressing OsREX1 exhibit reduced CPDs in response to UV-B and increased tolerance of UV and other mutagens (Kunihiro et al. 2014).

1.3.2.2.5 Endonuclease activity: the next step of damage verification

The first protein identified in human NER was XPA. Later, research revealed that the role of XPA was in the last step of recognition along with XPD of the TFIIH complex. XPA facilitates the arrival of XPF-ERCC1 to the damaged site to introduce incisions in the damaged DNA (Fig. 1.4). The Zn finger of XPA is the DNA binding region. XPA acts as a bridge between the TFIIH complex for damage recognition and the ERCC1-XPF endonuclease for damaged DNA incision and also binds to RPA, an important single strand binding protein (Alekseev and Coin 2015). XPF-ERCC1 catalyzes the 5' incision and adds one free hydroxyl radical to the 3'

end for repair synthesis. XPG catalyzes the 3' excision to complete the damaged DNA site excision. XPG also interacts with PCNA to facilitate repair synthesis (Petruseva et al. 2014).

The human ERCC1 homologue is *Saccharomyces cerevisiae* Rad10p, which is 29% identical at the amino acid level. It is a single stranded endonuclease that, along with the XPF homologue Rad1p, cleaves off the UV damaged DNA strand. Yeast Rad2p is the homologue of human XPG, which is another single stranded DNA endonuclease and a component of the NEF3 complex (Sarangi et al. 2014) (Table 1.1).

In plants, homologues of ERCC1, XPF, XPG, and RPA have been identified but not an XPA homologue. The Arabidopsis AtERCC1 homolog, UV REPAIR DEFICIENT 7 (UVR7), interacts with AtXPF (Vannier et al. 2009). AtXPF has 37% amino acid identity to the human homolog. The AtXPF mutant was also identified as *UV hypersensitive 1* (*uvh1)*. A complementation study revealed that UVH1 is a homologue of yeast RAD1 and is involved in dark excision repair (Fidantsef et al. 2000). An AtXPG point mutant, *uvh3*, is also UV sensitive as well as exhibits premature aging (Liu et al. 2001). The *XPG* homologue in rice, *OsSEND1*, is upregulated in response to UV (Furukawa et al. 2003). Plant RPA homologues were first identified in rice. Three OsRPA70, three OsRPA32, and one OsRPA14 have been identified. *OsRPA70A* mutants exhibit defects in mutagen sensitivity and fertility (Ishibashi et al. 2001; Ishibashi et al. 2006). Arabidopsis has five AtRPA70, two AtRPA32, and two AtRPA14 homologues (Shultz et al. 2007). The AtRPA70A/B double mutants are UV sensitive (Takashi et al. 2009).

1.3.2.2.6 Ligation and DNA synthesis

Mammals have enzymes and proteins that are common to both regular DNA replication and DNA ligation and damage repair. DNA polymerase δ and ε and factors such as PCNA, RFC,

and RPA are actively involved in DNA synthesis. The ATP dependent five subunit RFC complex interacts with PCNA to synthesize the DNA strand from the 3' OH end. PCNA interacts with DNA polymerase to initiate the synthesis (Petruseva et al. 2014) (Fig. 1.4).

In yeast, PCNA (proliferating cell nuclear antigen) is encoded by *POL30* and has a similar role as mammalian PCNA in repair. The PCNA complex embraces the damaged DNA for repair (Chakraborty et al. 2016).

PCNA and RFC homologues have been identified in plants (Table 1.1). Arabidopsis has two PCNA homologues, AtPCNA1 and AtPCNA2, involved in sliding gate activity in DNA replication. AtPCNA2 has similar roles to yeast Pol30 (Xue et al. 2015). The AtPOLλ in Arabidopsis, a mammalian homologue of DNA polymerase λ, is believed to have role in NER (Roy et al. 2011).

1.3.2.3 TC-NER

The transcription coupled NER (TC-NER) machinery detects damage indirectly, via the stalled RNA polymerase II. TC-NER initiates when RNA polymerase II elongation is interrupted by a damaged lesion. Two proteins, Cockayne Syndrome complementation group A (CSA) and B (CSB), are recruited by RNA Polymerase II to the damaged strand to proceed with repair (Dijk et al. 2014). CSA and CSB further assemble with the common NER players and TC-NER specific proteins to form the core TC-NER machinery. Proteins involved in mammalian TC-NER include UV-stimulated scaffold protein A (UVSSA) (Schwertman et al. 2013; Spivak 2005), ubiquitin-specific-processing protease 7 (USP7; or ubiquitin C-terminal hydrolase 7) (Li et al. 2002; Schwertman et al. 2013), XPA-binding protein 2 (XAB2) (Lagerwerf et al. 2011; Nakatsu et al. 2000), high mobility group nucleosome-binding domain-containing protein 1 (HMGN1; also known as non-histone chromosomal protein HMG14) (Fousteri and Mullenders 2008;

Landsman et al. 1989), and transcription elongation factor TFIIS (Fousteri and Mullenders 2008; Yoo et al. 1991). These proteins are involved in various stages of TC-NER. UVSSA removes RNA polymerase from the damaged site, facilitating the ability of other proteins to carry out TC-NER. USP7 is a deubiquitinating enzyme that forms a complex with UVSSA and stabilizes CSB (Schwertman et al. 2013). XAB2 interacts with XPA, CSA, and CSB, as well as RNA polymerase II. Mammalian CSB is 168 kDa nuclear protein from the SWI/SNF family, which recruits additional NER factors for repair. Mammalian CSA is 46 kDa WD40 repeat family protein, which possesses five WD repeat domains, facilitating interaction with the DDB1-CUL4 E3 ligase. CSA directly interacts with RNA Pol II and is recruited to the damaged site after CSB to form a complex in a damage dependent manner (Saijo 2013). TFIIS is required for RNA Pol II transcript elongation at the transcription arrested site. Subsequently, the common repair process in both GG-NER and TC-NER is based on further recruitment of factors by TFIIH. TFIIH, like XPA and recruitment protein A (RPA), prepare for dual incision by XPG and XPF-ERCC1 (Marteijn et al. 2014; Zhang et al. 2012).

Yeast TC-NER also results in the rapid removal of stalled RNA polymerase II from the lesion site on the transcribed strand. The DNA dependent ATPase Rad26p, the homologue of mammalian CSB, is a SWI2/SNF2 family chromatin remodeling protein which participates in TC-NER (Li 2015). The *Saccharomyces cerevisiae* homologue of mammal CSA is Rad28p. The loss of function *rad28* mutant did not demonstrate increased sensitivity for UV damage. However the *rad28* mutant was sensitive to UV in the presence of the *rad7* and *rad16* mutants and prone to mutation upon UV exposure (Bhatia et al. 1996).

The yeast homologue of mammalian USP7 is ubiquitin binding protein (UBP) 15p. This protein is involved in the processing of ubiquitin precursors (Amerik et al. 2000). Yeast SYF1p

is the homologue of mammalian XAB2, which is a part of the splicosome for pre-RNA splicing (Ben-Yehuda et al. 2000) (Table 1.1).

TC-NER has been shown to result in the preferential repair of the transcribed strand of actively transcribed genes in animals, yeast, and bacteria. Recently this preferential rapid repair of transcribed strands was shown to also occur in plants, thus TC-NER is also important in plant systems (Fidantsef and Britt 2012). An Arabidopsis homologue of XAB2 has been identified which is a tetratricopeptide repeat (TPR) like superfamily protein predicted to exhibit RNA processing activity, but its role in NER has yet to be examined (Kunz et al. 2005). USP7 has two homologues in Arabidopsis, Ubiquitin like protease 12 (UBP12) and Ubiquitin like protease 13 (UBP13). Both of the proteins have ubiquitin specific protease activity (Liu et al. 2008). Mammalian CSB has an Arabidopsis homologue named Chromatin Remodelling 8 (CHR8), which has helicase as well as DNA, ATP, and nucleic acid binding domains (Kunz et al. 2005). *CHR8* RNAi lines are sensitive to UV (Shaked et al. 2006). Two mammalian CSA homologs have been identified in Arabidopsis, AtCSA1A and AtCSA1B. They are 92% identical DWD proteins and have been found to interact with the DDB1-CUL4A-E3 complex. Loss of function mutants are sensitive to UV and result in reduced or slow removal of photoproducts. The overexpression of AtCSA1A also resulted in hypersensitivity to UV (Biedermann and Hellmann 2010; Zhang et al. 2010). TFIIS has an Arabidopsis homologue AtTFIIS/RDO2 (Reduced Dormancy 2), which initiates the efficient RNA Pol II elongation and complements yeast TFIIS. Arabidopsis TFIIS RNAi mutants lines showed reduced seed dormancy thus are involved in seed development (Grasser et al. 2009).

Thus NER is a conserved multistep procedure with homologues in mammalian, plant, and yeast systems (Table 1.1, Fig. 1.4). While the role of XPC/Rad4p has been well studied in

mammals and yeast, its function in plants is relatively uncharacterized. In this thesis I will examine the role of Arabidopsis RAD4 in UV tolerance. In addition, we have identified plant homologues of yeast Rad7p, and will characterize the role of Rad7p homologues in a multicellular system for the first time.

In Chapter 2, I examine the role of Arabidopsis RAD4 and RAD23 in Arabidopsis UV tolerance.

Chapter 2. RAD4 and RAD23/HMR contribute to Arabidopsis UV tolerance

Triparna Lahari, Janelle Lazaro, and Dana F. Schroeder

Department of Biological Sciences, University of Manitoba, Winnipeg, MB R3T 2N2

Published in a special issue of Genes on DNA Damage Responses in Plants

Author contributions: Janelle Lazaro assisted with yeast two hybrid analysis and genotyping *rad23* lines, and assayed adult UV tolerance in *rad23* lines. All other experiments were performed by Triparna Lahari.

2. RAD4 and RAD23/HMR contribute to Arabidopsis UV tolerance

2.1 Abstract

In plants, exposure to solar ultraviolet (UV) light is unavoidable, resulting in DNA damage. Damaged DNA causes mutations, replication arrest, and cell death; thus efficient repair of the damaged DNA is essential. A light-independent DNA repair pathway called Nucleotide Excision Repair (NER) is conserved throughout evolution. For example, the damaged DNA binding protein Radiation sensitive 4 (Rad4p) in *Saccharomyces cerevisiae* is homologous to the mammalian NER protein Xeroderma Pigmentosum complementation group C (XPC). In this study, we examined the role of the *Arabidopsis thaliana* Rad4p/XPC homologue (AtRAD4) in plant UV tolerance by generating overexpression lines.AtRAD4 overexpression, both, with and without an N-terminal yellow fluorescent protein (YFP) tag, resulted in increased UV tolerance. YFP-RAD4 localized to the nucleus and UV treatment did not alter this localization. We also used yeast two hybrid analysis to examine the interaction of AtRAD4 with Arabidopsis RAD23 and found that RAD4 interacted with RAD23B as well as with the structurally similar protein HEMERA (HMR). In addition, we found that *hmr* and *rad23* mutants exhibited increased UV sensitivity. Thus, our analysis suggests a role for RAD4 and RAD23/HMR in plant UV tolerance.

2.2 Introduction

All living organisms have an inherent ability to protect their genetic integrity against naturally occurring environmental mutagens. Ultraviolet (UV) light is one of the most common and unavoidable environmental sources of DNA damage. UV induces dipyrimidine photolesions

in DNA such as cyclobutane pyrimidine dimers (CPDs) and 6,4 photoproducts (6-4PPs) (Rastogi et al. 2010). Damaged DNA arrests cellular processes such as replication and transcription. A failure to repair DNA damage ultimately leads to disturbances of gene expression, mutations, and apotosis. The mechanisms for the protection and repair of DNA are well conserved (Sugasawa 2011). The single step light dependent damage repair, called photoreactivation, is carried out by photolyase enzymes in the presence of blue light. Light independent multistep DNA repair is called nucleotide excision repair (NER) (Ganpudi and Schroeder 2011). Defective NER in humans can result in xeroderma pigmentosum (XP), Cockayne syndrome (CS), and trichothiodystrophy (Laine and Egly 2006) Xeroderma pigmentosum results in hypersensitivity to UV radiation and increased risk of skin cancer. Eight genetic complementation groups (A to G, V) have been identified for XP to date (Dijk et al. 2014).

The initiation of NER varies depending on the location of the damage. The repair of transcribed DNA strands is known as transcription coupled-NER (TC-NER). Damage recognition in TC-NER is performed by Cockayne syndrome A and B proteins (CSA and CSB) (Saijo 2013). In contrast, global genomic NER (GG-NER) is the repair of untranscribed DNA across the entire genome (Sugasawa 2010). In mammalian GG-NER, UV-induced lesions recruit the UV-damaged DNA binding (DDB) protein complex, DDB1–DDB2–CUL4A–RBX1 . The DDB complex then recruits the Xeroderma Pigmentosum complementation group C (XPC) complex to the damaged site. The mammalian XPC complex consists of XPC, hRAD23B, and Centrin 2 (CEN2), a small calcium-binding EF-hand protein. Damage recognition by the XPC complex is followed by damage verification by the basal transcription factor IIH (TFIIH) complex and XPA. During verification by TFIIH, two helicases, XPD and XPB, open the double helix with their ATPase activity. Replication protein A (RPA), along with the endonucleases XPG and XPF-ERCC1, become active after damage verification, resulting in a

dual incision at the damaged site, , and the removal of the damage. Finally, repair synthesis completes the repair (Matsumoto et al. 2015).

The yeast (*Saccharomyces cerevisiae*) XPC orthologue, Rad4p (Radiation sensitive 4), has an activity that is similar to that of its mammalian counterpart. Rad4p, along with yeast Rad23p, forms a complex to recognize UV-damaged DNA. This complex is recruited by Rad7p/Rad16p. Rad4p is ubiquitinated and degraded after damage recognition (Gillette et al. 2006).

The GG-NER process is similar in plants, mammals, and yeast (Ganpudi and Schroeder 2011). Plant homologues of Rad23p have been reported first in *Arabidopsis thaliana*, rice, and *Daucus carrota* (Schultz and Quatrano 1997; Sturm and Lienhard 1998). In *Arabidopsis thaliana* the RAD23 family includes four members, RAD23A, RAD23B, RAD23C, and RAD23D, which are also involved in the transfer of ubiquitinated proteins to the 26S proteasome (Farmer et al. 2010). In addition, Chen et al. (2010) identified a novel protein in the Arabidopsis phytochrome nuclear body, HEMERA, previously known as pTAC12 (Chen et al. 2010; Pfalz et al. 2006). HEMERA was found to be structurally similar to RAD23 and partially complements Rad23p function in yeast (Chen et al. 2010). Studies involving the loss of Arabidopsis CEN2 confirmed its role in NER (Molinier et al. 2004). AtCEN2 interacts with the Arabidopsis homologue of human XPC (AtRAD4) via an EF-hand $Ca2^{+}$ binding domain. This domain is required for CEN2 function in NER (Liang et al. 2006). In plants, the role of AtRAD4 in DNA repair has yet to be studied in detail. In this study, we investigate the role of AtRAD4 in UV tolerance and its interaction with RAD23 and HMR.

2.3 Materials and methods

2.3.1 Plant material and growth conditions

In these studies the Columbia-0 (Col-0) ecotype was used as the wild type control. The *HEMERA* (At2g34640) partial loss of function allele *hmr-22* (Qiu et al. 2015) was kindly provided by Dr. Meng Chen, UC Riverside. The lines *rad23a-1* (SALK_064980 in At1g16190), *rad23b-1* (SALK_076360 in At1g79650), *rad23c-1* (SALK_068091 in At3g02540), and *rad23d-1* (SALK_014137 in At5g38470) (Farmer et al. 2010) were ordered from the Arabidopsis Biological Resource Center (ABRC), Columbus, OH, USA. Unfortunately, we were unable to identify homozygotes in the *rad23d-1* line, so *rad23a-c* were used for analysis. The seeds were sterilized (10 min in 70% ethanol, 0.5% Triton X-100 followed by 10 min in 95% ethanol) and plated on Linsmaier and Skoog (LS) medium (Caisson, Smithfield, UT, USA) containing 0.6% sucrose and 0.86% phytoblend (Caisson). The seeds were cold-stratified at 4 ^{0}C for 2 days, followed by growth in an incubator at 20 ^{0}C, 50% relative humidity and long day conditions for 14 days. Seedlings were transplanted to soil on the 14th day for further growth in long-day conditions (16 h light and 8 h dark) provided by fluorescent bulbs (100 M photons m^{-2} s^{-1}). The temperature was maintained at 20 ^{0}C and the relative humidity at 50%. The soil used for growth was Sunshine mix no. 1 (SunGro, Bellevue,WA, USA).

2.3.2 Generation of overexpression lines

Overexpression lines were generated using the *RAD4* (At5g16630) cDNA in the pENTR223 vector (G16664) obtained from the ABRC. The *RAD4* cDNA was cloned into pEarleyGate100 (CaMV 35S:RAD4) and pEarleyGate104 (CaMV 35S:YFP-RAD4) using Gateway technology (Earley et al. 2006). The pEarleyGate vectors were also obtained from the ABRC. Wild-type Arabidopsis Col-0 was transformed via agrobacterium-mediated

transformation (Weigel and Glazebrook 2002) and the transformed generation (T1) was screened with BASTA selection. Homozygous T3 plants were used for the experiments.

2.3.3 RNA extraction and qRT-PCR

Col-0 and RAD4 overexpression lines were grown on LS plates in long-day conditions for 7 days. The RNA was extracted from 50 seedlings per sample using the RNeasy plant minikit (Qiagen, Hilden, Germany) including DNase treatment. cDNA was synthesized from RNA with the Maxima First Strand cDNA synthesis kit (Fermentas, Waltham, MA, USA). Transcript levels were checked with the *RAD4* cDNA specific primers RAD4_c671F (GTAAAGGCACAGCGGAAGAG) and RAD4_c780R (CCCAGGTTTTAAGGATGCAA). *EF1α* (At5g60390) (CTGGAGGTTTTGAGGCTGGTAT, CCAAGGGTGAAAGCAAGAAGA) was used to normalize the sample loading (Hossain et al. 2012; Jain et al. 2006). Real-time PCR was performed using SsoFast EvaGreen Supermix (Bio-Rad, Hercules, CA, USA) and the CFX Connect Real time PCR detection system (Bio-Rad) was used for analysis. Two biological replicates were performed per genotype, the data were normalized versus *EF1α,* and the mean values were calculated and expressed as relative to the levels in the Col-0 control.

2.3.4 UV sensitivity assays

The seeds were sterilized and plated on LS medium (Caisson) containing 0.6% sucrose and 0.86% phytoblend. The plates were kept at 4 ^{0}C for 2 days for cold stratification followed by vertical growth for 3 days at 20 ^{0}C in long-day conditions. The three-day-old plants were exposed to 0 or 1000 J UV-C m^{-2} (shortwave UV lamp XX-15S, UVP/LLC, Upland, CA, USA) and wrapped with aluminium foil to prevent photoreactivation. The plants were then rotated 90° and grown in the dark for 3 days. Plates were then scanned on a Perfection 1260 scanner (Epson,

Suwa, Japan), and hypocotyl and root growth were measured for the indicated number of seedlings (n) using ImageJ.

In the light-versus-dark UV sensitivity assay, the seeds were grown in the same conditions as above. Three-day-old seedlings were exposed to 0 or 1000 J m^{-2} UV-C, followed by 2 days growth in light or dark. The roots were measured and analyzed as above.

In the adult assay, the seedlings were grown in the above conditions on LS medium and transplanted to soil at two weeks of age. At three weeks of age, the plants were exposed to 0, 300, or 600 J m^{-2} of UV-C, followed by 3 days of growth in dark conditions, then returned to long-day conditions. After 2-3 days of growth in the light, individual leaves were scored as either undamaged (green) or damaged (yellow or brown) and data were expressed as percentage of undamaged leaves (green leaves/total leaves) for six plants per genotype per treatment. In the adult UV sensitivity assays, *uvh1-1* was used as the positive control (Harlow et al. 1994).

2.3.5 Protein localization

Yellow fluorescent protein (YFP)-tagged RAD4 T3 and control seeds were sterilized and cold stratified for 2 days at 4 ^{0}C. The seedlings were grown on LS medium for 3 days in the dark following a 6 h light treatment to initiate germination. The slides were prepared with 2-3 seedlings per slide in distilled water and were observed under an AXIO Imager Z1 Microscope (Zeiss, Oberkochen, Germany) equipped with Axio Vision 4.8 software using YFP (Filter Set YFP-2427B-000, Semrock Inc., Rochester, NY, USA) and DAPI (Zeiss Filter Set 02 (488002-9901-000) filters. DAPI (Sigma-Aldrich Canada, Oakville, ON, Canada) staining (10 µg/ml) (Kapuscinski 1995) was done for 10 min. For UV treatments, the seedlings were exposed to 1000 J UV-C m^{-2} and then observed.

2.3.6 Yeast two hybrid analysis

RAD4 protein interactions were investigated using the Matchmaker gold yeast two-hybrid system (Clontech, Mountian View, CA, USA). The cDNAs of *RAD4* (ABRC clone U16664), *RAD23B* (ABRC clone U09913), and *DDB2* (At5g58760) (ABRC clone U61992) were cloned into pGADT7 (Leu selection) and pGBKT7 (Trp selection) via standard cloning or Gateway technology. *RAD4* pGADT7 was digested with SacI enzyme to remove the C-terminal fragment of RAD4 then ligated to construct *RAD4N* pGADT7 (1-368/866 aa). To construct *RAD4N* pGBKT7 (1-371/866 aa), *RAD4* pGBKT7 was digested with PstI to remove the C terminal end of RAD4, followed by re-ligation. *HEMERA* pGADT7 and pGBKT7 were kindly provided by Dr. Meng Chen, UC Riverside. Diploid yeast strains were plated via a series of five fold dilutions on both double drop-out (-trp -leu) control and quadruple drop-out (-ade –his –leu -trp) selection medium along with the positive p53/T (murine p53/ SV40 large T-antigen) and negative Lam/T (Lamin/ SV40 large T-antigen) control. Protein interaction resulted in the expression of *ADE2* and *HIS3* reporters and growth on the selective medium. On the control medium, Ade- colonies sometimes turn reddish over time while Ade+ colonies remain pale.

2.3.7 Statistical analysis

A Student's two-tailed t-test was performed to compare the overexpression lines or mutants with Col-0 wild type. Values of $p \leq 0.05$ were considered to be statistically significant. Each experiment was repeated at least twice, and representative data are shown.

2.4 Results

Initially, we attempted to examine the *AtRAD4* loss of function phenotype by examining two Salk T-DNA insertion lines (SALK_135310, SALK_020675) and one FLAG T-DNA line (FLAG_005E11) (Alonso et al. 2003; Samson et al. 2002). The T-DNA insertions in the Salk lines are beyond the 3' end of the *RAD4* transcript, so they do not disrupt the coding sequence. The analysis of *RAD4* transcript levels in these two lines showed no decrease in *RAD4* levels (data not shown). Thus, these two lines are not suppressed or silenced and are not *RAD4* loss of function alleles. The insertion site of the FLAG T-DNA line is in exon 11. However, no homozygotes were found in the segregating populations, suggesting that *RAD4* loss of function results in gamete or embryo lethality.

Thus, in order to examine the role of AtRAD4 in UV tolerance, we utilized a gain of function approach by generating overexpression lines using pEarleyGate vectors (Earley et al. 2006). Two overexpression (CaMV 35S driven) constructs were generated, one with an N-terminal YFP tag in the pEarleyGate104 vector, and one without a tag in the pEarleyGate100 vector. Both these constructs were transformed into the Col-0 wild-type background, transformed lines were generated, and overexpression was confirmed in the homozygous T3 lines (Fig. 2.1a,b). The tagless RAD4 overexpression lines showed increased UV tolerance in both the root and hypocotyl (Fig. 2.1c). This increased UV tolerance occurred only when the plants were incubated in the dark following UV treatment, but not when they were incubated in the light (Fig. 2.1e), consistent with a role in dark repair (nucleotide excision repair). In adult plants, RAD4 overexpression resulted in decreased damage following UV treatment and dark incubation (Fig. 2.1g, S2.1), and, therefore, increased UV tolerance, in contrast to UV-sensitive control *uvh1-1,* which is defective in defective in the Arabidopsis XPF endonuclease homologue (Harlow et al. 1994). Similarly, YFP-RAD4 overexpression also resulted in increased UV tolerance in dark incubated hypocotyls, roots, and adult leaves (Fig. 2.1d,h), but not in light

incubated roots (Fig. 2.1f). Thus, RAD4 overexpression results in increased UV tolerance, and the N-terminal YFP tag does not appear to interfere with RAD4 function.

In order to determine RAD4 cellular localization, we examined YFP fluorescence in the YFP-RAD4 line. YFP-RAD4 was found to be nuclear-localized, as confirmed by DAPI staining (Fig. 2.2a). While the Arabidopsis SubCellular Proteomic Database (SUBA) (Tanz et al. 2013) predicts nuclear, plastid, and mitochrondrial localization for RAD4, both the consensus algorithms SUBAcon (Hooper et al. 2014) and PSI (Plant Subcellular localization integrative predictor) (Liu et al. 2013) predict nuclear localization of AtRAD4, with scores of 0.998 and 0.708, respectively. AtRAD4 appeared to be localized throughout the nucleus, consistent with the prediction of the Sub-nuclear Compartments Prediction System (Version 2.0) (Lei and Dai 2005) which predicts nucleoplasm and nuclear lamina localization for AtRAD4. This localization was not altered by UV treatment (Fig. 2.2b).

Yeast two hybrid analysis was used to examine the interactions between the Arabidopsis GG-NER components. Arabidopsis *RAD4* and *DDB2* homologues were cloned into yeast two hybrid vectors and tested for interaction, however no growth on the selective medium, indicative of interaction, was observed (Fig. S2.2). In addition, RAD4 did not interact with itself in this assay (Fig. S2.3).

We then tested for the interaction between XPC complex components AtRAD4 and RAD23B. Interestingly, the RAD23 GAL4 DNA-binding domain fusion alone (RAD23 pGBKT7) resulted in growth even in the absence of RAD4 (Fig. S2.4a), suggesting that RAD23 possesses some transcriptional activation activity. However, the RAD23 pGADT7 (activation domain) and RAD4 pGBKT7 (binding domain) constructs did not result in growth alone, but did together, indicating an interaction (Fig. S2.4b). The N terminal half (1-368 / 866 aa) of RAD4 was found to be sufficient for RAD23B interaction (Fig. 2.3).

We also tested for the interaction between RAD4 and the RAD23-like protein HEMERA. Both RAD4 and the RAD4 N-terminal half (1-371 / 866 aa) were able to interact with HMR in yeast two hybrid analysis (Fig. 2.4). This result is consistent with the ability of HEMERA to partially rescue yeast *rad23* UV sensitivity (Chen et al. 2010). To examine the role of HMR in Arabidopsis UV tolerance we performed UV assays using a viable *hmr* loss of function allele, *hmr-22* (Qiu et al. 2015). The seedlings of *hmr-22* exhibited increased UV sensitivity in both roots and hypocotyls (Fig. 2.5a), indicating that HMR contributes to Arabidopsis UV tolerance. This sensitivity was specific to dark conditions (Fig. 2.5b).

Since the RAD23-like protein HMR contributes to UV tolerance, we examined UV sensitivity in *rad23a, rad23b*, and *rad23c* mutants. The mutant *rad23a* exhibited sensitivity in dark grown roots (Fig. 2.6a) while *rad23b* was sensitive in both dark-grown roots and hypocotyls (Fig. 2.6b). The mutant *rad23c* was sensitive in dark-grown hypocotyls only (Fig. 2.6c). In adult plants, *rad23a* and *rad23b* exhibited increased leaf damage and, therefore, increased sensitivity (Fig. 2.6d). Thus, despite a potential redundancy within the RAD23 family, *rad23* single mutants were sensitive to UV damage.

2.5 Discussion

The DNA damage recognition factor XPC/RAD4 has been well studied in both mammalian (Dupuy and Sarasin 2016) and yeast systems (Min and Pavletich 2007) with respect to its role in the repair of UV-damaged DNA. In this study, we examined the role of Arabidopsis RAD4 in UV tolerance using a gain of function strategy. AtRAD4 overexpression lines, both with and without YFP tags, resulted in a significant increase in UV tolerance in hypocotyls, roots, and adults, indicating that increased AtRAD4 results in increased UV tolerance. This result

suggests that RAD4 is limiting during Arabidopsis nucleotide excision repair of UV-damaged DNA, and is the first genetic evidence that RAD4 contributes to this process in plants.

Our results are in contrast to findings in yeast, where ScRad4p overexpression in the wild type did not result in increased UV tolerance. However, ScRad4p overexpression did result in partial rescue of UV sensitivity in *rad23* mutants, consistent with the proposed role of Rad23p in Rad4p stabilization (Xie et al. 2004). Human *XPC* was found to be overexpressed in hepatocellular carcinoma cells, and may contribute to chemotherapeutic resistance in these cells (Fautrel et al. 2005). The role of XPC overexpression was also studied with respect to p53 turnover in the presence and absence of UV. In the absence of UV, XPC overexpression did not affect p53 turnover. However, in the presence of UV, XPC overexpression resulted in increased p53 degradation, indicating a role for XPC in p53 turnover (Krzeszinski et al. 2014). Thus, the effect of XPC/RAD4 overexpression varies between systems.

The overexpression of other Arabidopsis NER components, for example DDB2 and DDB1a, was also shown to increase UV tolerance (Al Khateeb and Schroeder 2009; Molinier et al. 2008). Extracts of plants overexpressing AtCEN2 exhibited increased repair of UV-damaged DNA (Liang et al. 2006). In contrast, the overexpression of the transcription-coupled repair component AtCSA resulted in decreased UV tolerance (Biedermann and Hellmann 2010).

The dark-specific UV tolerant phenotype in RAD4 overexpression lines is consistent with AtRAD4 acting during nucleotide excision repair. To determine if RAD4 exhibited nuclear localization, consistent with this role, we examined AtRAD4 cellular localization and found it to be nuclear-localized. UV treatment did not affect this pattern. In general, our localization results are in agreement with those generated by in silico localization prediction analysis (Hooper et al. 2014; Lei and Dai 2005; Liu et al. 2013; Tanz et al. 2013).

In yeast, ScRad4p was found to be localized in both the cytoplasm and the nucleus in a GFP-tagged localization study of yeast proteins (Huh et al. 2003). Later, the response of ScRad4p to DNA damaging agents was studied. ScRad4p was found throughout the cell in control conditions, and localized in the nucleus after treatment with a DNA-damaging agent (Li et al. 2010). Mammalian XPC was observed in the nucleus using immunofluorescence (Van Der Spek et al. 1996). Although XPC is localized in the nucleus the localization is not homogenous. The heterogeneous localization of XPC was higher in areas of condensed chromatin (Hoogstraten et al. 2008). XPC was found to become enriched in the perichromatin region following UV irradiation (Solimando et al. 2009).

The localization of other Arabidopsis NER components was also examined using fluorescent tags. Like AtRAD4, DDB2 is localized diffusely throughout the nucleus (Biedermann and Hellmann 2010; Molinier et al. 2008). Initial studies in onion cells indicated that CUL4 and DDB1a were nuclear-localized while DDB1b localized to both the nucleus and the cytoplasm (Zhang et al. 2008). However, in studies of transgenic Arabidopsis lines, GFP-tagged DDB1a was observed in the cytoplasm, but shuttled to the nucleus after UV irradiation. The DNA damage response component ATR1 was required for DDB1a relocalization (Molinier et al. 2008). In another study, the XPC complex component AtCEN2 was observed in the cytoplasm in control conditions, but localized to the nucleus following UV irradiation (Liang et al. 2006). The transcription-coupled repair protein CSA exhibited a speckled pattern in the nucleus (Biedermann and Hellmann 2010), while the rice TFIIH component OsREX1 was also nuclear (Kunihiro et al. 2014). Since NER occurs in the nucleus following UV damage, it appears that NER components already in the nucleus remain in place, while those present in the cytoplasm in control conditions relocate to the nucleus in response to UV treatment.

We examined RAD4 interaction with other NER components using yeast two hybrid assays. We did not detect an interaction between AtRAD4 and the damage recognition factor DDB2 in this assay. The mammalian XPC was found to interact with DDB2; however this was not detected using yeast two hybrid analysis but via co-immunoprecipitation (Sugasawa et al. 2005). Other proteins, such as DDB1, would have been present in this case, suggesting that the cellular context of the DDB and XPC complexes, or perhaps in vivo post-translational modifications are is required for DDB2-XPC/RAD4 interaction.

We did detect an interaction between AtRAD4 and RAD23b via yeast two hybrid analysis and showed the RAD4 N-terminal half was sufficient for RAD23b interaction. This region (amino acids 1-368 / 866) corresponds to amino acid 1-270 / 755 in ScRad4p and 1-490 / 940 in mammalian XPC (Min and Pavletich 2007). In yeast, ScRad4p was also found to interact with Rad23p in yeast two hybrid analysis (Wang et al. 1997). Interestingly (den Dulk et al. 2008), found that the equivalent N-terminal ScRAD4 fragment did not interact with Rad23p in yeast two hybrid analysis, but the C-terminal half did. However, co-crystallization of yeast Rad4p and Rad23p revealed contacts between the two proteins in both N- and C-termini of Rad4p (Min and Pavletich 2007). In mammals, the C-terminal 160 amino acids of XPC were found to be essential for hRAD23a/b interaction in yeast two hybrid analysis (Li et al. 1997). In vitro pulldown experiments found two XPC regions, 495-606 and 606-734, that were necessary but not sufficient for hRAD23b interaction; however the 495-734 region was sufficient (Uchida et al. 2002).

We also found that AtRAD4 interacts with the RAD23-like protein HEMERA in yeast two hybrid assays. Again, the RAD4 N-terminal half was sufficient for this interaction. HMR was previously found to partially rescue UV sensitivity in yeast *rad23* mutants, where it presumably would interact with ScRAD4 (Chen et al. 2010). A C-terminally tagged HMR-CFP

fusion protein was found to be localized to the chloroplast, while the N-terminally tagged YFP-HMR was found to be localized in the nucleus and cytoplasm but not in the chloroplast (Chen et al. 2010). Thus, AtRAD4 and HMR could potentially interact in the nucleus; however this has yet to be assessed. HMR was shown to contribute to transcriptional activation (Gao et al. 2011; Qiu et al. 2015). We found that RAD23b was also able to activate transcription in yeast two hybrid assays.

Since RAD4 interacted with HMR and RAD23b, we examined the role of HMR and the RAD23 family in Arabidopsis UV tolerance. We found the *hmr* and *rad23* mutants to be UV-sensitive. This is somewhat surprising given that there are four RAD23 homologues in Arabidopsis that were found to act redundantly with respect to developmental phenotypes (Farmer et al. 2010). However, the *rad23d* mutants were found to exhibit UV-sensitive pollen development (Li et al. 2012). We found that *hmr* and *rad23a,b,c* all exhibit dark-specific UV sensitivity, consistent with roles for both HMR and the RAD23s in Arabidopsis nucleotide excision repair.

In conclusion, our studies have shown that AtRAD4 overexpression results in increased UV tolerance, and that AtRAD4 is nuclear localized. RAD23B and HMR interact with RAD4 and contribute to Arabidopsis UV tolerance. These results are consistent with a role for AtRAD4, RAD23, and HMR in plant GG-NER. These studies provide additional insights into the basis of plant DNA repair and provide the basis for potential future improvements of plant UV tolerance.

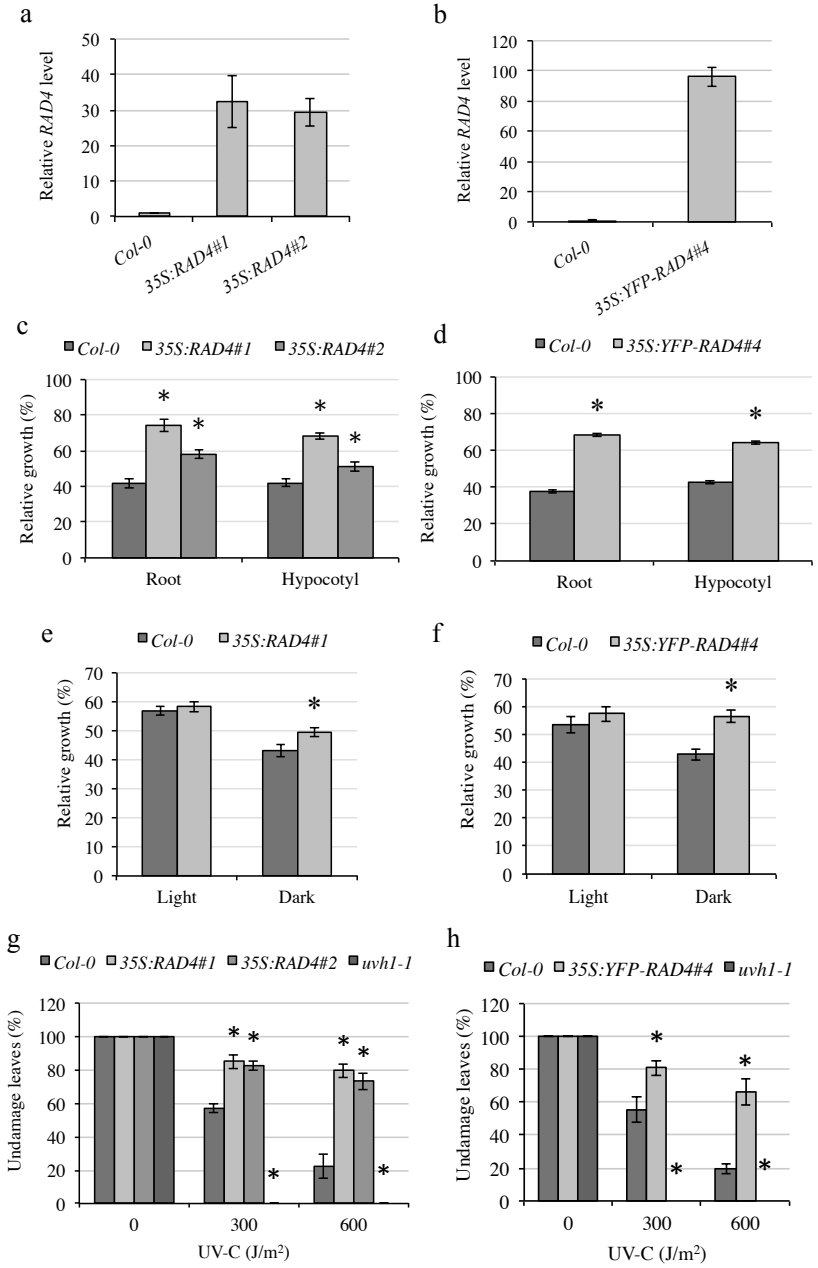

Fig. 2.1 RAD4 and YFP-RAD4 overexpression results in increased UV tolerance

RAD4 levels in (a) 35S:RAD4 overexpression lines and (b) 35S:YFP-RAD4 overexpression line, relative to control Col-0. The values are normalized relative to the reference gene *EF1α*. The error bars indicate SE (n=2). *(*c-h) UV tolerance in 35S:RAD4 and 35S:YFP-RAD4 overexpression lines. (c,d) Hypocotyl and root growth in dark-incubated seedlings analyzed 3 days after UV treatment, expressed as relative to the untreated controls (n=10). (e,f) Root growth in light- and dark-incubated seedlings analyzed 2 days after UV treatment, expressed as relative to the untreated controls (n=10). (g,h) Percentage of undamaged leaves in adult plants after 0, 300, or 600 J m^{-2} UV treatment followed by dark incubation (n=6). For c-h, the values are means ± SE, * = $p \leq 0.05$ for the overexpression lines vs Col-0 wild type in the same conditions.

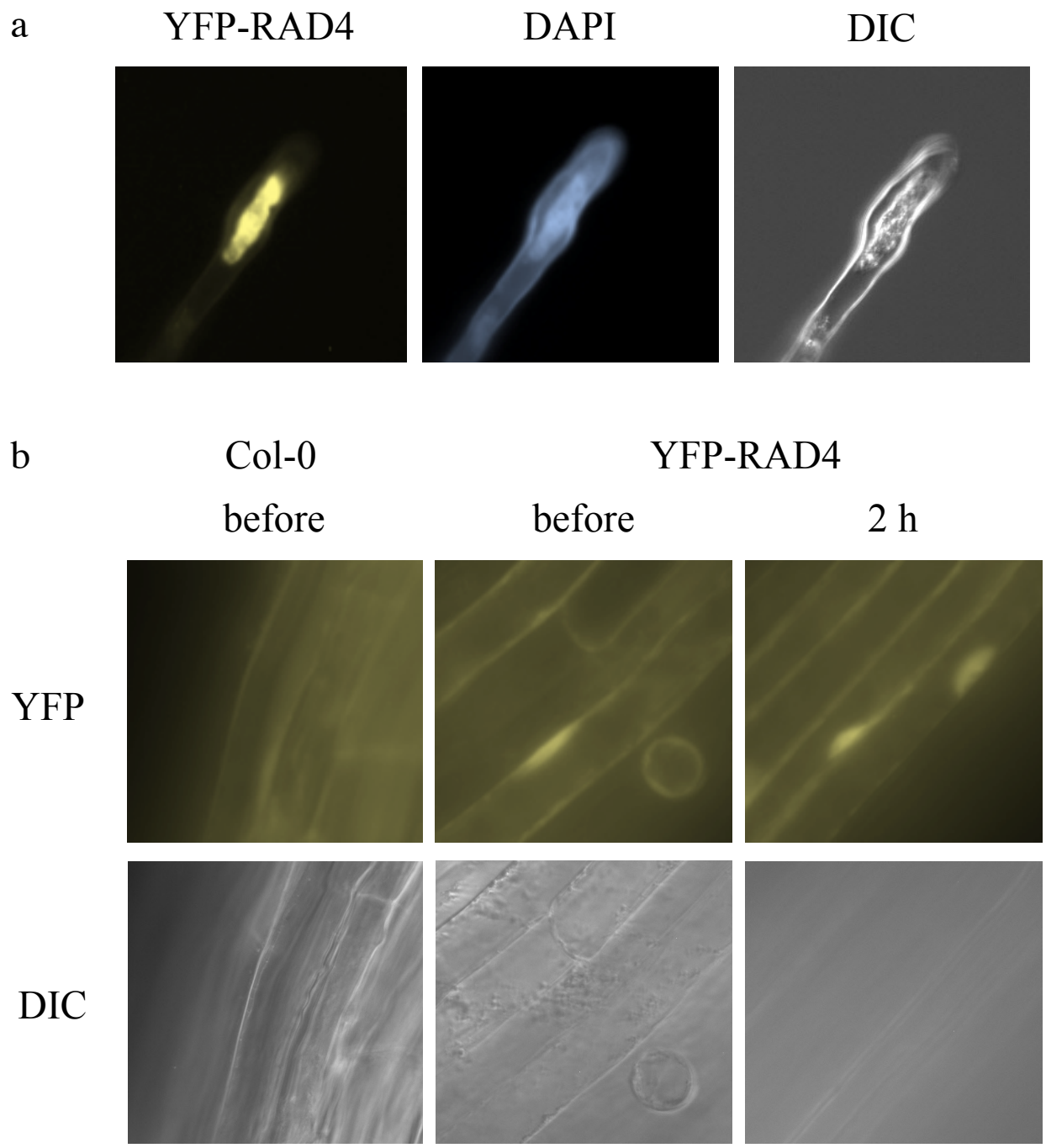

Fig. 2.2 YFP-RAD4 exhibits nuclear localization

(a) Root hair cells in three-day-old 35S:YFP-RAD4 dark-grown seedlings were examined under 40X magnification using YFP fluorescence, DAPI staining, and differential interference contrast (DIC). (b) YFP-RAD4 in three-day-old hypocotyl cells observed under a YFP filter (top) and DIC (bottom), before and after UV treatment, under 40X magnification.

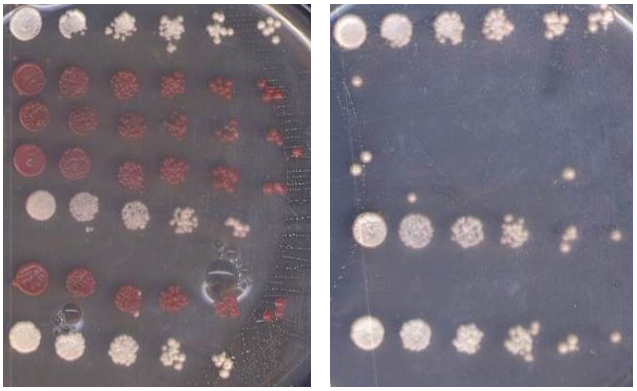

pGBKT7	pGADT7
P53	T
Lam	T
-	RAD23
RAD4	-
RAD4	RAD23
RAD4N	
RAD4N	RAD23

Fig. 2.3 Yeast two hybrid analysis of RAD4 N-terminus and RAD23B interaction

The RAD4 N-terminal half is sufficient to interact with RAD23B. Five-fold dilutions of the indicated diploid strains were plated on the double drop-out (-leu -trp) control plate on the left, and the quadruple drop-out (-leu -trp –ade -his) selection medium on the right. The interaction between p53 and T, resulting in growth on selective medium, is the positive control whereas Lam and T, which do not interact, are the negative control.

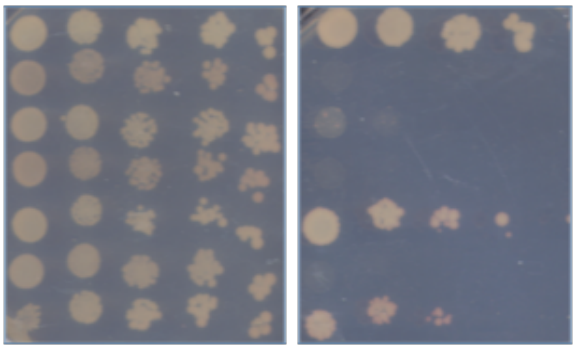

pGBKT7	pGADT7
P53	T
Lam	T
HMR	-
-	RAD4
HMR	RAD4
-	RAD4N
HMR	RAD4N

Fig. 2.4 Yeast two hybrid analysis of RAD4-HMR interaction

HMR interacted with both full length RAD4 and the RAD4 N-terminal half. Five-fold dilutions of the indicated diploid strains were plated on the double drop-out (-leu -trp) control plate on the left and the quadruple drop-out (-leu- trp –ade -his) selection medium on the right. The interaction between p53 and T, resulting in growth on the selective medium, is the positive control, whereas Lam and T, which do not interact, are the negative control.

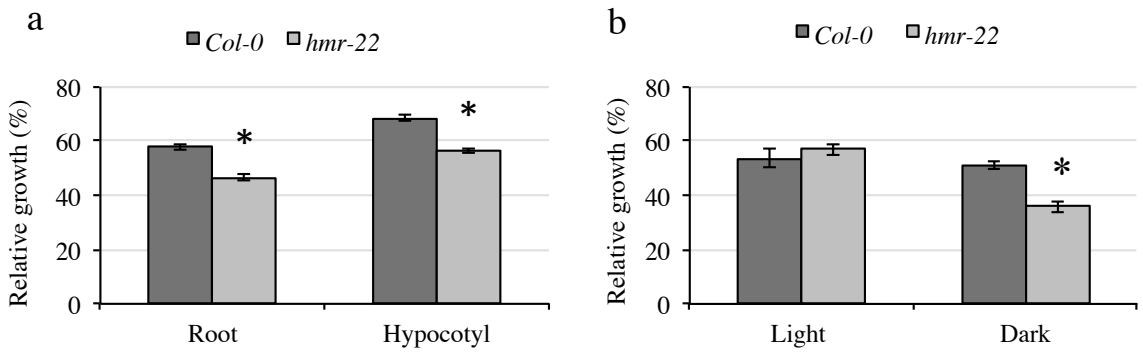

Fig. 2.5 The mutant *hmr* exhibits increased UV sensitivity

(a) Hypocotyl and root growth in dark-incubated seedlings analyzed 3 days after UV treatment expressed as relative to the untreated controls (n=20). (b) Root growth in light- and dark-incubated seedlings analyzed 2 days after UV treatment, expressed as relative to the untreated controls (n=20). The values are means ± SE, * = $p \leq 0.05$ for the mutant vs Col-0 wild type in the same conditions.

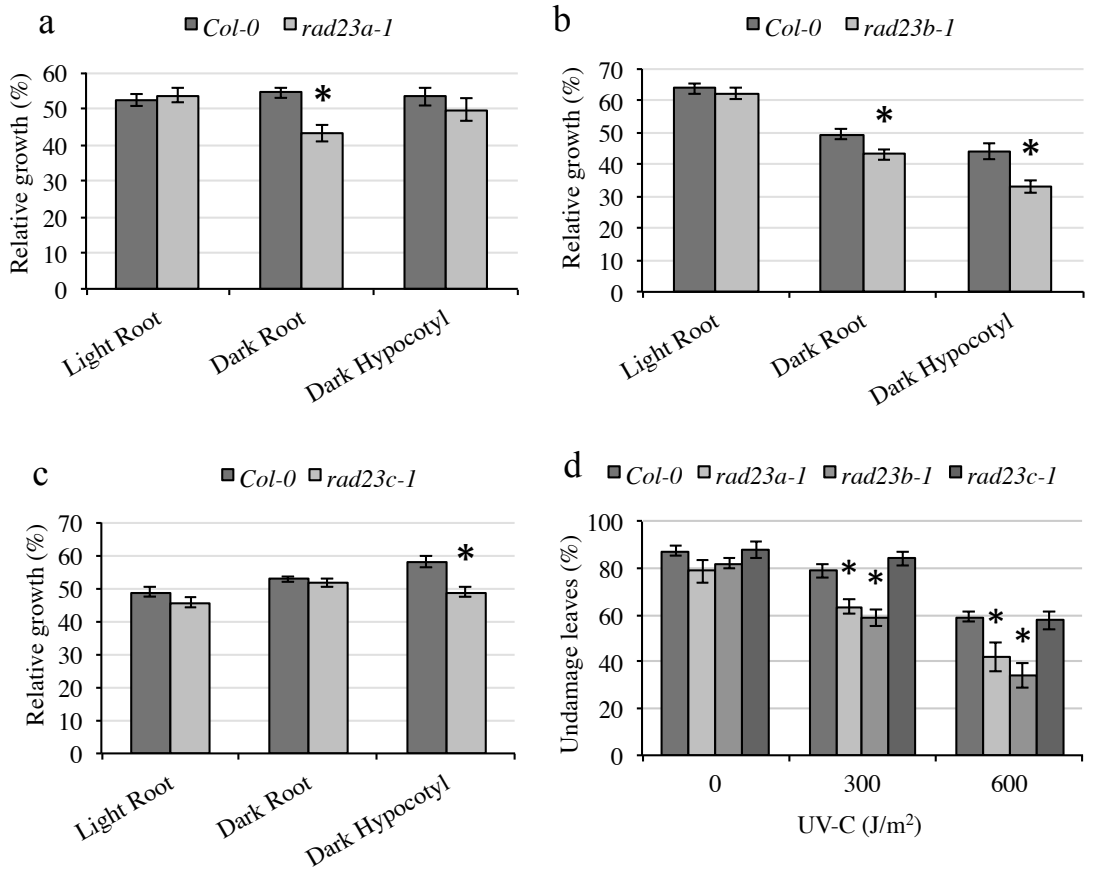

Fig. 2.6 Mutants of *rad23* exhibit increased UV sensitivity

(a-c) Relative root and hypocotyl growth in light- or dark-incubated seedlings analyzed 2 days after UV treatment (n=20). (d) Fraction of damaged leaves in adult plants after 0, 300, or 600 J m^{-2} UV treatment followed by dark incubation (n=6). The values are means ± SE, * = $p \leq 0.05$ for the mutant vs Col-0 wild type in the same conditions.

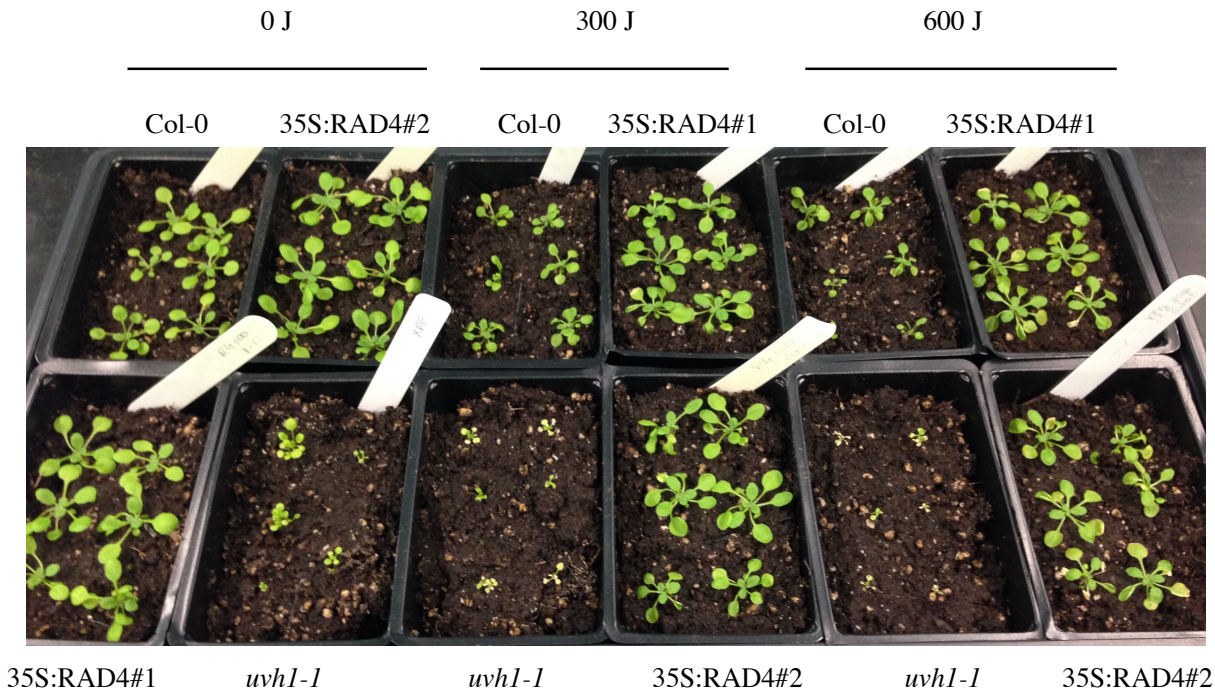

Fig. S2.1 RAD4 overexpression increases adult UV tolerance

21-day-old plants were treated with 0, 300, or 600 J m^{-2} UV-C followed by 3 days dark incubation and 3 days in long-day conditions. *uvh1-1* is the UV-sensitive control.

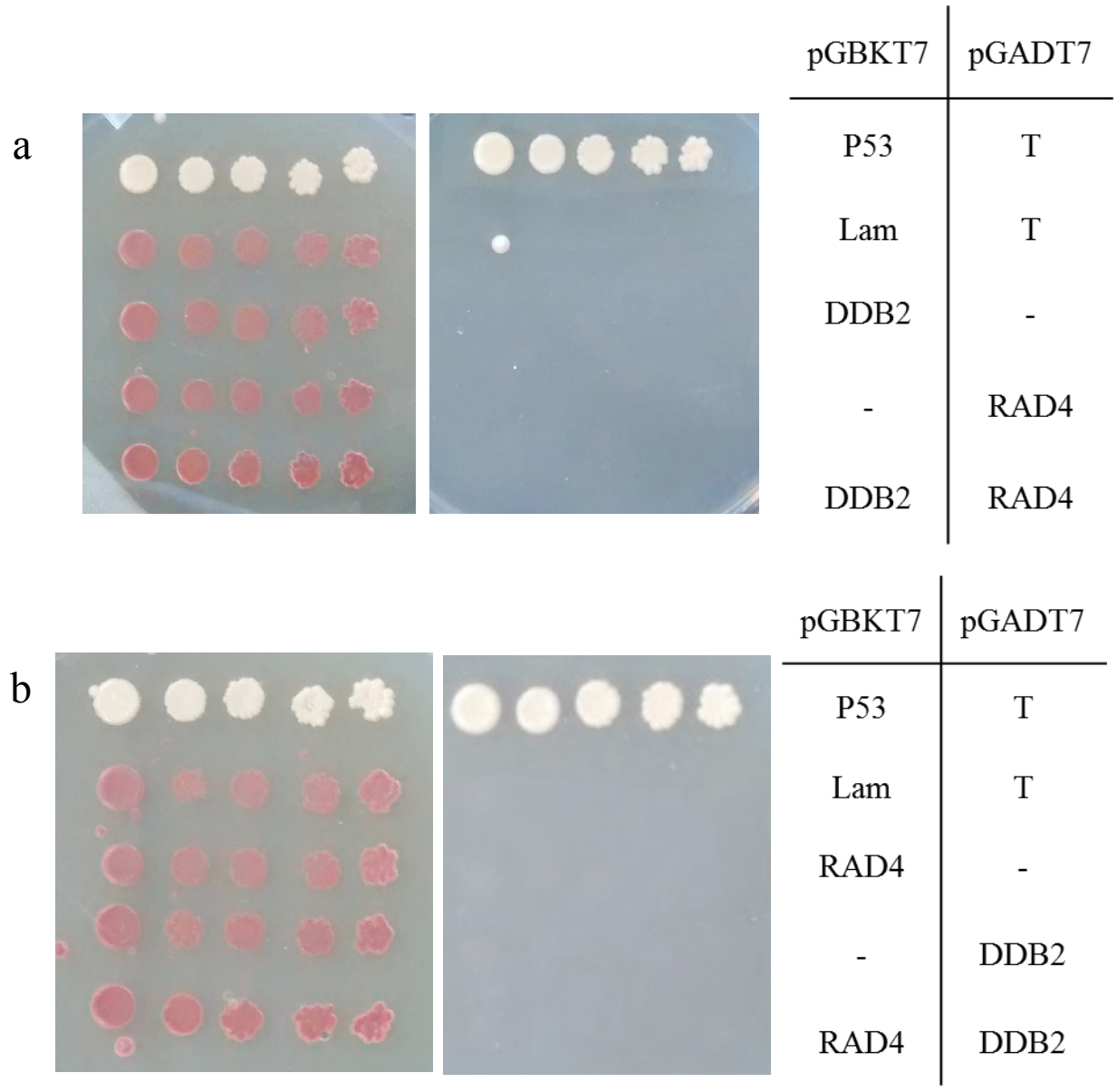

Fig. S2.2 Yeast two hybrid analysis of RAD4 DDB2 interaction

a) No interaction was observed between DDB2 pGBKT7 and RAD4 pGADT7. b) No interaction was observed between RAD4 pGBKT7 and DDB2 pGADT7. Five fold dilutions of the indicated diploid strains were plated on the double drop-out (-leu -trp) control plate on the left, and the quadruple drop-out (-leu –trp –ade -his) selection medium on the right. The interaction between p53 and T, resulting in growth on the selective medium, is the positive control, whereas Lam and T, which do not interact, are the negative control.

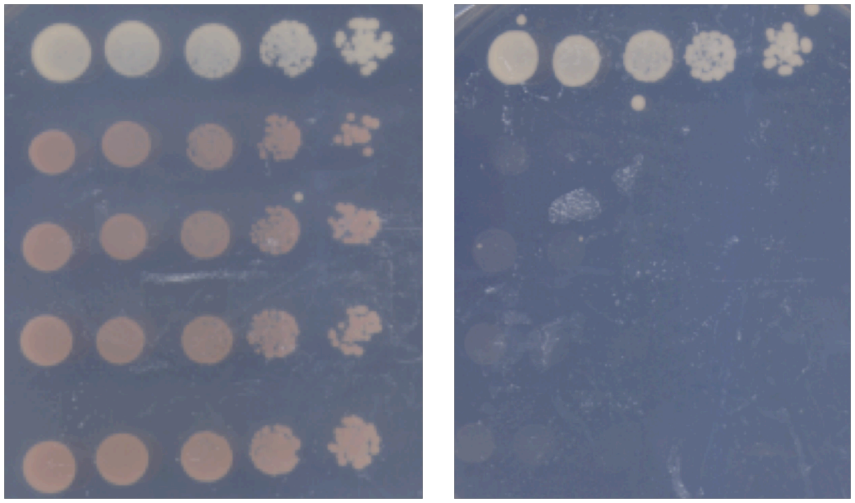

pGBKT7	pGADT7
P53	T
Lam	T
-	RAD4
RAD4	-
RAD4	RAD4

Fig. S2.3 Yeast two hybrid analysis of RAD4 self-interaction

No interaction was observed between RAD4 pGBKT7 and RAD4 pGADT7. Five fold dilutions of the indicated strains were plated on the double drop-out (-leu -trp) control plate on the left, and the quadruple drop-out (-leu -trp –ade -his) selective medium on the right. The interaction between p53 and T, resulting in growth on the selective medium, is the positive control, whereas Lam and T, which do not interact, are the negative control.

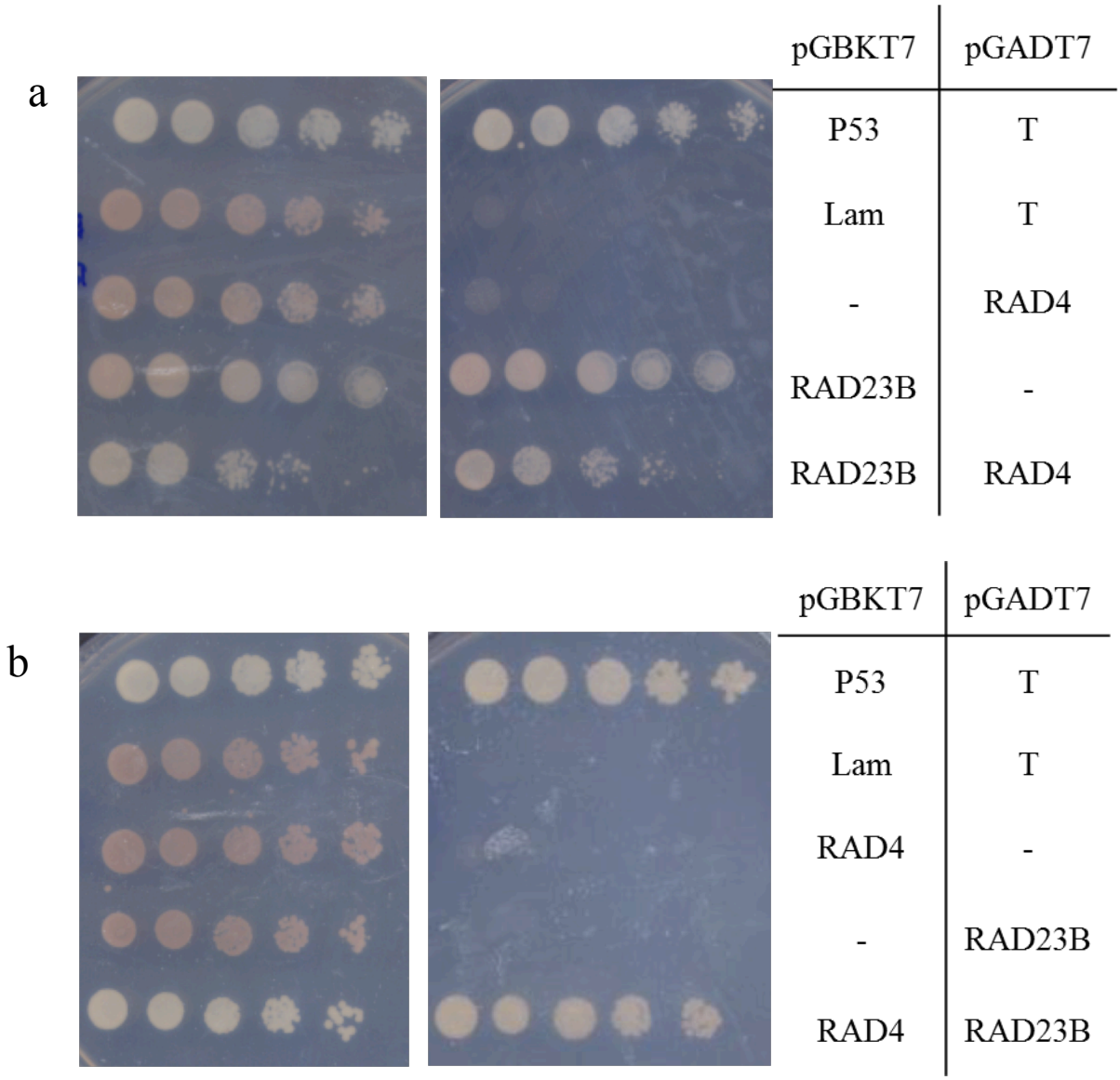

Fig. S2.4 Yeast two hybrid analysis of RAD4 RAD23B interaction

a) RAD23B pGBKT7 exhibited growth on selective medium with both empty pGADT7 and RAD4 pGADT7. b) Interaction was detected between RAD4 pGBKT7 and RAD23B. Five-fold dilutions of the indicated strains were plated on the double drop-out (-leu -trp) control plate on the left, and the quadruple drop-out (-leu-trp-ade-his) selective medium on the right. The interaction between p53 and T, resulting in growth on the selective medium, is the positive control, whereas Lam and T, which do not interact, are the negative control.

Chapter 3 contains the study of Arabidopsis *RAD7* genes. The role of Rad7p in *Saccharomyces cerevisiae* is well studied as a part of the GG-NER recognition complex. The Arabidopsis RAD7s are novel and homologous to yeast Rad7p.

Ch 3. RAD7 homologues contribute to Arabidopsis UV tolerance

Triparna Lahari, Janelle Lazaro, Jeff M. Marcus, and Dana F. Schroeder

Department of Biological Sciences, University of Manitoba, Winnipeg, MB R3T 2N2

To be submitted to Plant Science

Author contributions: Janelle Lazaro analyzed *RAD7c* expression, Jeff Marcus constructed the phylogenetic tree. All other experiments performed by Triparna Lahari.

Note: Results of yeast two hybrid analysis included here will not be included in the manuscript submitted to Plant Science

3. RAD7 homologues contribute to Arabidopsis UV tolerance

3.1. Abstract

Frequent exposure of plants to solar ultraviolet radiation (UV) results in damaged DNA. One mechanism of DNA repair is the multi-step, light independent pathway Global Genomic Nucleotide Excision Repair (GG-NER), which repairs UV-damaged DNA throughout the genome. GG-NER involves damage recognition, excision of the damaged strand, and repair. In mammals, DNA damage recognition is performed by the DAMAGED DNA BINDING protein 1 and 2 (DDB1/2) complex which recruits the XERODERMA PIGMENTOSA group C (XPC) / human RAD23D (HR23D) complex. In the yeast *Saccharomyces cerevisiae,* distinct proteins, RADIATION SENSITIVE 7 and 16 (Rad7p and Rad16p), recognize the damaged DNA strand and then recruit the XPC homologue Rad4p and Rad23p. The remainder of the proteins involved GG-NER are well conserved. DDB1, DDB2, XPC/RAD4, and RAD23 homologues have been described in the model plant *Arabidopsis thaliana*. In this study we characterize three Arabidopsis RAD7 homologues, RAD7a, RAD7b, and RAD7c. Loss of function alleles of each of the three RAD7 homologues were found to result in increased UV sensitivity. In addition RAD7b and RAD7c overexpression lines exhibited increased UV tolerance and YFP-tagged RAD7b and RAD7c localized to the nucleus. Thus RAD7 homologues contribute to UV tolerance in plants as well as in yeast. This is the first time any system has been shown to utilize both DDB1/2 and RAD7/16 during GG-NER damage recognition.

3.2 Introduction

Living organisms are exposed to solar ultraviolet (UV) rays. UV damages DNA, inhibiting replication and transcription, thus repair is essential for cellular viability. Repair of UV damaged DNA is performed by light dependent (light repair / photoreactivation) and light independent (dark repair) pathways. Light independent nucleotide excision repair (NER) is a conserved UV damaged DNA repair pathway present in mammalian, plant, and yeast systems. Global Genomic NER (GG-NER) repairs damaged DNA in untranscribed regions throughout the genome. GG-NER is a multistep process that involves damage recognition, damage verification, excision of the damaged strand, and repair synthesis (Petruseva et al. 2014). In mammals two complexes, one composed of UV damaged DNA binding protein (UV-DDB) 1 and 2, and the other including xeroderma pigmentosa complementation group C (XPC), human RAD23B (hr23B), and centrin 2 (CEN2), are responsible for damage recognition. Damage verification is done by the TFIIH complex including the XPB and XPD helicase subunits. Plants have homologs of DDB1, DDB2, RAD23, CEN2, and XPC (AtRAD4- Radiation Sensitive 4), as well as other GG-NER components (Ganpudi and Schroeder 2011)

In the yeast *Saccharomyces cerevisiae,* the XPC homolog Rad4p participates in damage recognition; however *S. cerevisiae* lacks DDB1 and DDB2 homologues, instead utilizing the distinct Rad7p/Rad16p complex. The Rad7p/Rad16p complex plays a role in UV damaged DNA recognition and Rad4p recruitment, similar to the role played by the DDB1/DDB2 complex in mammals (Gillette et al. 2006). Rad7p and Rad16p form a stoichiometric complex, NEF4 (Nucleotide Excision Repair Factor 4), to recognize the UV damaged DNA site and are GG-NER specific (Guzder et al. 1997). Rad16p has ATPase activity stimulated by DNA or chromatin, which is a signature of the SWI/SNF superfamily. Rad7p is a component of E3 ligase complexes

that ubiquitinate Rad4p. Rad4p, along with Rad23p, forms a complex that binds to damaged DNA sites directly and acts as a core component of NER (Waters et al. 2012). Rad4p forms the NEF2 complex with Rad23p to bind the DNA damage in coordination with NEF4 (Guzder et al. 1999). Rad4p is subject to ubiquitination and a cullin based E3 ubiquitin ligase is required for this process. Elongin C (Elc1p) interacts with the Rad7p/16p complex along with Cullin3 (Cul3p) for Rad4p degradation after recognition of UV damaged DNA (Gilette et al. 2006).

Homologues of all components of *S. cerevisiae* GG-NER exist in plants. For example, *RAD16* has two homologues in Arabidopsis (At1g05120, At1g02670) (Kunz et al. 2005). *Arabidopsis thaliana* has 6 Cullin homologues including CULLIN3a (CUL3a: At1g25830), and CULLIN3b (CUL3b: At1g69670) (Weber et al. 2005). The Arabidopsis Elc1p homologue (At5g59140) is a BTB/POZ domain protein (Risseeuw et al. 2003). In this study, we examine uncharacterized Arabidopsis Rad7p homologues by generating loss of function and overexpression lines followed by analysis of UV sensitivity.

3.3 Materials and methods

3.3.1 Phylogenetic tree construction

KEGG (Kyoto Encyclopedia of Genes and Genomes) (http://www.kegg.jp/) was used to identify the members of the RAD7 orthology group K15082 in *S. cerevisiae, S. pombe, A thaliana,* and rice *(Oryza sativa)*. The top RAD7 orthologue, as well as the top rice and Arabidopsis paralogues of the top orthologue, were used for analysis. Amino acid sequences from RAD7 orthologues were aligned in CLUSTAL Omega (Sievers et al. 2011) using the default amino acid settings and saved in NEXUS file format. The aligned amino acid sequences were then analyzed using the maximum parsimony criterion implemented in PAUP* version

4.0b8/4.0d78 using default settings unless otherwise specified (Swofford 2002). Heuristic searches of the dataset were conducted using the following options: 1 million maximum search replicates with random sequence addition, tree bisection and reconnection branch swapping on only the best trees, multiple trees saved at each step, and retention of all best trees. The bootstrap searches were conducted using the following settings: 1 million random sequence addition fast addition search replicates and retention of all groups consistent with 50% bootstrap consensus. When displaying trees, all nodes with less than 25% bootstrap consensus were collapsed. *S. cerevisiae* Grr1p, the yeast protein most closely related to Rad7p, was used as the outgroup.

3.3.2 Plant material and growth conditions

Columbia-0 (Col-0) was the *Arabidopsis thaliana* wildtype ecotype background for all SALK alleles (Alonso et al. 2003) and overexpression lines. Wassilevskija-4 (Ws-4) was the wildtype background for the *rad7c-3* FLAG allele (Brunaud et al. 2002; Samson et al. 2002). The T-DNA alleles *rad7a-1* (SALK_095626), *rad7a-2* (SALK_051730), *rad7a-3* (SALK_107725), *rad7b-2* (SALK_041396), *rad7c-1* (SALK_025534), and *rad7c-3* (FLAG_400G01) were obtained from the Arabidopsis Biological Resource Center (ABRC) Columbus, OH, USA and the Versailles Arabidopsis Stock Centre, Versailles, France. Plants were genotyped with respective gene and allele specific primers and standard T-DNA primers LBb1.3 (Salk lines) (ATTTTGCCGATTTCGGAAC) and Tag5 (FLAG line) (CTACAAATTGCCTTTTCTTATCGAC) (Table S3.1).

Seeds were sterilized (10 min in 70% ethanol, 0.5% Triton X-100 followed by 10 min in 95% ethanol) and plated on Linsmaier and Skoog (LS) medium (Caisson, Smithfiled, UT, USA) containing 0.6% sucrose and 0.86% phytoblend (Caisson) followed by cold stratification at 4^0C for 2 days. Plates were transferred to an incubator at 20^0C, 50% relative humidity, and long day

conditions (16 h light / 8 h dark) for 14 days for seedling growth. Fourteen-day-old seedlings were transplanted to soil (Sunshine mix no. 1, SunGro, Bellevue, WA, USA) and grown at 20 °C and 50% relative humidity in long day conditions provided by fluorescent bulbs (100 μM photons m^{-2} s^{-1}).

3.3.3 RNA extraction and RT-PCR

Plants were grown on LS plates in long day conditions for 7 days. RNA was extracted from 50 seedlings / genotype using the RNeasy plant mini kit (Qiagen, Hilden, Germany) according to the manufacturer's protocol including a DNase treatment. RNA was quantified using a spectrophotometer and 1 μg used to synthesize cDNA with the Maxima First Strand cDNA synthesis kit (Fermentas, Waltham, MA, USA). For semi-quantitative RT-PCR, RNA level was checked with cDNA specific primers after 28 cycles (*RAD7a* and *RAD7b*) or 35 cycles (*RAD7c*) using the primers listed in Table S3.1. *Actin* was used as the loading control and amplified for 22 cycles. For real time PCR, cDNA was diluted 40 fold and qPCR performed using SsoFast EvaGreen Supermix (Bio-Rad, Hercules, CA, USA). An CFX Connect Real time PCR detection system (Bio-Rad), was used for analysis. The sample loading were normalized relative to *EF1α* control (At5g60390) (Table S3.1) (Hossain et al. 2012; Jain et al. 2006). Three technical replicates were analyzed per sample and mean values calculated. For *RAD7c* UV induction, seedlings were irradiated with 1000 J m^{-2} UV-C followed by 0, 6, or 24 h dark incubation.

3.3.4 Generation of overexpression constructs

The *RAD7b* cDNA (G67755) and *RAD7c* cDNA (G68392) Salk Gateway clones in the pENTR223 vector were ordered from the ABRC. Both cDNAs were cloned into pEarleyGate100

(CaMV 35S promoter) and pEarleyGate104 (CaMV 35S promoter plus N-terminal YFP tag) destination vectors using Gateway technology (Earley et al. 2006). The pEarleyGate vectors were also obtained from the ABRC. The constructs were then transformed into Col-0 wild type and the respective loss of function mutants by agrobacterium mediated transformation (Weigel and Glazebrook 2002). T1 plants were selected with BASTA selection (1:2000 dilution sprayed on 10 day old plants). Homozygous T3 lines were used for experiments.

3.3.5 Developmental parameter measurement and analysis

Seedlings were germinated and grown on LS medium for 2 weeks in long day conditions in an incubator followed by transplantion to soil. Flowering time was determined with respect to days, when the bud became visible, as well as total number of rosette and cauline leaves. Rosette diameter was measured at 4 weeks of age. Plant height, silique length, and number of shoots (apical dominance) were determined at 6 weeks of age.

3.3.6 UV sensitivity assays

In the seedling assay, seeds were sterilized and plated on LS medium containing 0.6% sucrose and 0.86% phytoblend with appropriate controls (Col-0 or Ws-4). Seeds were stratified at 4^0C for 2 days, then grown vertically at 20^0C in long day conditions for 3 days. The three-day-old seedlings were exposed to 1000 J m^{-2} UV-C (shortwave UV lamp XX-15S, UVP/LLC, Upland, CA, USA) followed by wrapping in aluminium foil to avoid photoreactivation. The plates were rotated by 90^o after UV treatment and scanned after 3 days using a Perfection 1260 scanner (Epson, Suwa, Japan). Hypocotyl and new root growth was measured for the indicated number of seedlings (n) with Image J software.

In the light vs dark UV sensitivity assay, the seeds were grown in the same conditions as above. Three-day-old seedlings were again exposed to 1000 J m^{-2} UV-C followed by 90^0 rotation. The plates were then incubated in long day or dark conditions respectively for 2 days, then scanned. Roots were measured with Image J software.

In the adult UV sensitivity assay, seedlings were grown in the above conditions on LS medium and transplanted to soil at 14 days of age. The 21-day-old plants were exposed to 0, 600, or 1000 J m^{-2} of UV-C, followed by 3 days of growth in dark conditions, then returned to long day conditions. After 2–3 days of growth in long day conditions, individual leaves were scored as either undamaged (green) or damaged (yellow or brown), and data were expressed as percentage of undamaged leaves (green leaves/total leaves) for six plants per genotype per treatment. In adult UV sensitive assays, *uvh1-1,* a point mutant in the Arabidopsis XPF endonuclease homologue, used as the positive control (Harlow et al. 1994).

3.3.7 Protein localization

The YFP-tagged T3 overexpression lines and controls were grown for 3 days in the dark. Slides were prepared with 2-3 seedlings in distilled water and observed under a Zeiss AXIO Imager Z1 Microscope (Zeiss, Oberkochen, Germany) equipped with AxioVision 4.8 software using YFP (Filter Set YFP-2427B-000, Semrock Inc.,Rochester, NY, USA) and DAPI (Zeiss Filter Set 02 (488002-9901-000)) filters. The protein localization was confirmed with DAPI (Sigma-Aldrich,Canada, Oakville, ON, Canada) staining (Kapuscinski 1995). A stock solution was prepared with 1 mg DAPI/ml dH_2O. The stock solution is diluted to a final concentration of 10 μg/ml working solution in 10 ml of water with 1% Triton. Seedlings were soaked in the diluted DAPI solution for 10-30 minutes. For UV treatments, seedlings were exposed to 1000 J m^{-2} UV-C followed by observation at various time points.

3.3.8 Yeast two hybrid analysis

Protein interactions were analyzed using the Matchmaker gold yeast two hybrid system (Clontech, Mountian View, CA, USA). *RAD7b, RAD7c, ELC1* (ABRC clone G10376), and *RAD4* (ABRC clone G16664) cDNAs were cloned into pGBKT7 and pGADT7 vectors via standard cloning or Gateway technology. Diploid yeast strains were plated via a series of five-fold dilutions on both double drop-out (-trp -leu) control and quadruple drop-out (-ade –his –leu -trp) selection medium along with the positive p53/T (murine p53/ SV40 large T-antigen) and negative Lam/T (Lamin/ SV40 large T-antigen) control. Protein interaction resulted in the expression of *ADE2* and *HIS3* reporters and growth on the selective medium.

3.3.9 Statistical analysis

A two-tailed student's t-test was performed to compare the mutant or overexpression line with the relevant wild type. Values of $p \leq 0.05$ was considered to be statistically significant. Each experiment was repeated at least twice, and representative data are shown.

3.4 Results

We are interested in plant GG-NER, including the GG-NER specific protein AtRAD4/XPC. We used the Arabidopsis Interactions Viewer (AIV) (http://bar.utoronto.ca/interactions/cgi-bin/arabidopsis_interactions_viewer.cgi) to identify potential interaction partners of AtRAD4. Among other data sources, the AIV predicts interaction of proteins based on interaction in homologous systems (Geisler-Lee et al. 2007). AIV results included the expected high interlog confidence interaction of AtRAD4 with

RAD23D (At5g38470) and RAD23A (At1g16190) (Table S3.2). The AIV also predicted medium interlog confidence interaction with XPB2 (At5g41360), RAD23C (At3g02540), XPB1 (At5g41370), and CENTRIN2 (At3g47010). Interestingly, two novel RNI (RiboNuclease Inhibitor) - like superfamily proteins derived from At2g06040 and At4g15475 were also predicted to interact with AtRAD4 with high and medium interlog confidence values. The AIV indicated that *S. cerevisiae* homologs existed for these genes, and WU-BLAST2 analysis revealed that the proteins derived from At2g06040 and At4g15475 are the closest Arabidopsis homologues of *Saccharomyces cerevisiae* Rad7p (Table S3.3). Thus we refer to these as *AtRAD7a* (At2g06040) and *AtRAD7b* (At4g15475). The AIV also predicted high to medium confidence interactions between AtRAD7a and AtRAD7b and Arabidopsis RAD16 and ELC1 homologues. Another uncharacterized RNI-like superfamily protein derived from At5g21900 was found to be the closest protein match to AtRAD7a (At2g06040); thus we refer to it as AtRAD7c. The Genemania prediction server (Warde-Farley et al. 2010) predicts interaction of the related proteins RAD7a and RAD7c with AtRAD4, RAD16, and ELC1. The model organism orthology database P-POD: Princeton Protein Orthology Database (Heinicke et al. 2007) groups Arabidopsis RAD7a, RAD7b, and RAD7c with ScRAD7 in several phylogenic trees. Our own phylogenic analysis groups RAD7a and RAD7c with *S. cerevisiae* Rad7p and *S. pombe* Rad7p homologue rhp7 (Fig. S3.1), while RAD7b clusters with several related Arabidopsis F-box/Leucine Rich Repeat (LRR) proteins including EBF1/2 (Guo and Ecker 2003), SKP2A/B (del Pozo et al. 2006) and SLOMO (Lohmann et al. 2010). Homologues of Arabidopsis RAD7a,b,c exist thoroughout the plant kingdom, for example, as shown here, in rice (Fig. S3.1). The RAD7a/c duplication seems to be specific to the Brassicaceae, since clear RAD7a and RAD7c homologues exist in *Arabidopsis lyrata* and *Brassica rapa,* but not in other plants (EggNOG) (Huerta-Cepas et al. 2015). Arabidopsis RAD7a,b,c and ScRad7p contain multiple

LRR motifs and AMN1 domains (Marchler-Bauer et al. 2014) (Fig. S3.2). RAD7b also contains an F box and was previously identified as FBL4 (Xiao and Jang 2000). AtGenExpress data (Schmid et al. 2005) reveal that *RAD7b* is expressed throughout development (Fig. S3.3). *RAD7a* is expressed at lower levels than *RAD7b*, but is upregulated in pollen. *RAD7c* is unfortunately not on the Arabidopsis array.

In order to study the role of the three Arabidopsis RAD7 homologues in UV tolerance, we identified loss of function alleles in public collections (Fig. 3.1a). The T-DNA insertions for *rad7a-2* and *rad7a-3* are in the sixth and third exon respectively, while *rad7a-1* is in the fourth intron. All three *rad7a* alleles are complete RNA nulls (Fig. 3.1b). The T-DNA insertion for *rad7b-2* is in the second exon, and is also an RNA null (Fig. 3.1c). For *RAD7c,* the T-DNA insertion in *rad7c-1* is in the promoter region while *rad7c-3* (in the Ws-4 background) is in the third exon. *rad7c-3* is also an RNA null (Fig. 3.1d). *RAD7c* RNA level was found to increase by 17 fold 24 h afer UV treatment, while induction did not occur to the same extent in the *rad7c-1* allele, suggesting that T-DNA insertion in this allele interferes with UV regulation of *RAD7c* expression (Fig. 3.1e).

The *rad7* loss of function mutants were examined for adult developmental phenotypes, such as flowering time in days and leaves, rosette diameter, height, silique length, and apical dominance (Fig. S3.4, S3.5). No significant differences from wildtype phenotypes were observed except for early flowering time in days in *rad7c-3*.

UV sensitivity assays were performed on *RAD7* loss of function seedlings. *rad7a-1, rad7a-2,* and *rad7a-3* all exhibited significantly increased UV sensitivity in roots and hypocotyls relative to wild type Col-0 (Fig. 3.2a). The effect of variable UV dose on representative allele *rad7a-3* was also examined. Hypocotyl growth in *rad7a-3* was reduced relative to wild type at all three doses of UV (Fig. 3.2b). Root growth was significantly reduced at 1000 and 1500 J m^{-2}

only (Fig. 3.2c). Thus the *rad7a* mutants exhibit increased UV sensitivity in both hypocotyls and roots.

We also performed variable dose UV assays on *rad7b* and *rad7c*. For *rad7b-2*, hypocotyl growth was significantly reduced only at the intermediate dose (1000 J m^{-2}) (Fig. 3.3a), while root growth was reduced relative to wild type at both the low (500 J) and intermediate (1000 J m^{-2}) doses of UV (Fig. 3.3b). In *rad7c-1,* hypocotyl growth was reduced at all three UV doses (Fig. 3.4a), while root growth was reduced at intermediate and high UV doses (Fig. 3.4b). The *rad7c* null allele *rad7c-3* also showed significantly reduced hypocotyl and root growth compared to wild type Ws-4 following 1000 J m^{-2} UV treatment (Fig. 3.4c). Thus the *rad7b* and *rad7c* mutant seedlings are also sensitive to UV damage.

In order to determine if the UV sensivity in the *rad7* mutants was specific to dark repair, consistent with a role in nucleotide excision repair, we performed UV treatments followed by either light or dark incubation. For all three genes root UV sensitivity was specific to dark conditions (Fig. 3.5).

We also examined UV sensitivity in adult plants (Fig. 3.6). Three week old wildtype Col-0 showed increased damage with increased UV dose. The UV sensitive control *uvh1-1*, a point mutant in the Arabidopsis XPF endonuclease homologue (Harlow et al. 1994), showed complete damage, i.e. death, following either UV treatment. *rad7a-1* and *rad7a-2* showed increased leaf damage compared to wildtype Col-0 at intermediate (300 J m^{-2}) and high (600 J m^{-2}) doses of UV while *rad7a-3* showed increased damage at the high dose of UV only. *rad7b-2* mutants showed increased damage at the intermediate dose only. Thus, the *rad7a* and *rad7b* adults are also sensitive to UV. In contrast, *rad7c-3* adults did not show significantly increased leaf damage compared to Ws-4 (Fig. S3.6).

Next, to verify that the loss of function phenotypes we observed were due to defects in the *RAD7* genes, we performed rescue experiments. cDNA clones of *RAD7b* and *RAD7c* in Gateway entry vectors were obtained from the ABRC and cloned into the pEarleygate vectors pEG100 (CaMV 35S promoter) and pEG104 (CaMV 35S promoter and N-terminal YFP tag) (Earley et al. 2006). These constructs were then transformed into their respective mutant backgrounds. Overexpression of the tagless cDNAs via the pEG100 vector rescued both the *rad7b* and *rad7c* loss of function phenotypes in the both root and hypocotyl (Fig. S3.7a,b). Thus the *rad7b-2* and *rad7c-3* mutants were rescued by their respective cDNAs, indicating that the UV sensitivity we observe is due to defects in these genes. Overexpression of the YFP-tagged pEG104 versions of the cDNAs in their respective mutants resulted in partial rescue of *rad7b-2* and near complete rescue of *rad7c-3* (Fig. S3.7c,d).

To examine overexpression phenotypes of *RAD7b* and *RAD7c* we overexpressed the tagless and YFP-tagged cDNAs in the Col-0 wildtype background. Tagless and YFP-tagged RAD7b and RAD7c overexpression lines showed significantly increased UV tolerance in hypocotyl, root, and adults relative to wild type, and this tolerance was dark specific (Fig. 3.7-3.10). Thus RAD7b and RAD7c overexpression is sufficient to increase UV tolerance. Increased UV tolerance with and without the YFP epitope tag indicates that the YFP tag did not appear to interfere with RAD7b and RAD7c function.

We then used these YFP-tagged lines to examine the cellular localization of RAD7b and RAD7c. We found that both YFP-RAD7b and YFP-RAD7c exhibited nuclear localization (Fig. 3.11, 3.12). Closer inspection showed that YFP-RAD7b exhibited a punctate speckled pattern within the nucleus, while YFP-RAD7c was diffusely localized throughout the nucleus. These patterns did not obviously change following UV treatment.

The AIV predicted interaction between RAD4 and the RAD7 homologues, so we tested for interaction using yeast two hybrid assays. However, we did not detect interaction between RAD4 and RAD7b (Fig. S3.8) or RAD4 and RAD7c (Fig. S3.9a) in this assay. Interestingly, RAD7c fused to the GAL4 DNA binding domain was able to activate transcription alone, resulting in growth on selective media (Fig. S3.9b), suggesting that RAD7c possesses a transcriptional activation domain. We also did not detect interaction between RAD7b and itself (Fig. S3.10a), or RAD7b and RAD7c (Fig. S3.10b). Finally, we did not detect interaction between RAD7b or RAD7c and RAD7/16 complex component ELC1 (Fig. S3.11).

3.5 Discussion

In this study we identified three Arabidopsis homologues of *S. cerevisiae* RAD7 and determined their roles in plants by examining loss of function alleles. The only developmental phenotype observed in the loss of function lines was slightly reduced flowering time in *rad7c-3*. Thus the RAD7 homologues do not appear to play significant non-redundant roles in development, but may have redundant functions. In *S. cerevisiae rad7* mutants are viable but exhibit a very strong defect in vacuolar fragmentation (Michaillat and Mayer 2013). In *S. pombe,* RAD7 homologue (*rhp7*) mutants are also viable but exhibit a slow vegetative cell growth phenotype (Sideri et al. 2015).

Our phylogenic analysis indicates that while Arabidopsis RAD7a and RAD7c are closely related to the rice, *S. cerevisiae* and *S. pombe* RAD7 homologues, RAD7b clusters with other F-box/LRR proteins. F-boxes facilitate interaction with SKP1/ASK1; thus F-box proteins are components of SCF-cullin1-type E3 ubiquitin ligase complexes (Xiao and Jang 2000). Members of this clade include EBF1 and EBF2, negative regulators of ethylene signalling that target EIN3

and related transcription factors for degradation (Guo and Ecker 2003), and have recently been shown to also degrade light signalling factor PIF3 (Dong et al. 2017). SKP2A degrades cell cycle regulator DPB (del Pozo et al. 2006), a process that is enhanced by direct auxin binding (Jurado et al. 2010), while SKP2B degrades cyclin-dependent kinase inhibitor KRP1 (Ren et al. 2008) and represses lateral root formation (Manzano et al. 2012). SLOMO is required for correct timing of aerial organ initiation, but its direct degradation targets are not known (Lohmann et al. 2010). Other global genomic repair factors are also E3 ubiquitin ligases. DDB1/2 are components of a CUL4-type complex (Groisman et al. 2003) while yeast Rad7p/Rad16p forms a CUL3-type complex (Gilette at al 2006). It will be interesting to determine if the Arabidopsis RAD7 proteins form E3 ubiquitin ligase complexes and if so, what type. It will also be interesting to determine if EBF1/2, SKP2A/B, or SLOMO play roles in UV tolerance.

In the *rad7a* mutants, *rad7a-3* would be expected to generate the shortest truncated protein, therefore generating the strongest allele, followed by *rad7a-1* and *rad7a-2*. In seedling UV sensitivity assays, all three alleles exhibited UV sensitivity in both roots and hypocotyls. Similar sensitivity was observed in all three alleles in roots, while in hypocotyls *rad7a-1* was slightly but significantly more sensitive than *rad7a-3*. In adults, *rad7a-1* was again the most sensitive, followed by *rad7a-2* and *rad7a-3*. Thus in both seedlings and adults *rad7a-3* is surprisingly the weakest of the *rad7a* alleles, while *rad7a-1* is the strongest.

With respect to *RAD7c* alleles, *rad7c-3* is a RNA null allele while *rad7c-1* exhibits normal levels of *RAD7c* in control conditions. Nonetheless both alleles exhibit increased UV sensitivity in seedlings. *RAD7c* is induced by UV treatment in wildtype but not to the same extent in *rad7c-1*, thus this lack of induction appears to result in UV sensitivity.

UV sensitivity in the *rad7a, rad7b,* and *rad7c* mutants is all specific to dark conditions, suggesting that these genes contribute to GG-NER dark repair rather than photolyase-based light

repair of DNA damage. *Saccharomyces cerevisiae rad7* mutants exhibit UV sensitivity and Rad7p is required for GG-NER (Cox and Parry 1968; Verhage et al. 1994). The *S. pombe* RAD7 homologue also contributes to NER (Lombaerts et al. 1999).

We examined RAD7b and RAD7c cellular localization using YFP-tagged proteins and found that both proteins localized to the nucleus. The Arabidopsis SubCellular Proteomic Database (SUBA3) (Tanz et al. 2013) predicts nuclear, plastid, mitochrondrial, and extracellular localization for both proteins; however consensus algorithm SUBAcon (Hooper et al. 2014) predicts nuclear localization for both RAD7b (score .787) and RAD7c (score .999). In contrast the PSI (Plant Subcellular localization integrative predictor) consensus algorithm (Liu et al. 2013) predicts both nuclear (score 0.457) and cytoplasmic localization (score 0.411) for RAD7b and nuclear localization for RAD7c (score 0.850). Within the nucleus, RAD7b localized both diffusely and to speckles, while RAD7c was diffusely localized. These patterns do not agree with those predicted by the Sub-nuclear Compartments Prediction System (Version 2.0) (Lei and Dai 2005), which predicts nuclear lamina localization for both proteins. We did not observe a detectable effect of UV treatment on RAD7b and RAD7c localization.

GFP-tagged *S. cerevisiae* Rad7p exhibits nuclear localization and this pattern does not change following treatment with the DNA damaging agents hydroxyurea and methyl methanesulfonate (Tkach et al. 2012). *S. pombe* RAD7 homologue rhp7 localizes to the nucleus and mitotic spindle pole body (Matsuyama et al. 2006).

Many Arabidopsis proteins have been found to exhibit specific subnuclear localization patterns, such as the phytochrome photoreceptors (Van Buskirk et al. 2012). In addition, DNA repair in mammals has been linked to specific subnuclear patterns (Dellaire and Bazett-Jones 2007).

We used yeast two hybrid analysis to investigate the interaction of RAD7b and RAD7c with RAD4 and ELC1 but could not detect any interaction in this assay. In *S. cerevisiae*, Rad7p interacts with Rad4p in yeast two hybrid assays (Wang et al. 1997). *S. cerevisiae* Rad7p has also been shown to interact with Elongin C; however this interaction was detected via immunoprecipitation, not via yeast two hybrid analysis (Gillette et al. 2006). In *S. pombe*, the RAD7 homologue, *Rhp7*, and the RAD4 homologue, *Rhp42*, exhibit genetic interaction, but physical interaction has not been explored (Marti et al. 2003). Interaction between Rhp7 and the *S. pombe* elongin C homologue has not been reported.

In mammals, damage recognition in GG-NER is performed by the DDB1/2 complex (Sugasawa et al. 2005). In yeast, this step is performed by the Rad7p/16p complex (Guzder et al. 1997). In Arabidopsis, DDB1a, DDB1b, and DDB2 have been shown to participate in UV tolerance (Al Khateeb and Schroeder 2009; Biedermann and Hellmann 2010; Ganpudi and Schroeder 2013; Koga et al. 2006; Molinier et al. 2008). Here we show that RAD7 homologues are also involved in Arabidopsis UV tolerance. This is the first time RAD7s have been shown to function in a multicellular organism and the first time any system has been found to utilize both DDB1/2 and RAD7/16. This work expands our concept of plant NER from a purely mammalian model to one which draws on the strengths of a number of systems to protect its genome from relentless exposure to solar UV.

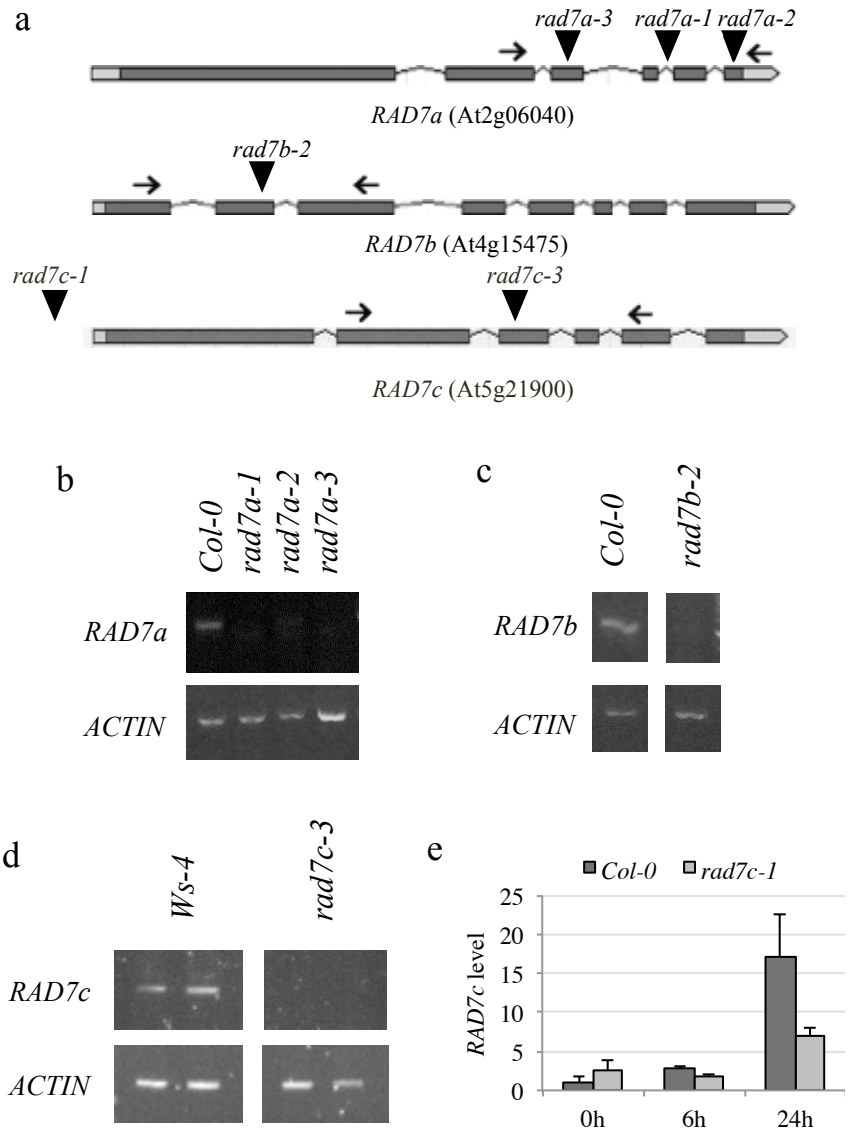

Fig. 3.1 Loss of function alleles of RAD7 homologues

a) Schematic diagram of *RAD7a* (At4g06040), *RAD7b* (At4g15475), and *RAD7c* (At5g21900) genes. Boxes indicate exons and lines indicate introns. T-DNA insertion alleles *rad7a-1* (SALK_095626), *rad7a-2* (SALK_051730), *rad7a-3* (SALK_107725), *rad7b-2* (SALK_041396), *rad7c-1* (SALK_025534), and *rad7c-3* (FLAG_400G01) are shown. Arrows indicate primers used in semi-quantitaive RT-PCR analysis below. b) Semi-quantitative RT-PCR of *RAD7a* and *Actin* control in wildtype Col-0 and *rad7a* loss of function alleles. c) Semi-quantitative RT-PCR of *RAD7b* and *Actin* control in wildtype Col-0 and *rad7b-2*. d) Semi-quantitative RT-PCR of *RAD7c* and *Actin* control in wildtype Ws-4 and *rad7c-3* loss of function allele. e) UV induction of *RAD7c* in wild type Col-0 and *rad7c-1*. *RAD7c* level after 1000 J m^{-2} UV-C treatment was normalized versus *EF1α* and expressed as relative to the Col-0 control. Error bars indicate SE of three technical replicates.

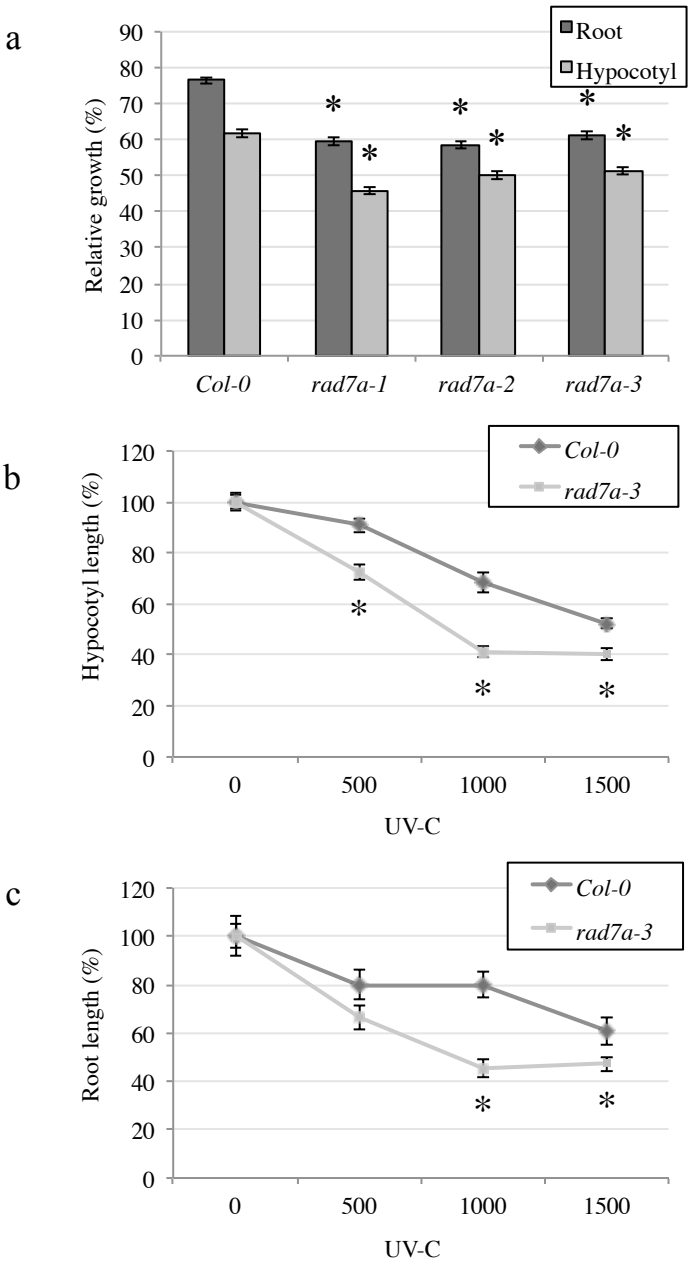

Fig. 3.2 *rad7a* mutant seedlings exhibit increased UV sensitivity

a) Relative root and hypocotyl lengths after exposure to 1000 J m^{-2} UV-C irradiation followed by three days of dark incubation. b) Relative hypocotyl length after exposure to 500, 1000, or 1500 J m^{-2} UV-C irradiation followed by three days of dark incubation. c) Relative root length after exposure to 500, 1000, or 1500 J m^{-2} UV-C irradiation followed by three days of dark incubation. Data is expressed as length relative to unirradiated control of the same genotype. Values are means ± SE (n=10), * = $p \leq 0.05$.

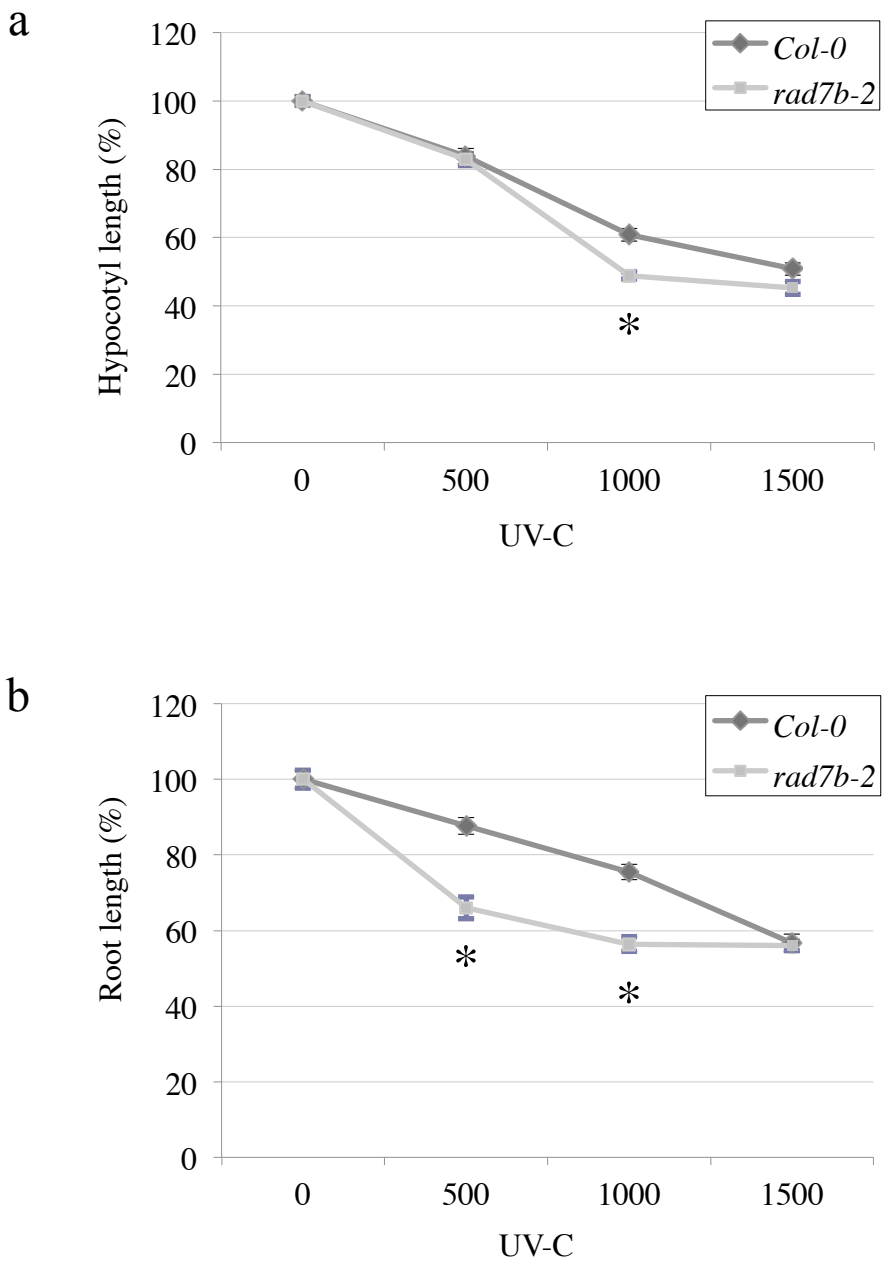

Fig. 3.3 *rad7b* mutant seedlings exhibit increased UV sensitivity.

a) Relative hypocotyl length after exposure to 500, 1000, or 1500 J m^{-2} UV-C irradiation followed by three days of dark incubation. b) Relative root length after exposure to 500, 1000, or 1500 J m^{-2} UV-C irradiation followed by three days of dark incubation. Data is expressed as length relative to unirradiated control of the same genotype. Values are means ± SE (n=10), * = $p \leq 0.05$ of mutants vs wild type.

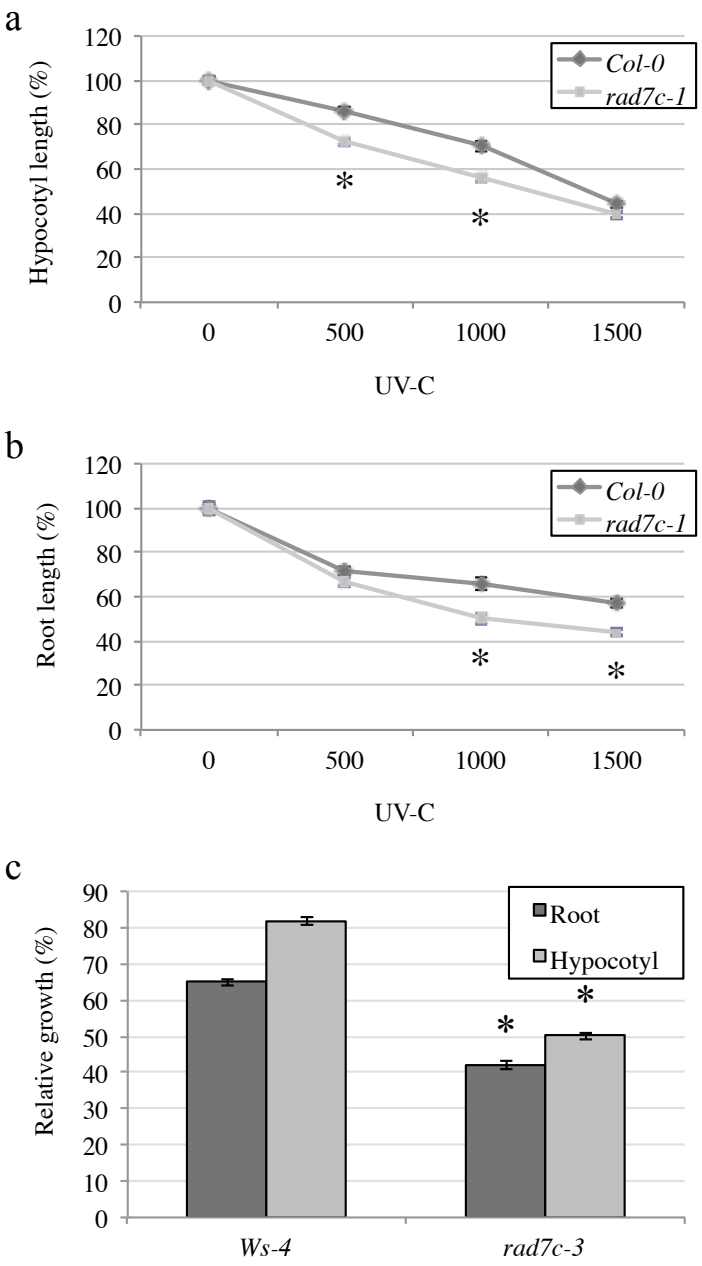

Fig. 3.4 *rad7c* mutant seedlings exhibit increased UV sensitivity.

a) *rad7c-1* relative hypocotyl length in after exposure to 500, 1000, or 1500 J m^{-2} UV-C irradiation followed by three days of dark incubation. b) Relative root length after exposure to 500, 1000, or 1500 J m^{-2} UV-C irradiation followed by three days of dark incubation. Data is expressed as length relative to unirradiated control of the same genotype. c) Relative root and hypocotyl growth of *rad7c-3* allele after 1000 J m^{-2} UV exposure. Values are means ± SE (n=10), * = $p \leq 0.05$ of mutants vs wild type.

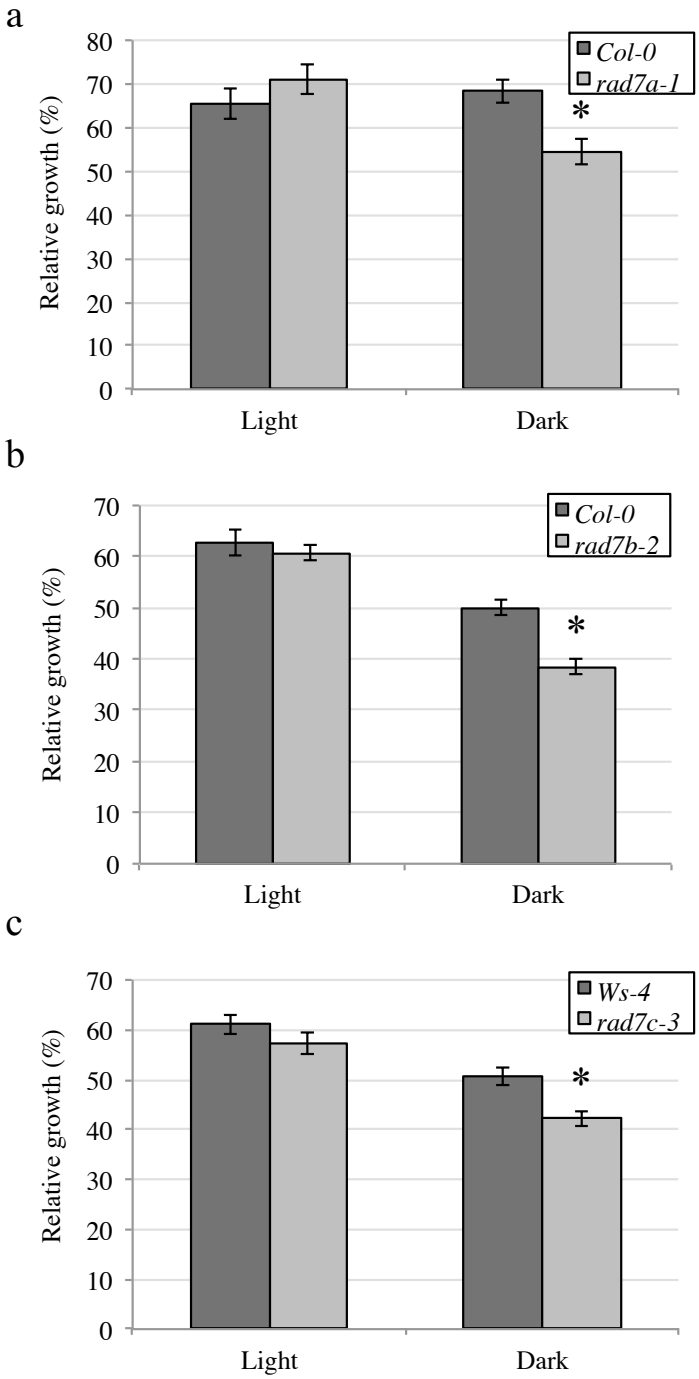

Fig. 3.5 *rad7* mutant seedlings exhibit dark specific UV sensitivity

Relative root length of *rad7a* (a), *rad7b* (b), and *rad7c* (c) after exposure to 1000 J m^{-2} UV-C irradiation followed by two days of light or dark incubation. Data is expressed as length relative to unirradiated control of the same genotype. Values are means ± SE (n=10), * = $p \leq 0.05$ of mutants vs wild type.

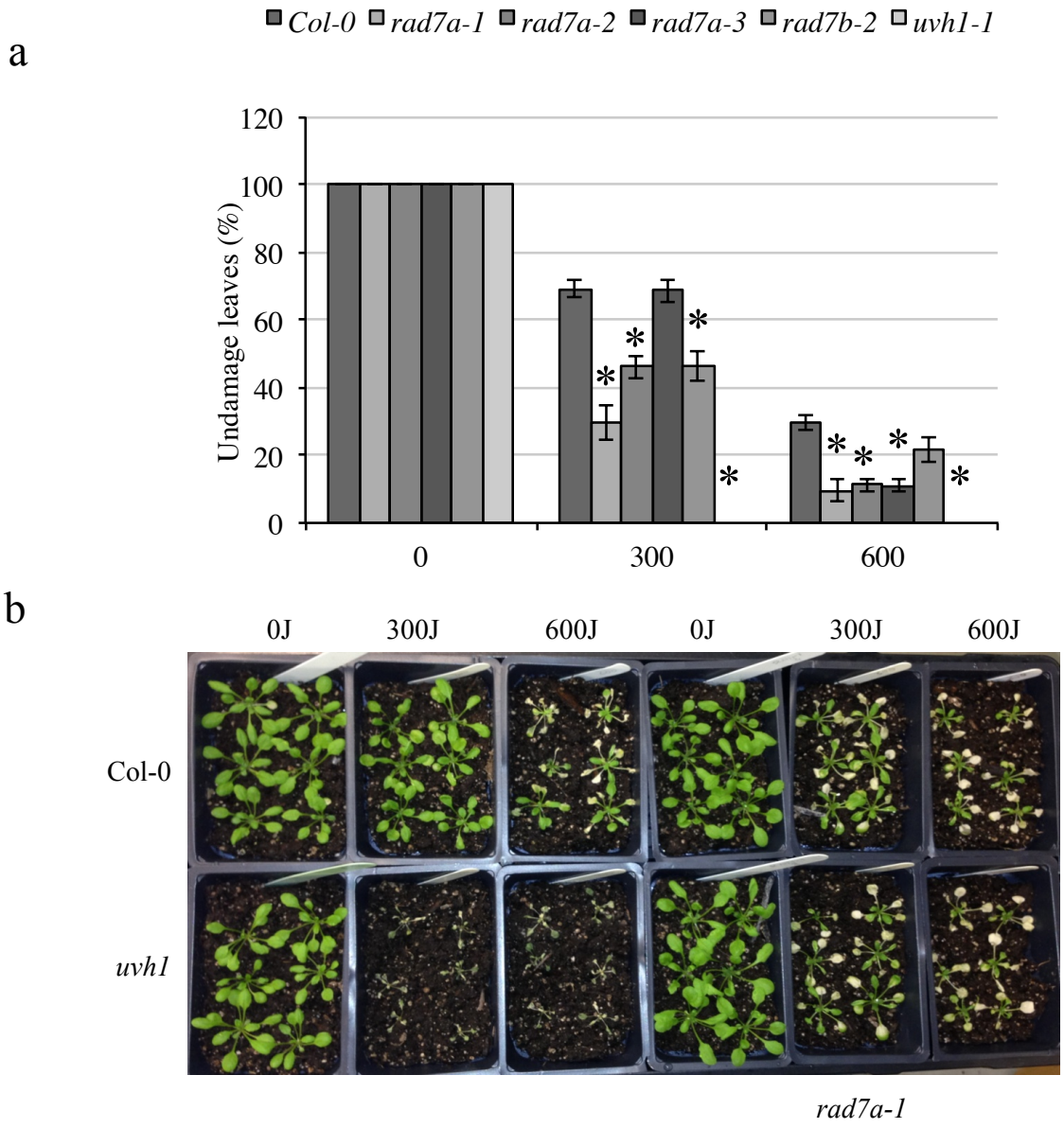

Fig. 3.6 *rad7a* and *rad7b* adults exhibit increased UV sensitivity

a) Percentage undamaged leaves after exposure to 0, 300, or 600 J m^{-2} UV-C irradiation followed by three days of dark incubation and 3 days in long day conditions. Values are means ± SE (n=6), * = $p \leq 0.05$ of mutants vs wild type. b) Representative image of the adult UV-sensitivity assay above, including positive and negative controls Col-0 and *uvh1-1* and *rad7a-1*. UV dose in J m^{-2} is indicated at the top.

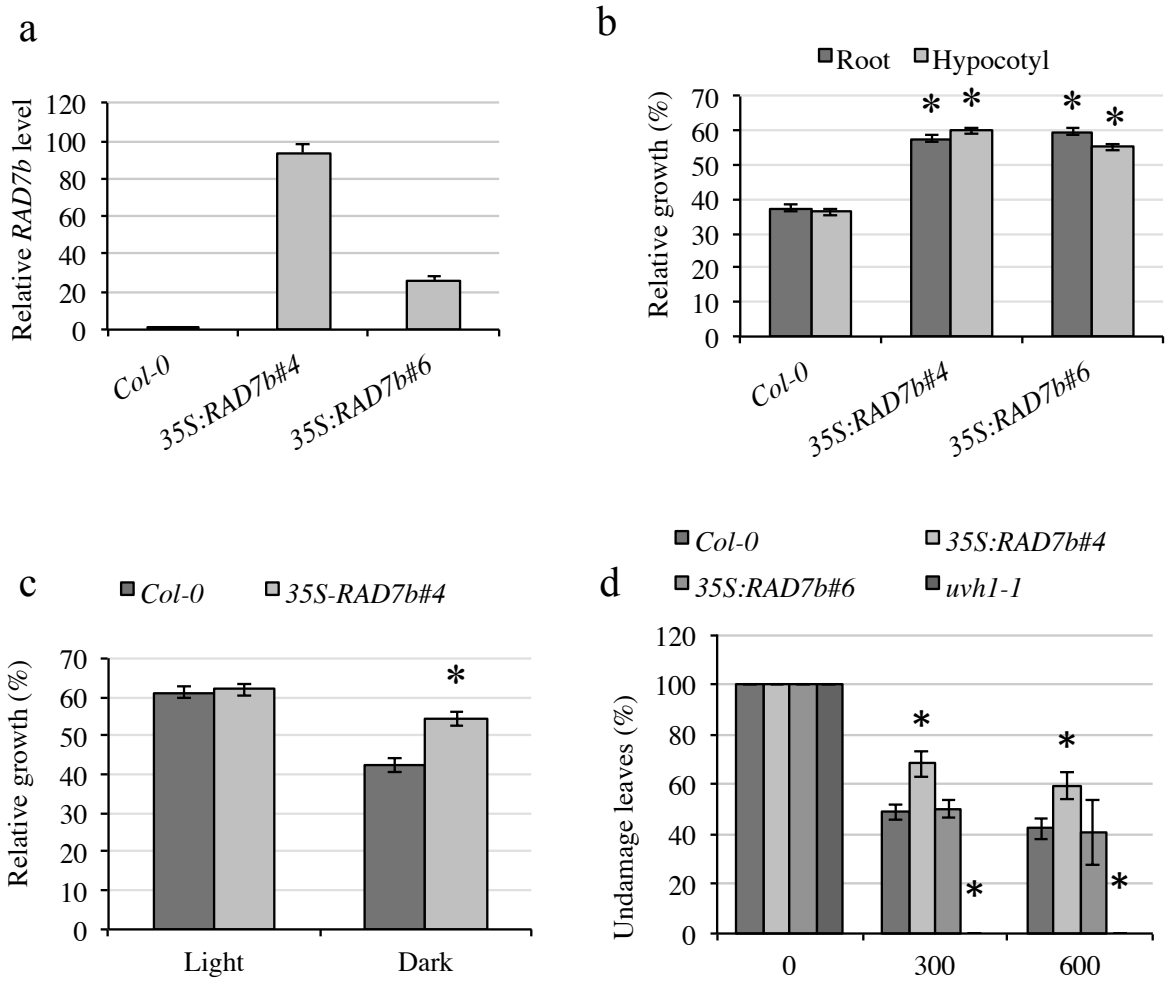

Fig. 3.7 RAD7b overexpression results in increased UV tolerance

a) *RAD7b* level in 35S:RAD7b overexpression line relative to control Col-0. Values are normalized relative to the reference gene *EF1α*. Error bars indicate SE of 3 technical replicates. b) UV tolerance in 35S:RAD7b overexpression line. Hypocotyl and root growth in dark incubated seedlings analyzed 3 days after UV treatment expressed as relative to untreated controls (n=10). c) Root growth in light and dark-incubated seedlings analyzed 2 days after UV treatment, expressed as relative to untreated controls (n=10). d) Percentage undamaged leaves in adult plants after 0, 300, or 600 J m^{-2} UV treatment followed by dark incubation and 3 days in long day conditions (n=6). For b-d values are means ± SE, * = $p \leq 0.05$ of overexpression line vs Col-0 wildtype.

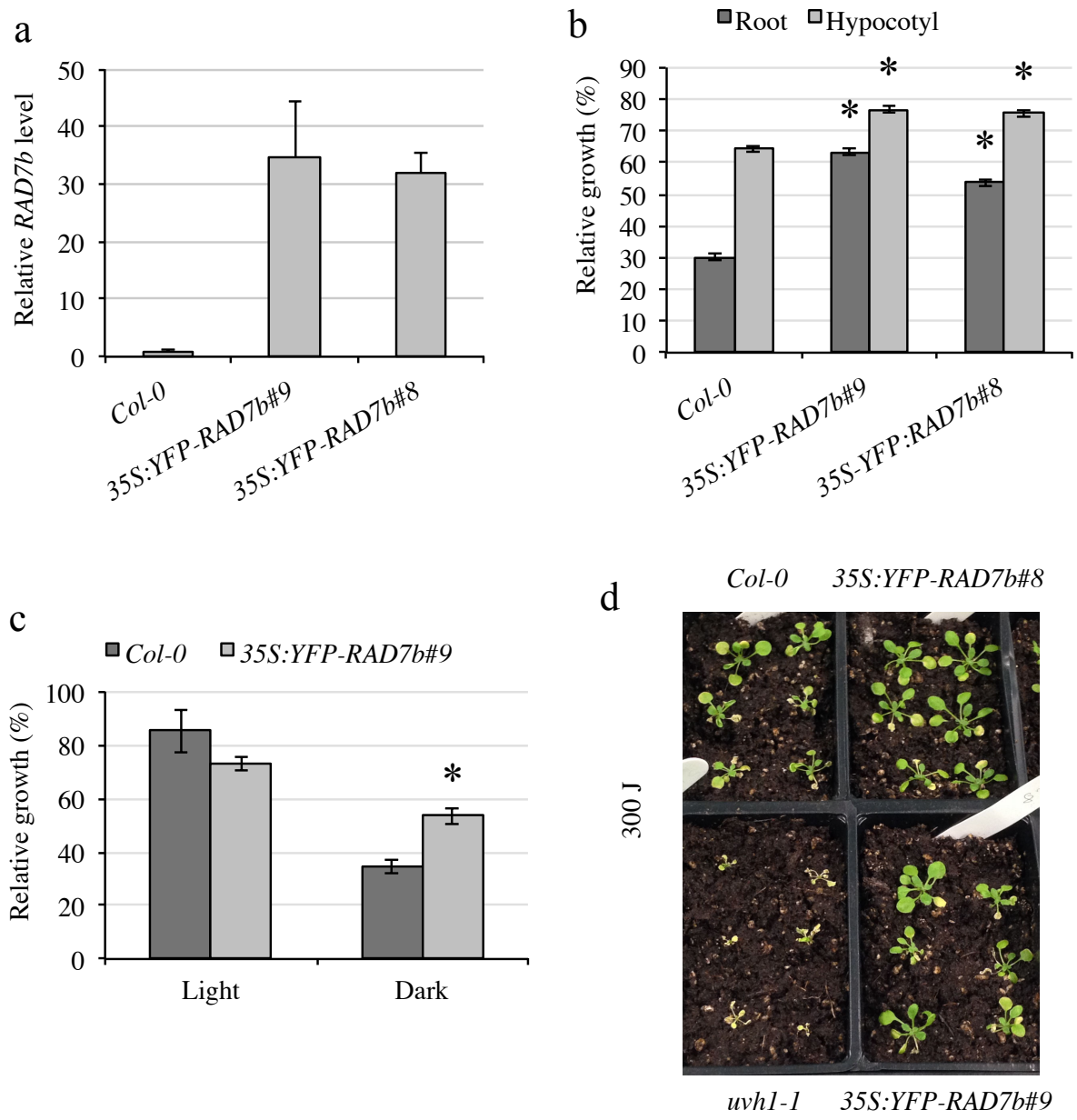

Fig. 3.8 YFP-RAD7b overexpression results in increased UV tolerance

a) *RAD7b* level in 35S:YFP-RAD7b overexpression line relative to control Col-0. Values are relative to the reference gene *EF1α*. Error bars indicate SE of 3 technical replicates. b) Relative hypocotyl and root growth in seedlings exposed to 1000 J m^{-2} UV followed by 3 days dark incubation relative to untreated control (n=10). c) Relative to untreated controls (n=10) root growth was measured in 2 days light and dark-incubated seedlings after UV treatment. * = $p \leq$ 0.05 of overexpression lines vs Col-0 wildtype. d) Representative image of wildtype Col-0, *uvh1-1*, and two YFP-RAD7b overexpression lines following 300 J m^{-2} UV-C treatment.

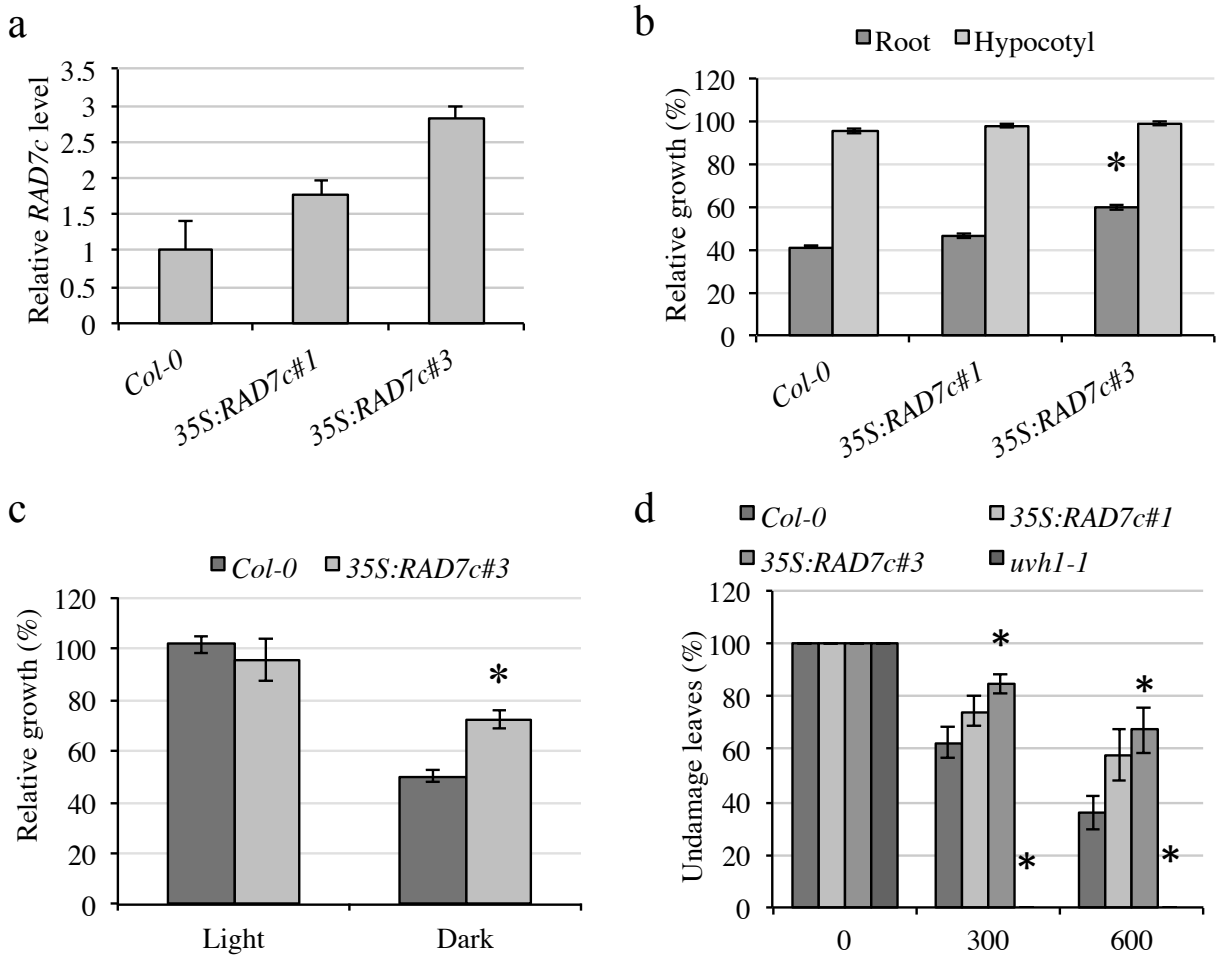

Fig. 3.9 RAD7c overexpression results in increased UV tolerance

a) *RAD7c* level in 35S:RAD7c overexpression line relative to control Col-0. Values are relative to the reference gene *EF1α*. Error bars indicate SE of 3 technical replicates. b) Relative hypocotyl and root growth in seedlings exposed to 1000 J m^{-2} UV followed by 3 days dark incubation relative to untreated control (n=10). c) Relative to untreated controls (n=10) root growth was measured in 2 days light and dark-incubated seedlings after UV treatment. d) Percentage undamaged leaves in adult plants after 0, 300, or 600 J m^{-2} UV treatment followed by dark incubation and 3 days in long day conditions (n=6). For b-d values are means ± SE, * = $p \leq$ 0.05 of overexpression lines vs Col-0 wildtype.

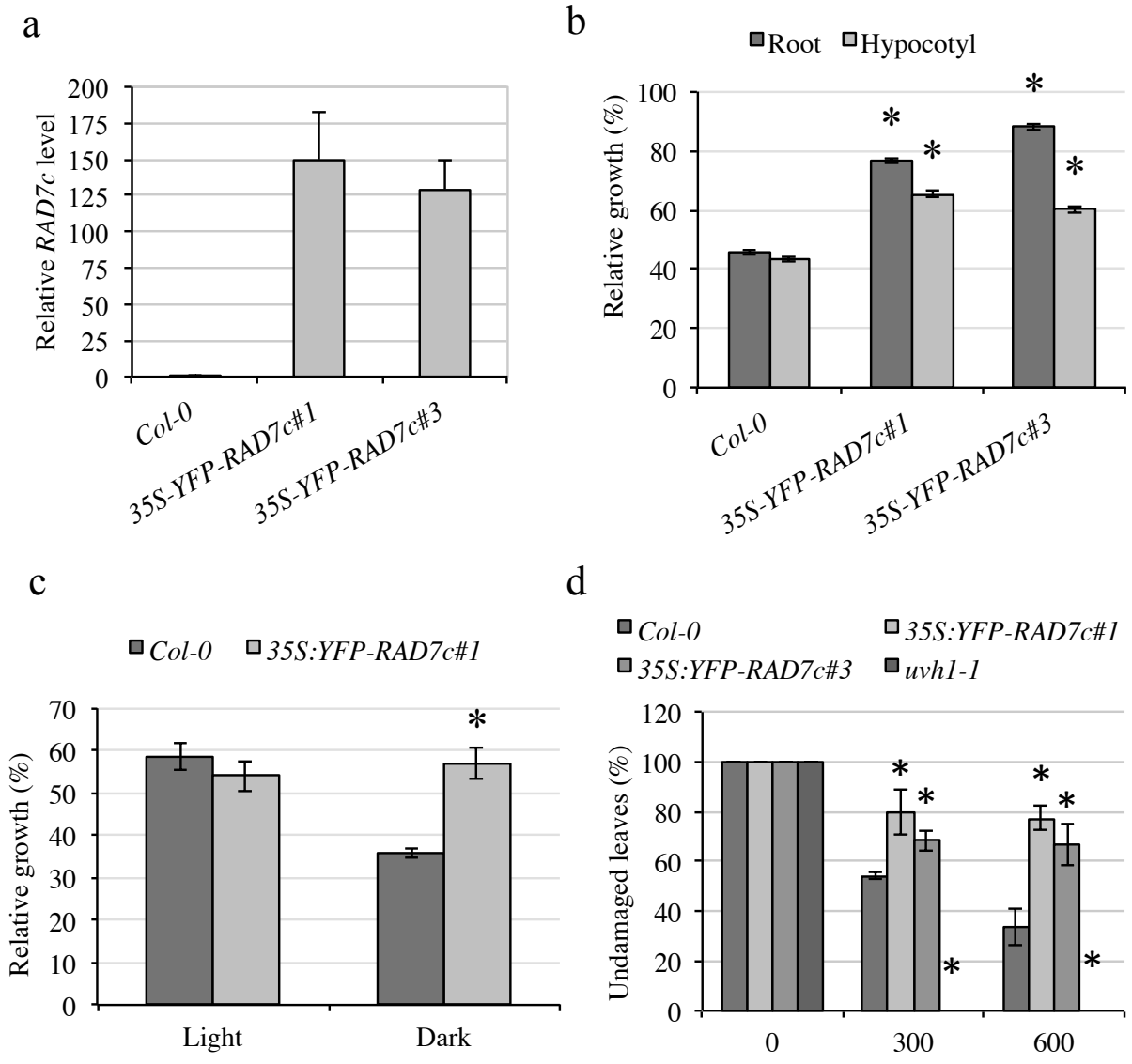

Fig. 3.10 35S:YFP-RAD7c overexpression results in increased UV tolerance

a) *RAD7c* level in 35S:YFP-RAD7c overexpression line relative to control Col-0. Values are relative to the reference gene *EF1α*. Error bars indicate SE of 3 technical replicates. b) Relative hypocotyl and root growth in seedlings exposed to 1000 J m^{-2} UV followed by 3 days dark incubation relative to untreated control (n=10). c) Relative to untreated controls (n=10) root growth was measured in 2 days light and dark-incubated seedlings after UV treatment. d) Percentage undamaged leaves in adult plants after 0, 300, or 600 J m^{-2} UV treatment followed by dark incubation and 3 days in long day conditions (n=6). For b-d values are means ± SE, * = $p \leq$ 0.05 of overexpression lines vs Col-0 wildtype.

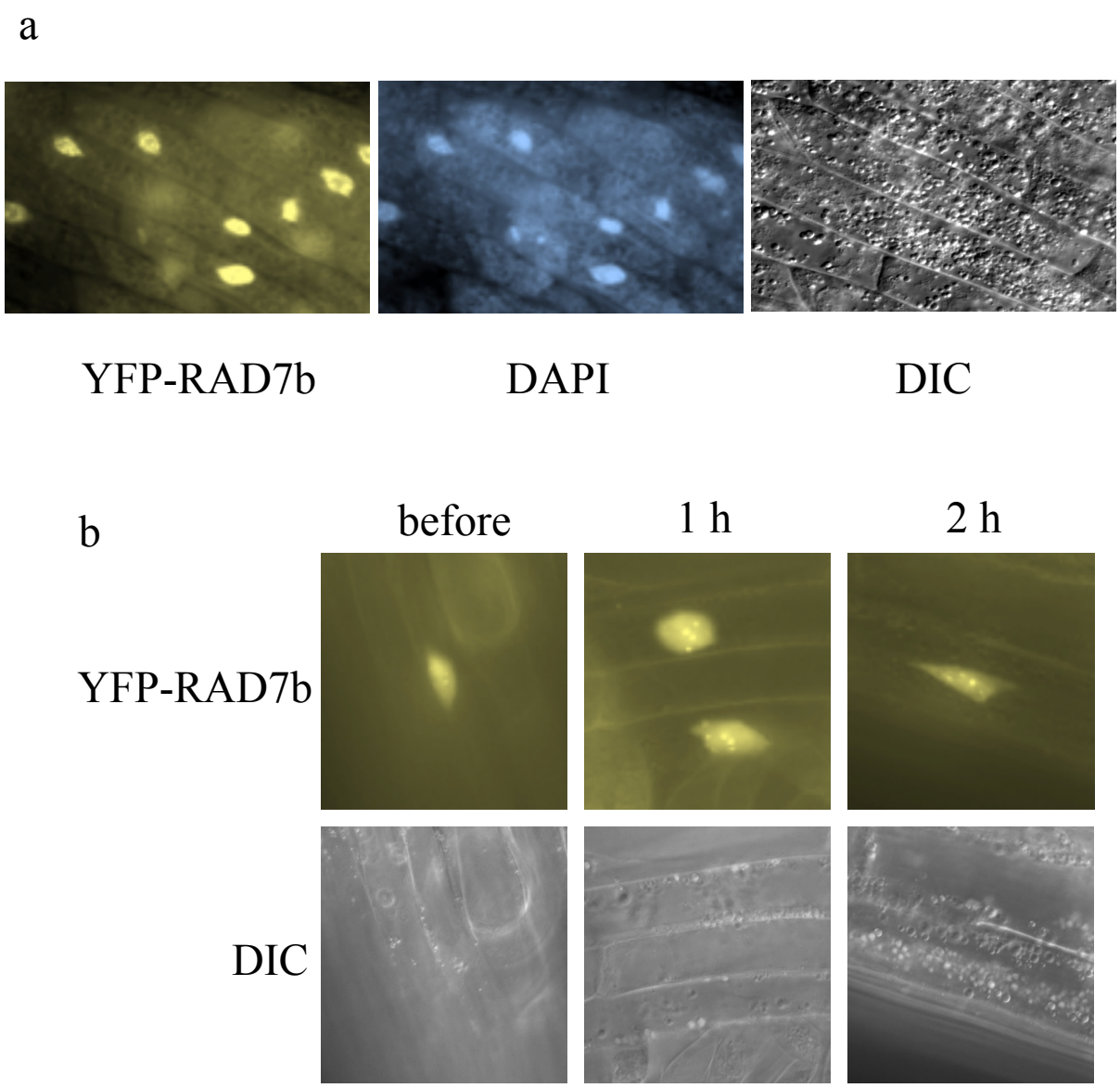

Fig. 3.11 YFP-RAD7b localizes to nuclear speckles

a) Hypocotyl cells in three day old 35S:YFP-RAD7b dark grown seedlings were examined under 40X magnification for YFP fluorescence, DAPI staining, and DIC. b) 35S:YFP-RAD7b root cells observed before UV treatment, and one and two hours after UV treatment under a YFP filter (top) and DIC (bottom).

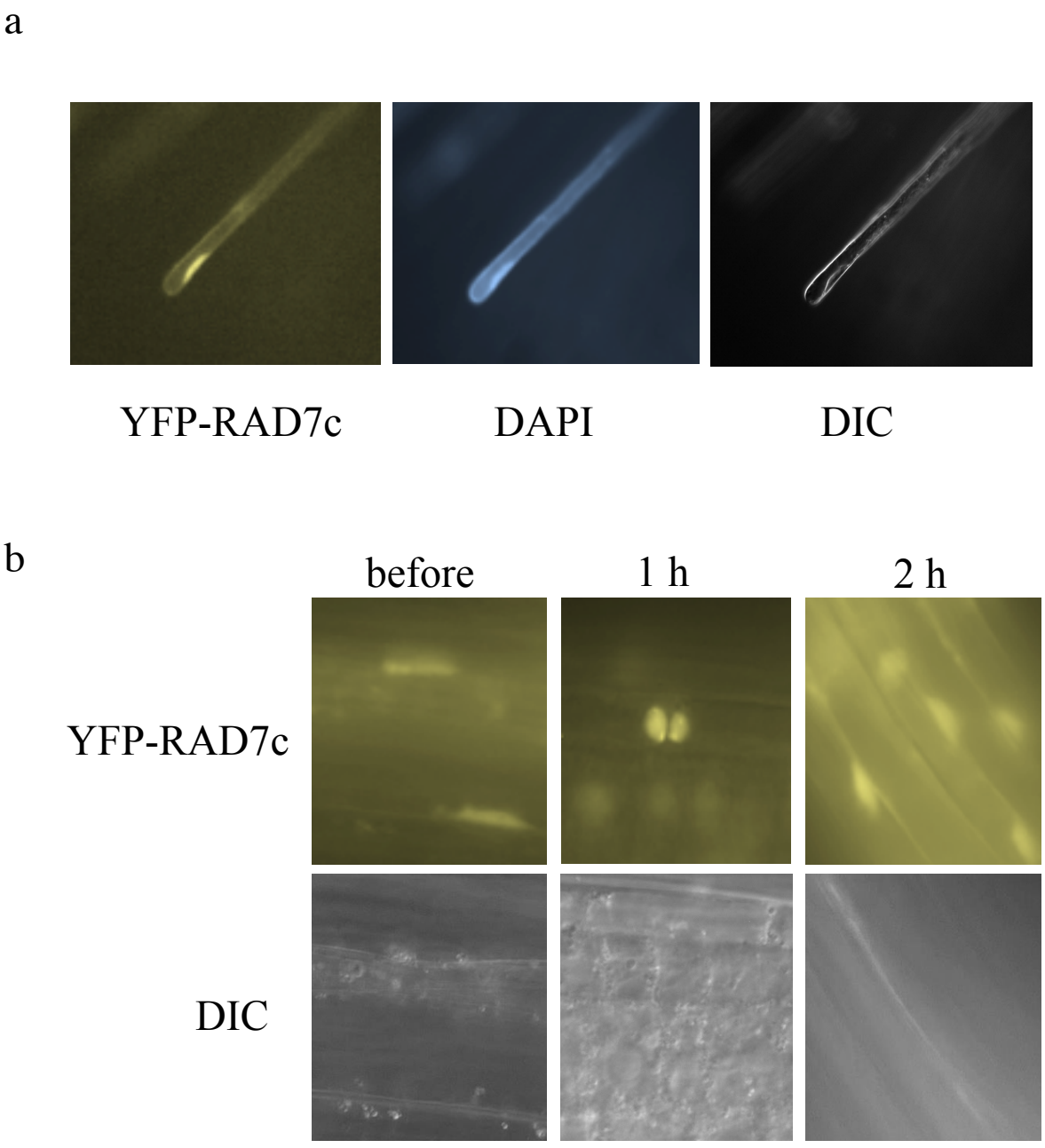

Fig. 3.12 YFP-RAD7c exhibits nuclear localization

a) Root hair cells in three day old 35S:YFP-RAD7c dark grown seedlings were examined under 40X magnification for YFP fluorescence, DAPI staining, and DIC. b) 35S:YFP-RAD7c root cells observed before UV treatment, and one and two hours after UV treatment under a YFP filter (top) and DIC (bottom).

Table S3.1 Primers used in this study (5' -> 3')

Genotyping		
RAD7a	Rad7a-1F: CTGAAGCAGCTGATTTTGACC	Rad7a-1R: AAAAAGAAGCAAAGCAGAGGG
	Rad7a-2F: ATTTGATATGGTGACATGGCC	Rad7a-2R: GGTTCTCTCTGCCCTTTCTTG
	Rad7a-3F: TGACTGCATCCAAAGACCTTC	Rad7a-3R: ATCTATAAGTGGTGCATGCCG
RAD7b	Rad7b-2F: TAAGGCAAGTGTCCTTCCATG	Rad7b-2R: CCTCTCTCCTTCCCCAGTATG
RAD7c	Rad7c-1PR: AATAGTTTGGTTGGCTAGGCC	Rad7c-1R: TTCTTCCATCTCCACGTCTTG
	Rad7c-3F: GAACTTGGCACCTACACTTGG	Rad7c-3R: ATCGTGCATTGAGGATTCTTG
Semi-quantitative RT-PCR		
RAD7a	Rad7a-1F: CTGAAGCAGCTGATTTTGACC	Rad7a-C TCAGTTATCAGAAAGGTGGCCTAA
RAD7b	Rad7b-1F GCTATACAATGCCAATCGCTC	Rad7b-1R: ATCCATGTCGACGAACGTATC
RAD7c	Rad7c-c701F GCGGAAGATCGATGACGGAT	Rad7c-c1387R TGGCAAGCGAAAAAGCAGTC
Actin	CTGGAACAAGACTTCTGGGC	GGTGATGAAGCACAATCCAAG
qPCR		
EEF1α	CTGGAGGTTTTGAGGCTGGTAT	CCAAGGGTGAAAGCAAGAAGA
RAD7b	Rad7b-c239F TCCCTCCTATCTCGTCGCTT	Rad7b-c343R CCCACGTTTTCTTTTTGGGGA
RAD7c	Rad7c-c1539F ATTTGGATGGACGCAGGTGG	Rad7c-c1666R TGGCACCTACACTTGGGTAAA

Table S3.2 Arabidopsis Interaction Viewer predictions of AtRAD4 (At5g16630) interacting proteins

Interolog confidence value	Interolog confidence	Protein 2	Protein 2 annotation
210	High	At5g38470	RAD23D_Rad23 UV excision repair protein family
56	High	At1g16190	RAD23A__Rad23 UV excision repair protein family
14	High	At2g06040	RNI like superfamily protein
8	Medium	At5g41360	ATXPB2_XPB2_Homologue of xeroderma pigmentosum complementation group B2
8	Medium	At3g02540	RAD23-3_RAD23C__Rad23 UV excision repair protein family
6	Medium	At4g15475	RNI like superfamily
4	Medium	At5g41370	ATXPB1_XPB1__homologue of xeroderma pigmentosum complementation group B 1
4	Medium	At3g47010	CEN2__centrin 2

Table S3.3 Results of WU-BLAST2.0 search of *S. cerevisiae* Rad7p versus TAIR10 proteins.

Sequences producing high-scoring segment pairs:		High Score	Smallest sum probability P(N)	N
AT2G06040.1	CONTAINS InterPro DOMAIN/s: Leucine-rich repeat, cysteine-containing subtype	146	6.8e-09	2
AT4G15475.1	F-box/RNI-like superfamily protein	146	9.6e-08	1
AT2G25490.1	EBF1, FBL6 | EIN3-binding F box protein 1	142	2.7e-07	1
AT1G77000.1	ATSKP2;2, SKP2B | RNI-like superfamily protein	128	3.8e-06	1
AT1G77000.2	SKP2B | RNI-like superfamily protein	128	3.8e-06	1
AT5G23340.1	RNI-like superfamily protein	123	1.7e-05	1
AT5G01720.1	RNI-like superfamily protein	116	0.00020	1

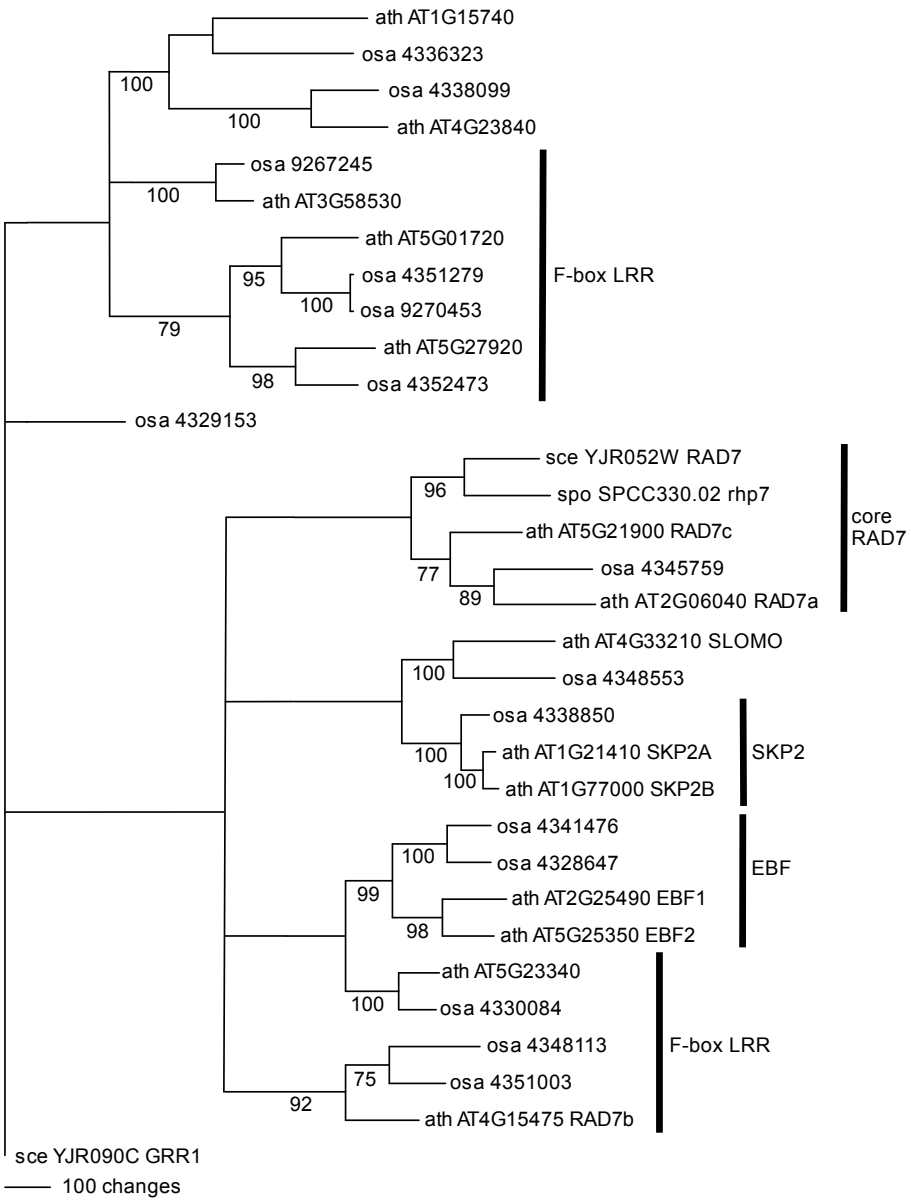

Fig. S3.1 Phylogenetic tree of RAD7 orthologues

Phylogenetic analysis of RAD7 amino acid sequences produced a single most parsimonious tree of 8231 steps. However, many of the nodes had very weak (<25%) bootstrap support, and so were collapsed in the final tree. Unlabelled nodes had 25-50% bootstrap support while nodes with over 50% bootstrap support are indicated. A well-defined core RAD7 clade includes RAD7 homologues from yeast (sce, spo), rice (osa), and RAD7a and RAD7c from Arabidopsis (ath), which derive from KEGG group K15082. Other well-defined lineages are made up of SKP2 (KEGG K03875) and EBF (KEGG K14515) orthologues. Proteins containing F-box LRR domains (KEGG K10268) appear to be found in at least 2 distinct lineages. *S. cerevisiae* Grr1p, the *S. cerevisiae* protein most closely related to ScRad7p, was used as the outgroup.

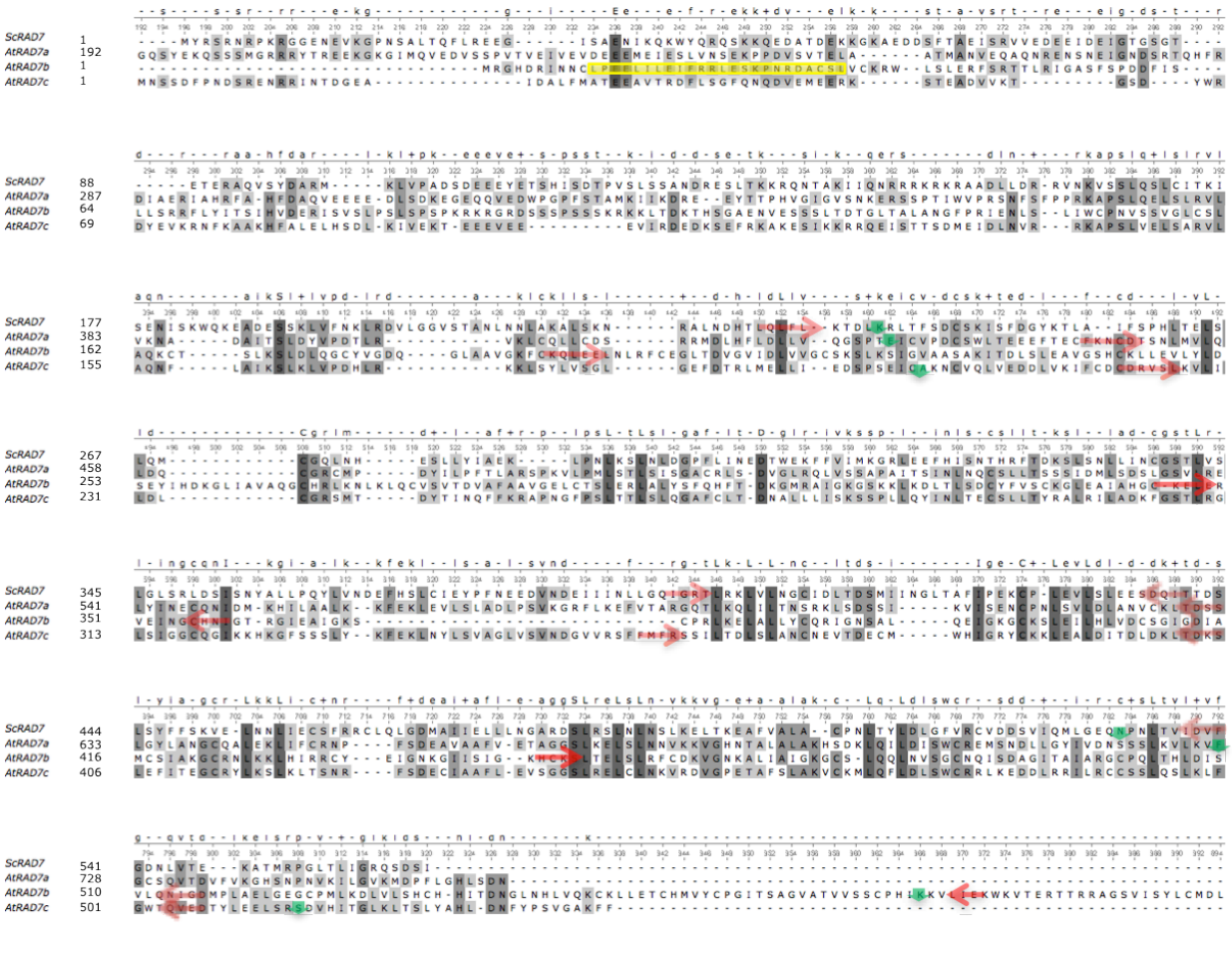

Fig. S3.2 Alignment of RAD7 homologues

S. cerevisiae (NP_012586.1) and Arabidopsis RAD7 protein sequences (NP_178661.2, NP_567467.1, NP_680178.1) aligned using NCBI Cobalt (Papadopoulos and Agarwala 2007) then formatted using Ugene (Okonechnikov et al. 2012). Yellow box indicates F box domain, red arrows indicate the start (right facing) and stop (left facing) of AMN1 domains and the green arrows indicate the start and stop of a continuous series of LRR domains (10 LRRS in ScRad7p, AtRAD7a, and AtRAD7c and 16 LRRs in AtRAD7b).

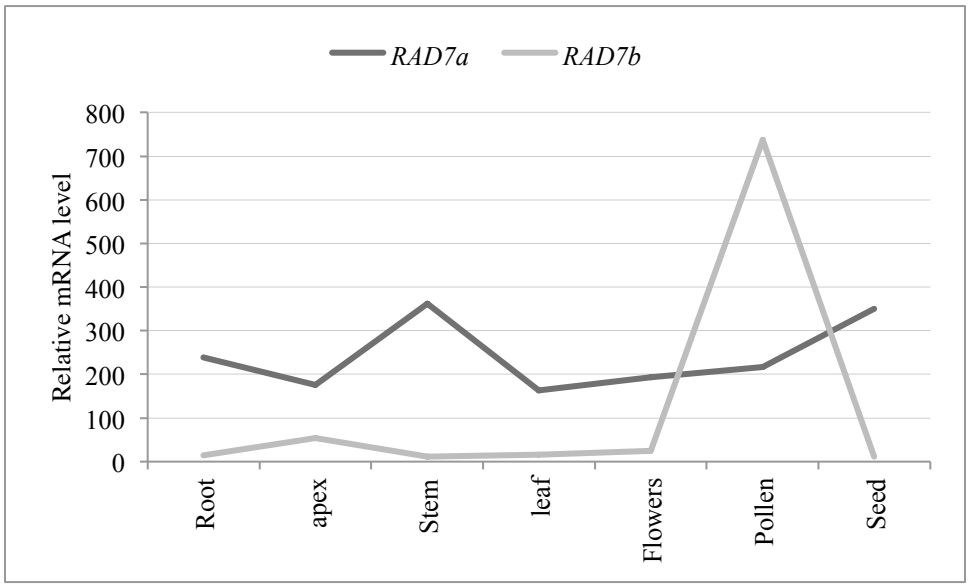

Fig. S3.3 *RAD7a* and *RAD7b* transcript level via AtGeneExpress

RAD7a and *RAD7b* transcript level in wild type in root (21 days), stem (2nd internode, 21+ days), leaf (cauline, 21+ days), shoot apex (21 days), flowers (stage 9, 21+ days), pollen (mature, 6 wks), and seed (stage 10, w/o siliques; green cotyledons embryos, 8 wks). Data from Schmid et al. (2005) visualized with AtGenExpress.

.

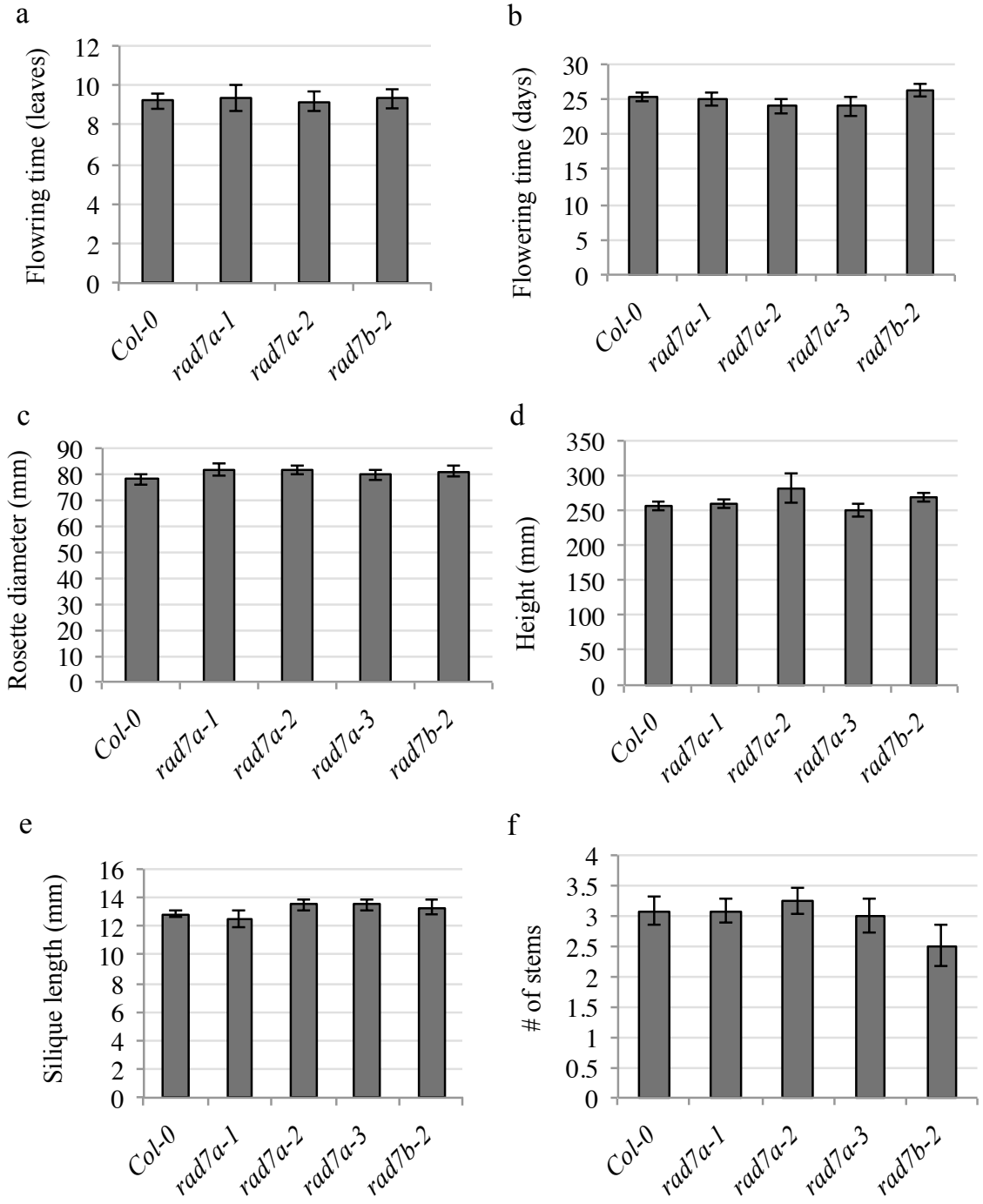

Fig. S3.4 Phenotypic analysis of *rad7a* and *rad7b* adults

a) Flowering time (number of leaves). b) Flowering time (days). c) Rosette diameter. d) Height. e) Silique length. f) Apical dominance (number of stems). Values are means ± SE (n= 12).

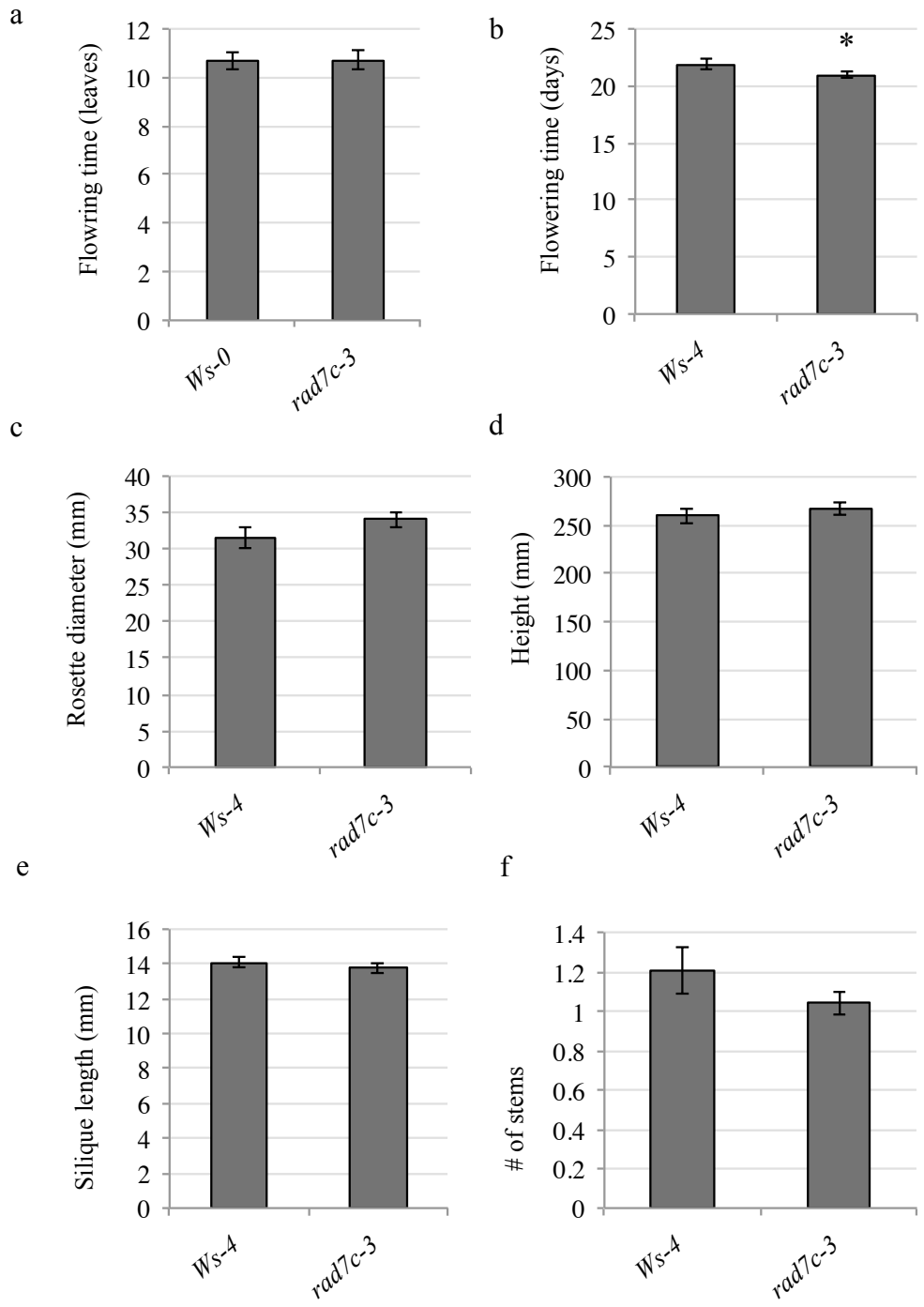

Fig. S3.5 Phenotypic analysis of *rad7c* adults

a) Flowering time (days). b) Flowering time (number of leaves). c) Rosette diameter. d) Height. e) Silique length. f) Apical dominance (number of stems). Values are means ± SE (n= 12), * = $p \leq 0.05$ of mutants vs wild type.

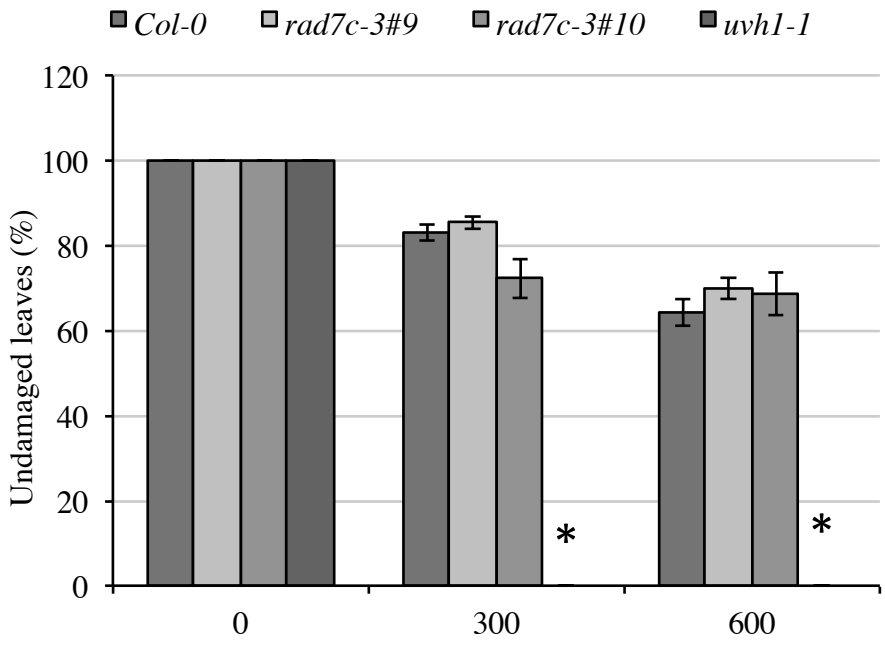

Fig. S3.6 *rad7c-3* adults do not exhibit increased UV sensitivity

Percentage undamaged leaves after exposure to 0, 300, or 600 J m^{-2} UV-C irradiation followed by three days of dark incubation. Values are means ± SE (n=6), * = $p \leq 0.05$ of mutants vs wild type. Note that the *uvh1-1* controls were 100% damaged after 300 or 600 J m^{-2} UV-C irradiation.

a

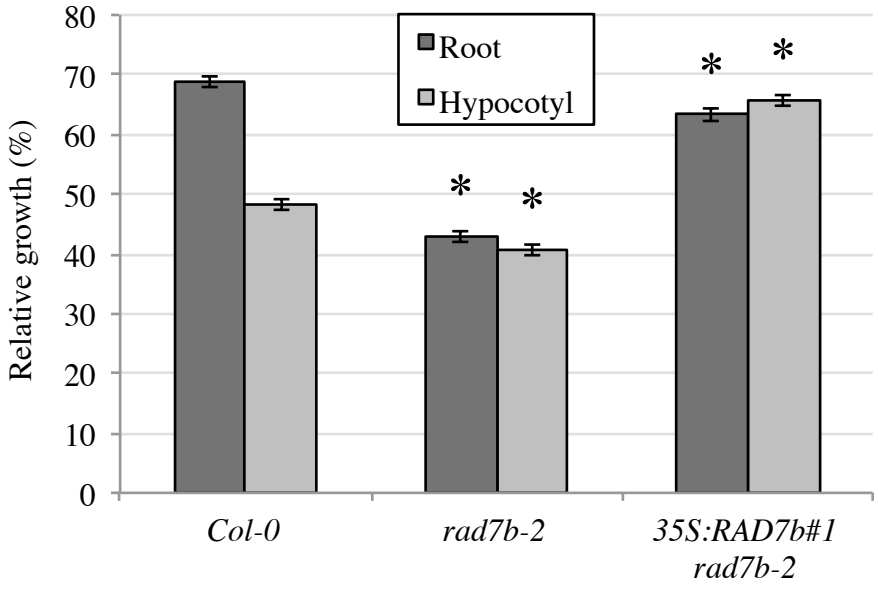
Root
Hypocotyl
Relative growth (%)
80
70
60
50
40
30
20
10
0
*
*
*
*
Col-0
rad7b-2
35S:RAD7b#1
rad7b-2

b

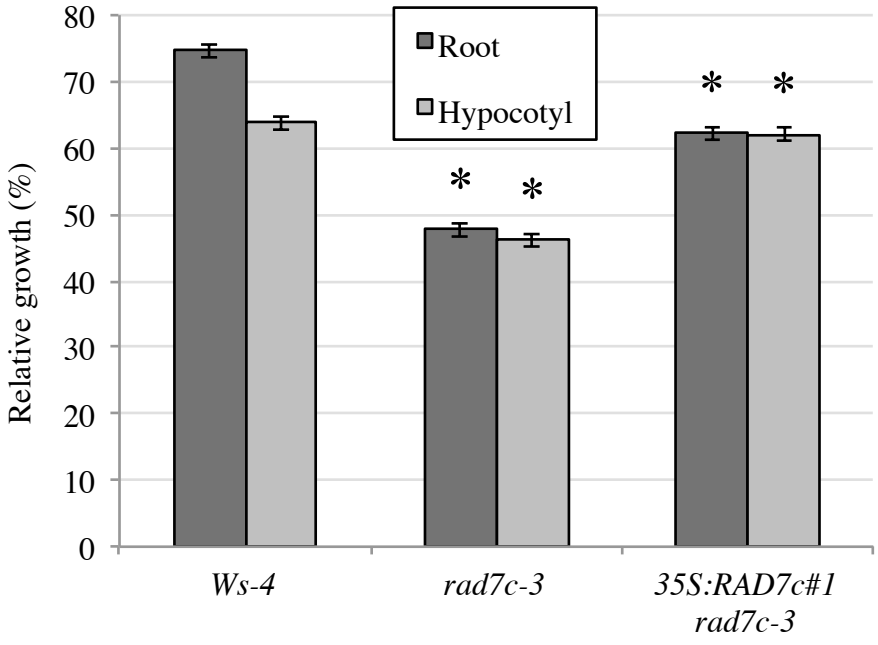
Root
Hypocotyl
Relative growth (%)
80
70
60
50
40
30
20
10
0
*
*
*
*
Ws-4
rad7c-3
35S:RAD7c#1
rad7c-3

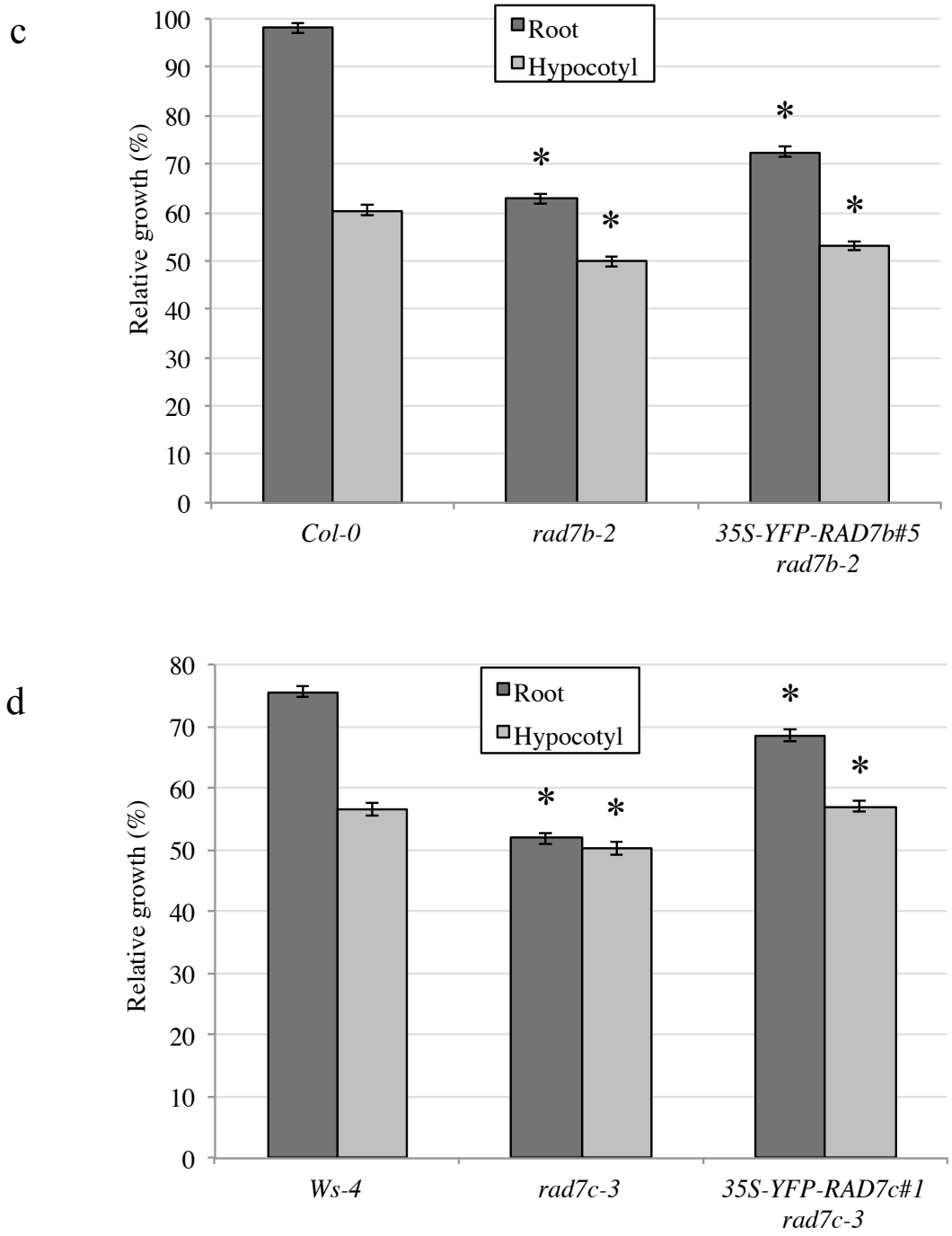

Fig. S3.7 Overexpression of RAD7b and RAD7c rescues seedling UV sensitivity

a) 35S:RAD7b in *rad7b-2*. b) 35S:RAD7c in *rad7c-3*. c) 35S:YFP-RAD7b in *rad7b-2*. d) 35S:YFP-RAD7c in *rad7c-3*. Relative root and hypocotyl lengths after exposure to 1000 J m^{-2} UV-C irradiation followed by three days of dark incubation. Data are expressed as length relative to the unirradiated control of the same genotype. Values are means ± SE (n=10), * = $p \leq 0.05$ of mutants vs wild type or overexpression line vs mutant control.

a

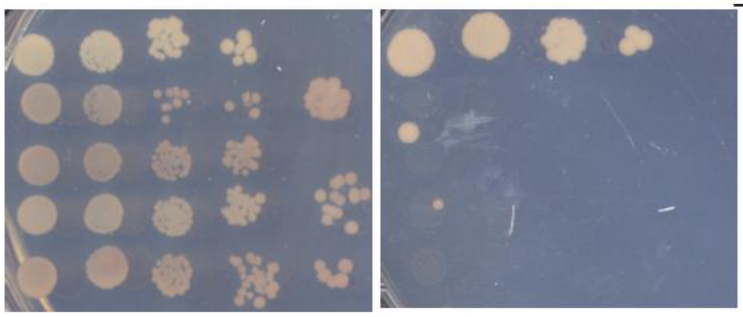

pGBKT7	pGADT7
P53	T
Lam	T
-	RAD4
RAD7b	-
RAD7b	RAD4

b

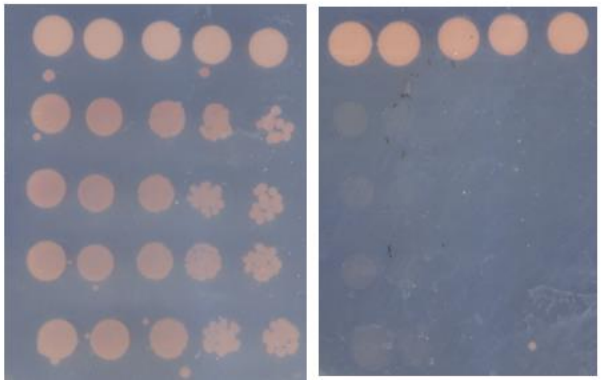

pGBKT7	pGADT7
P53	T
Lam	T
RAD4	-
-	RAD7b
RAD4	RAD7b

Fig. S3.8 Yeast two hybrid analysis of RAD7b RAD4 interaction

a) No interaction was observed between RAD7b pGBKT7 and RAD4 pGADT7. b) No interaction was observed between RAD4 pGBKT7 and RAD7b pGADT7. Five-fold dilutions of the indicated diploid strains were plated on the double drop-out (–leu, –trp) control plate on the left, and the quadruple drop-out (–leu, –trp, –ade, –his) selection medium on the right. The interaction between p53 and T, resulting in growth on the selective medium, is the positive control, whereas Lam and T, which do not interact, are the negative control.

a

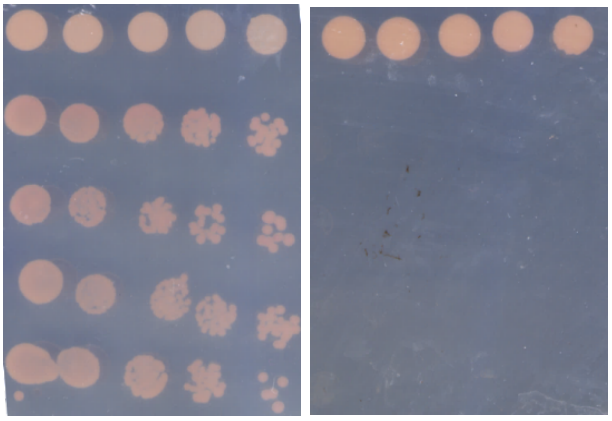

pGBKT7	pGADT7
P53	T
Lam	T
RAD4	-
-	RAD7c
RAD4	RAD7c

b

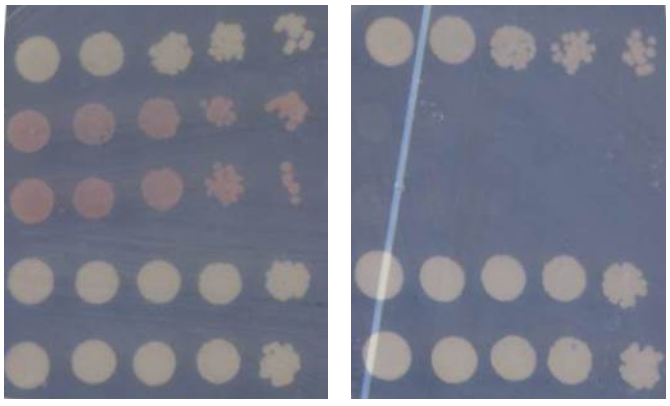

pGBKT7	pGADT7
P53	T
Lam	T
-	RAD4
RAD7c	-
RAD7c	RAD4

Fig. S3.9 Yeast two hybrid analysis of RAD7c RAD4 interaction

a) No interaction was observed between RAD4 pGBKT7 and RAD7c pGADT7. b) RAD7c pGBKT7 exhibited growth on selective media with both empty pGADT7 and RAD4 pGADT7. Five-fold dilutions of the indicated diploid strains were plated on the double drop-out (–leu, –trp) control plate on the left, and the quadruple drop-out (–leu, –trp, –ade, –his) selection medium on the right. The interaction between p53 and T, resulting in growth on the selective medium, is the positive control, whereas Lam and T, which do not interact, are the negative control.

a

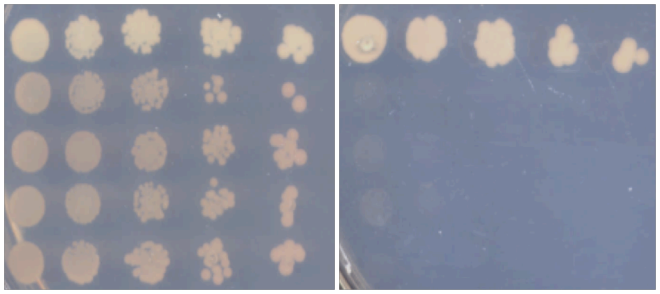

pGBKT7	pGADT7
P53	T
Lam	T
RAD7b	-
-	RAD7b
RAD7b	RAD7b

b

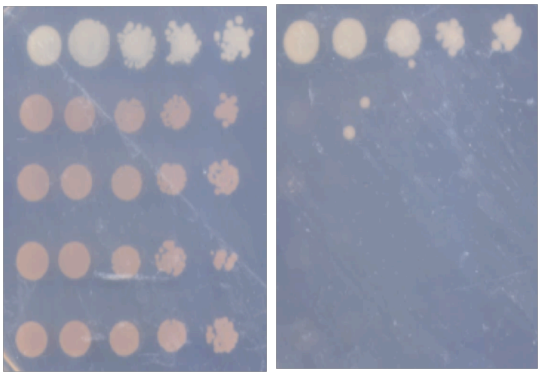

pGBKT7	pGADT7
P53	T
Lam	T
RAD7b	-
-	RAD7c
RAD7b	RAD7c

Fig. S3.10 Yeast two hybrid analysis of RAD7b RAD7c interaction

a) No interaction was observed between RAD7b pGBKT7 and RAD7b pGADT7. b) No interaction was observed in between RAD7b pGBKT7 and RAD7c pGADT7. Five-fold dilutions of the indicated diploid strains were plated on the double drop-out (–leu, –trp) control plate on the left, and the quadruple drop-out (–leu, –trp, –ade, –his) selection medium on the right. The interaction between p53 and T, resulting in growth on the selective medium, is the positive control, whereas Lam and T, which do not interact, are the negative control.

a

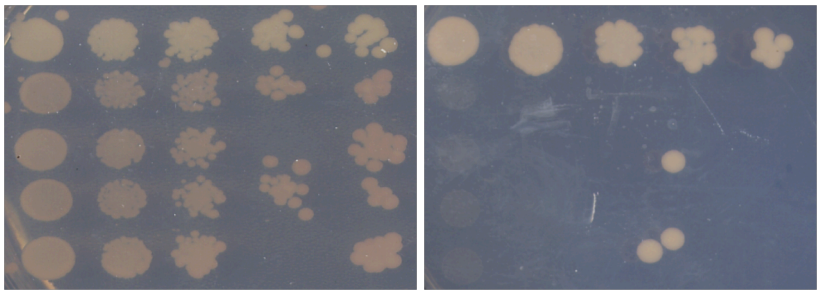

pGBKT7	pGADT7
P53	T
Lam	T
ELC1	-
-	RAD7b
ELC1	RAD7b

b

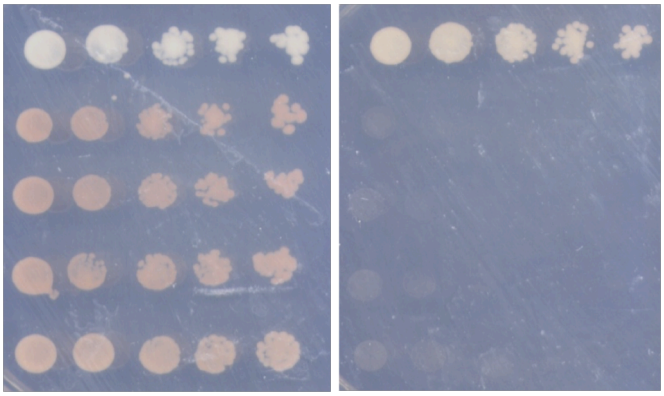

pGBKT7	pGADT7
P53	T
Lam	T
ELC1	-
-	RAD7c
ELC1	RAD7c

Fig. S3.11 Yeast two hybrid analysis of RAD7b/RAD7c ELC1 interaction

a) No interaction was observed between ELC1 pGBKT7 and RAD7b pGADT7. b) No interaction was observed in between ELC1 pGBKT7 and RAD7c pGADT7. Five-fold dilutions of the indicated diploid strains were plated on the double drop-out (–leu, –trp) control plate on the left, and the quadruple drop-out (–leu, –trp, –ade, –his) selection medium on the right. The interaction between p53 and T, resulting in growth on the selective medium, is the positive control, whereas Lam and T, which do not interact, are the negative control.

4. Discussion

4.1 General Discussion

Plants need sunlight for photosynthesis and cannot avoid daily exposure to sunlight due to their immovable nature. The ultraviolet rays (UV) in sunlight cause DNA damage by forming pyrimidine dimers including CPDs and 6-4 PP. These DNA lesions inhibit cellular activities such as replication and transcription. Plants have both light dependent and light independent DNA repair mechanisms. Light independent repair is a conserved process, nucleotide excision repair (NER), which identifies the damaged site, followed by excision of the damaged nucleotides and repair. NER of untranscribed DNA throughout the genome is called global genomic (GG) NER (Bray and West 2005). In GG-NER, damage recognition is performed by the DDB complex in mammals (Sugasawa 2010) and the Rad7p/Rad16P complex in yeast (Guzder et al. 1997). In plant GG-NER, DDB2, DDB1, and CUL4 have been shown to be required (Al Khateeb and Schroeder 2009; Koga et al. 2006; Molinier et al. 2008). In this thesis, I have shown for the first time that Arabidopsis RAD7 homologues are also involved in UV tolerance. Why would plants require both UV-DDB and RAD7/16 type damage recognition complexes? What do these complexes have in common and how do they differ?

In mammals, UV-DDB accumulates at the damaged site, binding to the photolesion, and initiates XPC binding. Crystal structure studies have revealed the lesion dependent structure of these proteins. DDB2 forms a β-propeller structure in the C terminal region that inserts into the lesion to flip out the damaged nucleotide (Sugasawa 2016). Single molecule analysis revealed that UV-DDB does not slide along DNA but jumps between DNA strands in three dimensions (Ghodke et al. 2014). DDB1 acts as a base to link the CUL4-RBX1 ubiquitin E3 ligase to DDB2. The DDB2 E3 ligase is activated upon damaged DNA binding, resulting in auto-ubiquitination

and degradation of DDB2, as well as ubiquitination of XPC, which does not result in degradation but in increased lesion affinity (Zhang and Gong 2016). In the context of chromatin, UV-DDB recognizes lesions in nucleosomal DNA, promotes histone eviction, and facilitates the interaction of other NER factors with the lesion. Chromatin remodelling by UV-DDB occurs via ubiquitination of histones H2A, H3, and H4 and interaction with chromatin remodelling enzymes such as GCN5 and p300 (Sugasawa 2016; Zhang and Gong 2016).

In GG-NER in the yeast *S. cerevisiae*, UV damaged DNA recognition is carried out by the Rad7p/Rad16p complex. The Rad7p/Rad16p complex can also contain Autonomously replicating sequence Binding Factor 1 (Abf1p) and binds the UV damage DNA in an ATP dependent manner. The Rad7p-Rad16p-Abf1p complex uses ATP hydrolysis energy to translocate and promotes a conformational change in DNA to facilitate Rad4p binding to the damaged site. Although Rad16p does not posses any helicase activity, it is homologous to SWI/SNF chromatin remodelling complex subunit Snf2 (Boiteux and Jinks-Robertson 2013). The Rad7p/Rad16p complex interacts with Gcn5p, resulting in histone H3 acetylation and chromatin opening, facilitating repair. Both the translocase and E3 ligase activities of the Rad16p complex are required for this activity (Waters et al. 2015). The Rad7p-Rad16p Elcp-Cul3p complex has E3 ubiquitin ligase activity and ubiquitinates Rad4p, resulting in its degradation (Boiteux and Jinks-Robertson 2013). Interestingly *rad7* mutants were recently found to accumulate ubiquitinated proteins, suggesting that Rad7p also regulates deubiquitination (Benoun et al. 2015).

Thus the DDB and RAD7 complexes perform similar functions, such as binding UV damaged DNA, recruiting and ubiquitinating XPC/Rad4p, and interacting with chromatin remodelling enzymes such as GCN5. In addition, neither UV-DDB nor the Rad7/16 complex are required for NER in vitro, suggesting that their role is to facilitate chromatin remodelling or

enhance affinity of NER factors which are present at lower concentrations in vivo than in vitro. There are differences between the two complexes however. Rad7/16 translocates along the DNA in an ATP dependent manner while UV-DDB jumps between strands and does not require ATP. In addition, while both complexes add ubiquitin to XPC/Rad4p, this results in Rad4p degradation in yeast but not XPC degradation in mammals (Boiteux and Jinks-Robertson 2013; Sugasawa 2016). Thus perhaps in plants these two activities are complementary. Plants are reliant on solar energy, so may have a higher demand for UV damaged DNA repair than other organisms. However, in contrast to mammals, plants can also utilize photolyases for repair. Recent evidence indicates that Arabidopsis DDB2 has a dual role in repair and DNA methylation (Schalk et al. 2016), thus perhaps RAD7/16 assists with damage recognition. However Arabidopsis *centrin 2* and *rad10/xpf* mutants exhibit alteration of methylation like *ddb2* mutants, suggesting that this effect involves the entire NER pathway (Schalk and Molinier 2016). In addition, plants do not have a clear ABF1 homologue; thus plant RAD7/16 may interact with DNA in a different manner than in yeast. Finally, in contrast to mammals and yeast, plants do not have a clear XPA homologue. Mammalian XPA interacts with both DDB2 and XPC, so perhaps double damage recognition in plants compensates for the lack of XPA (Sugitani et al. 2016).

Interestingly, GG-NER components appear to vary across systems. For example, *S. pombe* has Rad7p and Rad16p homologues, and lacks DDB2, but has a DDB1 homologue that functions in other CUL4 complexes (Jin et al. 2006). In *C. elegans* XPC and RAD23 homologues contribute to UV damage response (Lans et al. 2010) and DDB1 regulates destruction of CDT1 and DNA polymerase eta during DNA damage response (Hu et al. 2004; Kim and Michael 2008), but a clear DDB2 homologue is lacking (Tang and Chu 2002). In Drosophila, DDB1 contributes to genomic stability (Shimanouchi et al. 2006) and overexpression of human DDB2 results in increased UV tolerance (Sun et al. 2010); yet again a

clear DDB2 homologue is lacking (Tang and Chu 2002). Thus, given our findings of the role of RAD7 is Arabidopsis GG-NER, perhaps *C. elegans* and Drosophila also use an alterate, possibly RAD7-based, mechanism of damaged DNA recognition.

4.2 Future directions

We have examined the effect of overexpression of AtRAD4, its cellular localization, and interaction with RAD23B and HMR in yeast two hybrid assays. We have identified Arabidopsis RAD7 homologues, examined loss of function and overexpression lines, as well as the cellular localization of RAD7b and RAD7c. The following experiments would complement these studies.

While we have studied the effect of overexpression of AtRAD4, we did not examine the effect of AtRAD4 loss of function. AtRAD4 loss of function lines could be generated via RNAi gene silencing (Zamore et al. 2000). The ability of AtRAD4 and *S. cerevisiae* RAD4 to rescue the AtRAD4 loss of function phenotype could also be examined.

RAD7a rescue, overexpression, cellular localization, and yeast two hybrid experiments have yet to be performed. We have recently obtained *RAD7a* cDNA RAFL clones from Riken (Seki et al. 2002), which will be cloned into Gateway entry vectors to facilitate cloning into the pEG100 and pEG104 destination vectors, as well as into pGADT7 and pGBKT7 for yeast two hybrid analysis.

We have obtained *rad4* and *rad7* knockout mutants in *S. cerevisiae*. Preliminary experiments indicate that AtRAD4 and AtRAD7b fail to rescue their respective mutants (J. Lazaro, personal communication). However the ability of AtRAD7a and AtRAD7c to rescue UV sensitivity in the yeast *rad7* mutant has yet to be assessed.

Generating double or triple mutants among the *RAD7* loss of function alleles, followed by UV sensitivity study, would contribute information on gene interaction between the *RAD7* genes. In addition, *rad7 ddb2* double mutants would reveal the contribution of the mammalian and yeast damage recognition complexes to Arabidopsis UV tolerance.

While we would predict, based on homology, that RAD4 and the RAD7 homologues function in NER, in fact we have studied only UV sensitivity. A DNA repair assay, such as a photoproduct assay (Al Khateeb and Schroeder 2009) with loss of function and overexpression material would clarify the contribution of these genes to NER.

In yeast, Rad7p interacts with Rad4p, Rad16p, Elc1, and Cul3. Additional information of the role of the RAD7 complex in Arabidopsis could be obtained by examining UV tolerance in *RAD16, RAD16b, ELC1,* and *CUL3* loss of function and gain of function lines. The study of loss of function alleles of these genes is already in progress in our lab. While we have tested for interaction between Arabidopsis RAD7b, RAD7c, RAD4, and ELC1 in yeast two hybrid assays, we have yet to examine interaction with RAD16, RAD16b, or CUL3a. These cDNAs are not available in Gateway entry vectors. We have recently obtained a *CUL3a* cDNA from Riken (Seki et al. 2002) and plan to synthesize *RAD16* and *RAD16b* cDNAs. These cDNAs will be cloned into yeast two hybrid vectors in order to test for interaction. In addition, other interaction assays such as fluorescence resonance energy transfer (FRET), bimolecular fluorescence complementation (BiFC), and immunoprecipitation could be utilized to examine protein-protein interactions. Additional biochemical assays such as DNA binding and ubiquitination experiments could also be performed with the RAD7/16 complex.

4.3 Conclusion

In conclusion, in this study we have assessed the role of RAD4 and RAD7 homologues in Arabidopsis UV tolerance and shown for the first time that RAD7 homologues contribute to UV tolerance in plants. These results suggest that UV damage recognition in plants combines the strengths of both the mammalian and yeast systems and provide new insight into the mechanism of GG-NER in multicellular organisms.

5. References

Al Khateeb WM, Schroeder DF (2009) Overexpression of Arabidopsis damaged DNA binding protein 1A (DDB1A) enhances UV tolerance. Plant Molecular Biology 70: 371-383

Alekseev S, Coin F (2015) Orchestral maneuvers at the damaged sites in nucleotide excision repair. Cellular and Molecular Life Sciences 72: 2177-2186

Alonso JM, Stepanova AN, Leisse TJ, Kim CJ, Chen H, Shinn P, Stevenson DK, Zimmerman J, Barajas P, Cheuk R (2003) Genome-wide insertional mutagenesis of *Arabidopsis thaliana*. Science 301: 653-657

Amerik AY, Li S-J, Hochstrasser M (2000) Analysis of the deubiquitinating enzymes of the yeast *Saccharomyces cerevisiae*. Biological Chemistry 381: 981-992

Araki M, Masutani C, Takemura M, Uchida A, Sugasawa K, Kondoh J, Ohkuma Y, Hanaoka F (2001) Centrosome protein centrin 2/caltractin 1 is part of the xeroderma pigmentosum group C complex that initiates global genome nucleotide excision repair. Journal of Biological Chemistry 276: 18665-16872

Bais AF, McKenzie RL, Bernhard G, Aucamp PJ, Ilyas M, Madronich S, Tourpali K (2015) Ozone depletion and climate change: Impacts on UV radiation. Photochemical and Photobiological Sciences 14: 19-52

Ballaré CL, Caldwell MM, Flint SD, Robinson SA, Bornman JF (2011) Effects of solar ultraviolet radiation on terrestrial ecosystems. Patterns, mechanisms, and interactions with climate change. Photochemical and Photobiological Sciences 10: 226-241

Ben-Yehuda S, Dix I, Russell CS, McGarvey M, Beggs JD, Kupiec M (2000) Genetic and physical interactions between factors involved in both cell cycle progression and pre-mRNA splicing in *Saccharomyces cerevisiae*. Genetics 156: 1503-1517

Benoun JM, Lalimar-Cortez D, Valencia A, Granda A, Moore DM, Kelson EP, Fischhaber PL (2015) Rad7 E3 ubiquitin ligase attenuates polyubiquitylation of Rpn10 and Dsk2 following DNA damage in *Saccharomyces cerevisiae*. Advances in Biological Chemistry 5: 61944

Bernhardt A, Lechner E, Hano P, Schade V, Dieterle M, Anders M, Dubin MJ, Benvenuto G, Bowler C, Genschik P (2006) CUL4 associates with DDB1 and DET1 and its downregulation affects diverse aspects of development in *Arabidopsis thaliana*. The Plant Journal 47: 591-603

Bernhardt A, Mooney S, Hellmann H (2010) Arabidopsis DDB1a and DDB1b are critical for embryo development. Planta 232: 555-566

Bhatia PK, Verhage RA, Brouwer J, Friedberg EC (1996) Molecular cloning and characterization of *Saccharomyces cerevisiae RAD28*, the yeast homolog of the human *Cockayne syndrome A (CSA)* gene. Journal of Bacteriology 178: 5977-5988

Biedermann S, Hellmann H (2010) The DDB1a interacting proteins ATCSA 1 and DDB2 are critical factors for UV B tolerance and genomic integrity in *Arabidopsis thaliana*. The Plant Journal 62: 404-415

Boiteux S, Jinks-Robertson S (2013) DNA repair mechanisms and the bypass of DNA damage in *Saccharomyces cerevisiae*. Genetics 193: 1025-1064

Bornman JF, Barnes PW, Robinson SA, Ballare CL, Flint SD, Caldwell MM (2015) Solar ultraviolet radiation and ozone depletion-driven climate change: effects on terrestrial ecosystems. Photochemical and Photobiological Sciences 14: 88-107

Brash DE (1997) Sunlight and the onset of skin cancer. Trends in Genetics 13: 410-414

Bray CM, West CE (2005) DNA repair mechanisms in plants: crucial sensors and effectors for the maintenance of genome integrity. New Phytologist 168: 511-528

Brunaud Vr, Balzergue S, Dubreucq B, Aubourg Sb, Samson F, Chauvin Sp, Bechtold N, Cruaud C, DeRose R, Pelletier G (2002) T-DNA integration into the Arabidopsis genome depends on sequences of pre-insertion sites. EMBO Reports 3: 1152-1157

Cadet J, Anselmino C, Douki T, Voituriez L (1992) New trends in photobiology: Photochemistry of nucleic acids in cells. Journal of Photochemistry and Photobiology B: Biology 15: 277-298

Cadet J, Grand A, Douki T (2015) Solar UV radiation-induced DNA bipyrimidine photoproducts: formation and mechanistic insights. Photoinduced Phenomena in Nucleic Acids II. Springer, pp 249-275

Cadet J, Sage E, Douki T (2005) Ultraviolet radiation-mediated damage to cellular DNA. Mutation Research/Fundamental and Molecular Mechanisms of Mutagenesis 571: 3-17

Chakraborty U, George CM, Lyndaker AM, Alani E (2016) A delicate balance between repair and replication factors regulates recombination between divergent DNA sequences in *Saccharomyces cerevisiae*. Genetics 202: 525-540

Chen J-J, Mitchell DL, Britt AB (1994) A light-dependent pathway for the elimination of UV-induced pyrimidine (6-4) pyrimidinone photoproducts in Arabidopsis. The Plant Cell 6: 1311-1317

Chen M, Galvão RM, Li M, Burger B, Bugea J, Bolado J, Chory J (2010) Arabidopsis HEMERA/pTAC12 initiates photomorphogenesis by phytochromes. Cell 141: 1230-1240

Coldiron BM (1992) Thinning of the ozone layer: facts and consequences. Journal of the American Academy of Dermatology 27: 653-662

Costa R, Morgante PG, Berra CM, Nakabashi M, Bruneau D, Bouchez D, Sweder KS, Van Sluys MA, Menck CFM (2001) The participation of *AtXPB1*, the *XPB/RAD25* homologue gene from *Arabidopsis thaliana,* in DNA repair and plant development. The Plant Journal 28: 385-395

Cox BS, Parry JM (1968) The isolation, genetics and survival characteristics of ultraviolet light-sensitive mutants in yeast. Mutation Research/Fundamental and Molecular Mechanisms of Mutagenesis 6: 37-55

Dantuma NP, Heinen C, Hoogstraten D (2009) The ubiquitin receptor Rad23: at the crossroads of nucleotide excision repair and proteasomal degradation. DNA Repair 8: 449-460

de Boer J, Hoeijmakers JHJ (2000) Nucleotide excision repair and human syndromes. Carcinogenesis 21: 453-460

del Pozo JC, Diaz-Trivino S, Cisneros N, Gutierrez C (2006) The balance between cell division and endoreplication depends on E2FC-DPB, transcription factors regulated by the ubiquitin-SCFSKP2A pathway in Arabidopsis. The Plant Cell 18: 2224-2235

Dellaire G, Bazett-Jones DP (2007) Beyond repair foci: subnuclear domains and the cellular response to DNA damage. Cell Cycle 6: 1864-1872

den Dulk B, van Eijk P, de Ruijter M, Brandsma JA, Brouwer J (2008) The NER protein Rad33 shows functional homology to human Centrin2 and is involved in modification of Rad4. DNA Repair 7: 858-868

Dijk M, Typas D, Mullenders L, Pines A (2014) Insight in the multilevel regulation of NER. Experimental Cell Research 329: 116-123

Dupuy Al, Sarasin A (2016) DNA damage and gene therapy of xeroderma pigmentosum, a human DNA repair-deficient disease. Mutation Research/Fundamental and Molecular Mechanisms of Mutagenesis 776: 2-8

Earley KW, Haag JR, Pontes O, Opper K, Juehne T, Song K, Pikaard CS (2006) Gateway compatible vectors for plant functional genomics and proteomics. The Plant Journal 45: 616-629

Farmer LM, Book AJ, Lee KH, Lin YL, Fu H, Vierstra RD (2010) The RAD23 family provides an essential connection between the 26S proteasome and ubiquitylated proteins in Arabidopsis. The Plant Cell 22: 124-142

Fautrel A, Andrieux L, Musso O, Boudjema K, Guillouzo A, Langouët S (2005) Overexpression of the two nucleotide excision repair genes ERCC1 and XPC in human hepatocellular carcinoma. Journal of Hepatology 43: 288-293

Fidantsef AL, Britt AB (2012) Preferential repair of the transcribed DNA strand in plants. Frontiers in Plant Science 2: 105

Fidantsef AL, Mitchell DL, Britt AB (2000) The Arabidopsis *UVH1* gene is a homologue of the yeast repair endonuclease *RAD1*. Plant Physiology 124: 579-586

Fousteri M, Mullenders L (2008) Transcription-coupled nucleotide excision repair in mammalian cells: molecular mechanisms and biological effects. Cell Research 18: 73-84

Franklin WA, Doetsch PW, Haseltine WA (1985) Structural determinatlon of the ultraviolet light-induced thymine-cytosine pyrimidine-pyrimidone (6-4) photoproduct. Nucleic Acids Research 13: 5317-5325

Furukawa M, He YJ, Borchers C, Xiong Y (2003) Targeting of protein ubiquitination by BTB-Cullin 3-Roc1 ubiquitin ligases. Nature Cell Biology 5: 1001-1007

Ganpudi AL, Schroeder DF (2011) UV Damaged DNA Repair & Tolerance in Plants. INTECH Open Access Publisher

Ganpudi AL, Schroeder DF (2013) Genetic interactions of *Arabidopsis thaliana* damaged DNA binding protein 1B (DDB1B) with DDB1A, DET1, and COP1. G3: Genes| Genomes| Genetics 3: 493-503

Gao Z-P, Yu Q-B, Zhao T-T, Ma Q, Chen G-X, Yang Z-N (2011) A functional component of the transcriptionally active chromosome complex, Arabidopsis pTAC14, interacts with pTAC12/HEMERA and regulates plastid gene expression. Plant Physiology 157: 1733-1745

Geisler-Lee J, O'Toole N, Ammar R, Provart NJ, Millar AH, Geisler M (2007) A predicted interactome for Arabidopsis. Plant Physiology 145: 317-329

Ghodke H, Wang H, Hsieh CL, Woldemeskel S, Watkins SC, Rapic-Otrin V, Van Houten B (2014) Single-molecule analysis reveals human UV-damaged DNA-binding protein (UV-DDB) dimerizes on DNA via multiple kinetic intermediates. Proceedings of the National Academy of Sciences 111: E1862-E1871

Gillette TG, Yu S, Zhou Z, Waters R, Johnston SA, Reed SH (2006) Distinct functions of the ubiquitin-proteasome pathway influence nucleotide excision repair. The EMBO Journal 25: 2529-2538

Grasser M, Kane CM, Merkle T, Melzer M, Emmersen J, Grasser KD (2009) Transcript elongation factor TFIIS is involved in Arabidopsis seed dormancy. Journal of Molecular Biology 386: 598-611

Groisman R, Polanowska J, Kuraoka I, Sawada J-i, Saijo M, Drapkin R, Kisselev AF, Tanaka K, Nakatani Y (2003) The ubiquitin ligase activity in the DDB2 and CSA complexes is differentially regulated by the COP9 signalosome in response to DNA damage. Cell 113: 357-367

Guo H, Ecker JR (2003) Plant responses to ethylene gas are mediated by SCF EBF1/EBF2-dependent proteolysis of EIN3 transcription factor. Cell 115: 667-677

Guzder SN, Sung P, Prakash L, Prakash S (1997) Yeast Rad7-Rad16 complex, specific for the nucleotide excision repair of the nontranscribed DNA strand, is an ATP-dependent DNA damage sensor. Journal of Biological Chemistry 272: 21665-21668

Guzder SN, Sung P, Prakash L, Prakash S (1999) Synergistic interaction between yeast nucleotide excision repair factors NEF2 and NEF4 in the binding of ultraviolet-damaged DNA. Journal of Biological Chemistry 274: 24257-24262

Hannss R, Dubiel W (2011) COP9 signalosome function in the DDR. FEBS letters 585: 2845-2852

Harlow GR, Jenkins ME, Pittalwala TS, Mount DW (1994) Isolation of *uvh1*, an Arabidopsis mutant hypersensitive to ultraviolet light and ionizing radiation. The Plant Cell 6: 227-235

Heinicke S, Livstone MS, Lu C, Oughtred R, Kang F, Angiuoli SV, White O, Botstein D, Dolinski K (2007) The Princeton Protein Orthology Database (P-POD): a comparative genomics analysis tool for biologists. PLoS One 2: e766

Hershko A (2005) The ubiquitin system for protein degradation and some of its roles in the control of the cell division cycle. Cell Death & Differentiation 12: 1191-1197

Higa LA, Wu M, Ye T, Kobayashi R, Sun H, Zhang H (2006) CUL4-DDB1 ubiquitin ligase interacts with multiple WD40-repeat proteins and regulates histone methylation. Nature Cell Biology 8: 1277-1283

Hoogstraten D, Bergink S, Ng JMY, Verbiest VHM, Luijsterburg MS, Geverts B, Raams A, Dinant C, Hoeijmakers JHJ, Vermeulen W (2008) Versatile DNA damage detection by the global genome nucleotide excision repair protein XPC. Journal of Cell Science 121: 2850-2859

Hooper CM, Tanz SK, Castleden IR, Vacher MA, Small ID, Millar AH (2014) SUBAcon: a consensus algorithm for unifying the subcellular localization data of the Arabidopsis proteome. Bioinformatics 30: 3356-3364

Hossain Z, Amyot L, McGarvey B, Gruber M, Jung J, Hannoufa A (2012) The translation elongation factor eEF-1Bβ1 is involved in cell wall biosynthesis and plant development in *Arabidopsis thaliana*. PLoS One 7: e30425

Hu J, McCall CM, Ohta T, Xiong Y (2004) Targeted ubiquitination of CDT1 by the DDB1-CUL4A-ROC1 ligase in response to DNA damage. Nature Cell Biology 6: 1003-1009

Huerta-Cepas J, Szklarczyk D, Forslund K, Cook H, Heller D, Walter MC, Rattei T, Mende DR, Sunagawa S, Kuhn M (2015) eggNOG 4.5: a hierarchical orthology framework with improved functional annotations for eukaryotic, prokaryotic and viral sequences. Nucleic Acids Research 44: D286-D293

Huh W-K, Falvo JV, Gerke LC, Carroll AS, Howson RW, Weissman JS, O'Shea EK (2003) Global analysis of protein localization in budding yeast. Nature 425: 686-691

Ishibashi T, Kimura S, Furukawa T, Hatanaka M, Hashimoto J, Sakaguchi K (2001) Two types of replication protein A 70 kDa subunit in rice, *Oryza sativa*: molecular cloning, characterization, and cellular and tissue distribution. Gene 272: 335-343

Ishibashi T, Kimura S, Furukawa T, Sakaguchi K (2006) DNA repair mechanisms in UV-B tolerant plants. Jarq-Japan Agricultural Research Quarterly 40: 107-113

Jain M, Nijhawan A, Tyagi AK, Khurana JP (2006) Validation of housekeeping genes as internal control for studying gene expression in rice by quantitative real-time PCR. Biochemical and Biophysical Research Communications 345: 646-651

Jin J, Arias EE, Chen J, Harper JW, Walter JC (2006) A family of diverse Cul4-Ddb1-interacting proteins includes Cdt2, which is required for S phase destruction of the replication factor Cdt1. Molecular Cell 23: 709-721

Kapuscinski J (1995) DAPI: a DNA-specific fluorescent probe. Biotechnic & Histochemistry 70: 220-233

Kerr JB, McElroy CT (1993) Evidence for large upward trends of ultraviolet-B radiation linked to ozone depletion. Science 262: 1032-1034

Kim S-H, Michael WM (2008) Regulated proteolysis of DNA polymerase Î· during the DNA-damage response in *C. elegans*. Molecular Cell 32: 757-766

Koga A, Ishibashi T, Kimura S, Uchiyama Y, Sakaguchi K (2006) Characterization of T-DNA insertion mutants and RNAi silenced plants of *Arabidopsis thaliana* UV-damaged DNA binding protein 2 (AtUV-DDB2). Plant Molecular Biology 61: 227-240

Krasikova YS, Rechkunova NI, Maltseva EA, Pestryakov PE, Petruseva IO, Sugasawa K, Chen X, Min J-H, Lavrik OI (2015) Comparative analysis of interaction of human and yeast DNA damage recognition complexes with damaged DNA in nucleotide excision repair. Journal of Biological Chemistry 288: 10936-10947

Krzeszinski JY, Choe V, Shao J, Bao X, Cheng H, Luo S, Huo K, Rao H (2014) XPC promotes MDM2-mediated degradation of the p53 tumor suppressor. Molecular Biology of the Cell 25: 213-221

Kulandaivelu G, Lingakumar K, Premkumar A (1997) UV-B radiation. John Wiley & Sons, Inc

Kunihiro S, Kowata H, Kondou Y, Takahashi S, Matsui M, Berberich T, Youssefian S, Hidema J, Kusano T (2014) Overexpression of rice *OsREX1-S*, encoding a putative component of the core general transcription and DNA repair factor IIH, renders plant cells tolerant to cadmium-and UV-induced damage by enhancing DNA excision repair. Planta 239: 1101-1111

Kunz BA, Anderson HJ, Osmond MJ, Vonarx EJ (2005) Components of nucleotide excision repair and DNA damage tolerance in *Arabidopsis thaliana*. Environmental and Molecular Mutagenesis 45: 115-127

Lagerwerf S, Vrouwe M, Overmeer R, Fousteri M, Mullenders L (2011) DNA damage response and transcription. DNA Repair 10: 743-750

Laine J-P, Egly J-M (2006) When transcription and repair meet: a complex system. Trends in Genetics 22: 430-436

Landsman D, McBride OW, Soares N, Crippa MP, Srikantha T, Bustin M (1989) Chromosomal protein HMG-14. Identification, characterization, and chromosome localization of a functional gene from the large human multigene family. Journal of Biological Chemistry 264: 3421-3427

Lans H, Marteijn JA, Schumacher B, Hoeijmakers JH, Jansen G, Vermeulen W (2010) Involvement of global genome repair, transcription coupled repair, and chromatin remodeling in UV DNA damage response changes during development. PLoS Genet 6: e1000941

La Verde V, Trande M, D'Onofrio M, Dominici P, Astegno A (2018) Binding of calcium and target peptide to calmodulin-like protein CML19, the centrin 2 of *Arabidopsis thaliana.* International Journal of Biological Macromolecules 108:1289-1299

Lei Z, Dai Y (2005) An SVM-based system for predicting protein subnuclear localizations. BMC Bioinformatics 6: 291

Li L, Lu X, Peterson C, Legerski R (1997) XPC interacts with both HHR23B and HHR23A in vivo. Mutation Research/DNA Repair 383: 197-203

Li M, Chen D, Shiloh A, Luo J, Nikolaev AY, Qin J, Gu W (2002) Deubiquitination of p53 by HAUSP is an important pathway for p53 stabilization. Nature 416: 648-653

Li S (2015) Transcription coupled nucleotide excision repair in the yeast *Saccharomyces cerevisiae*: The ambiguous role of Rad26. DNA Repair 36: 43-48

Li X, Guo X, Zhao L, Zhang J, Tang D, Zhao X, Liu X (2012) Arabidopsis *rad23-4* gene is required for pollen development under UV-B light. African Journal of Biotechnology 11: 10161-10169

Li Y, Yan J, Kim I, Liu C, Huo K, Rao H (2010) Rad4 regulates protein turnover at a postubiquitylation step. Molecular Biology of the Cell 21: 177-185

Li YF, Kim S-T, Sancar A (1993) Evidence for lack of DNA photoreactivating enzyme in humans. Proceedings of the National Academy of Sciences 90: 4389-4393

Liang L, Flury S, Kalck V, Hohn B, Molinier J (2006) CENTRIN2 interacts with the Arabidopsis homologue of the human XPC protein (AtRAD4) and contributes to efficient synthesis-dependent repair of bulky DNA lesions. Plant Molecular Biology 61: 345-356

Liu L, Zhang Z, Mei Q, Chen M (2013) PSI: a comprehensive and integrative approach for accurate plant subcellular localization prediction. PLoS One 8: e75826

Liu Y, Wang F, Zhang H, He H, Ma L, Deng XW (2008) Functional characterization of the Arabidopsis ubiquitin-specific protease gene family reveals specific role and redundancy of individual members in development. The Plant Journal 55: 844-856

Liu Z, Hall JD, Mount DW (2001) Arabidopsis *UVH3* gene is a homologue of the *Saccharomyces cerevisiae RAD2* and human *XPG* DNA repair genes. The Plant Journal 26: 329-338

Liu Z, Hong S-W, Escobar M, Vierling E, Mitchell DL, Mount DW, Hall JD (2003) Arabidopsis *UVH6*, a homologue of human *XPD* and yeast *RAD3* DNA repair genes, functions in DNA repair and is essential for plant growth. Plant Physiology 132: 1405-1414

Liu Z, Wang L, Zhong D (2015) Dynamics and mechanisms of DNA repair by photolyase. Physical Chemistry Chemical Physics 17: 11933-11949

Lohmann D, Stacey N, Breuninger H, Jikumaru Y, Müller D, Sicard A, Leyser O, Yamaguchi S, Lenhard M (2010) SLOW MOTION is required for within-plant auxin homeostasis and normal timing of lateral organ initiation at the shoot meristem in Arabidopsis. The Plant Cell 22: 335-348

Lombaerts M, Peltola PH, Visse R, den Dulk H, Brandsma JA, Brouwer J (1999) Characterization of the *rhp7+* and *rhp16+* genes in *Schizosaccharomyces pombe*. Nucleic Acids Research 27: 3410-3416

Manova V, Gruszka D (2015) DNA damage and repair in plants-from models to crops. Frontiers in Plant Science 6: 885

Marchler-Bauer A, Derbyshire MK, Gonzales NR, Lu S, Chitsaz F, Geer LY, Geer RC, He J, Gwadz M, Hurwitz DI (2014) CDD: NCBI's conserved domain database. Nucleic Acids Research 43: D222-6.

Marteijn JA, Lans H, Vermeulen W, Hoeijmakers JHJ (2014) Understanding nucleotide excision repair and its roles in cancer and ageing. Nature Reviews Molecular Cell Biology 15: 465-481

Matsumoto S, Fischer ES, Yasuda T, Dohmae N, Iwai S, Mori T, Nishi R, Yoshino K-i, Sakai W, Hanaoka F (2015) Functional regulation of the DNA damage-recognition factor DDB2 by ubiquitination and interaction with xeroderma pigmentosum group C protein. Nucleic Acids Research 43: 1700-1713

Matsuyama A, Arai R, Yashiroda Y, Shirai A, Kamata A, Sekido S, Kobayashi Y, Hashimoto A, Hamamoto M, Hiraoka Y (2006) ORFeome cloning and global analysis of protein localization in the fission yeast *Schizosaccharomyces pombe*. Nature Biotechnology 24: 841-847

McKenzie RL, Aucamp PJ, Bais AF, Bjorn LO, Ilyas M (2007) Changes in biologically-active ultraviolet radiation reaching the Earth's surface. Photochemical and Photobiological Sciences 6: 218-231

McKenzie RL, Aucamp PJ, Bais AF, Björn LO, Ilyas M, Madronich S (2011) Ozone depletion and climate change: impacts on UV radiation. Photochemical and Photobiological Sciences 10: 182-198

Michaillat L, Mayer A (2013) Identification of genes affecting vacuole membrane fragmentation in *Saccharomyces cerevisiae*. PLoS One 8: e54160

Min JH, Pavletich NP (2007) Recognition of DNA damage by the Rad4 nucleotide excision repair protein. Nature 449: 570-575

Mitchell DL, Rosenstein BS (1987) The use of specific radioimmunoassays to determine action spectra for the photolysis of (6-4) photoproducts. Photochemistry and Photobiology 45: 781-786

Mitchell DL, Vaughan JE, Nairn RS (1989) Inhibition of transient gene expression in Chinese hamster ovary cells by cyclobutane dimers and (6-4) photoproducts in transfected ultraviolet-irradiated plasmid DNA. Plasmid 21: 21-30

Molinier J, Lechner E, Dumbliauskas E, Genschik P (2008) Regulation and role of Arabidopsis CUL4-DDB1A-DDB2 in maintaining genome integrity upon UV stress. PLoS Genet 4: e1000093

Molinier J, Ramos C, Fritsch O, Hohn B (2004) CENTRIN2 modulates homologous recombination and nucleotide excision repair in Arabidopsis. The Plant Cell 16: 1633-1643

Morgante PG, Berra CM, Nakabashi M, Costa RMA, Menck CFM, Van Sluys M-A (2005) Functional XPB/RAD25 redundancy in Arabidopsis genome: characterization of AtXPB2 and expression analysis. Gene 344: 93-103

Nevarez PA, Qiu Y, Inoue H, Yoo CY, Benfey PN, Schnell DJ, Chen M (2017) Mechanism of dual targeting of the phytochrome signaling component HEMERA/pTAC12 to plastids and the nucleus. Plant Physiology 173: 1953-1966

Nakatsu Y, Asahina H, Citterio E, Rademakers S, Vermeulen W, Kamiuchi S, Yeo J-P, Khaw M-C, Saijo M, Kodo N (2000) XAB2, a novel tetratricopeptide repeat protein involved in transcription-coupled DNA repair and transcription. Journal of Biological Chemistry 275: 34931-34937

Ng JM, Vermeulen W, van der Horst GT, Bergink S, Sugasawa K, Vrieling H, Hoeijmakers JH (2003) A novel regulation mechanism of DNA repair by damage-induced and RAD23-dependent stabilization of xeroderma pigmentosum group C protein. Genes and Development 17: 1630-1645

Ohta T, Michel JJ, Schottelius AJ, Xiong Y (1999) ROC1, a homolog of APC11, represents a family of cullin partners with an associated ubiquitin ligase activity. Molecular Cell 3: 535-541

Okonechnikov K, Golosova O, Fursov M, team U (2012) Unipro UGENE: a unified bioinformatics toolkit. Bioinformatics 28: 1166-1167

Ortolan TG, Chen L, Tongaonkar P, Madura K (2004) Rad23 stabilizes Rad4 from degradation by the Ub/proteasome pathway. Nucleic Acids Research 32: 6490-6500

Papadopoulos JS, Agarwala R (2007) COBALT: constraint-based alignment tool for multiple protein sequences. Bioinformatics 23: 1073-1079

Pani B, Nudler E (2017) Mechanistic insights into transcription coupled DNA repair. DNA Repair 56: 42-50

Park E, Guzder SN, Koken MH, Jaspers-Dekker I, Weeda G, Hoeijmakers JH, Prakash S, Prakash L (1992) *RAD25 (SSL2)*, the yeast homologue of the human xeroderma pigmentosum group B DNA repair gene, is essential for viability. Proceedings of the National Academy of Sciences 89: 11416-11420

Petruseva IO, Evdokimov AN, Lavrik OI (2014) Molecular mechanism of global genome nucleotide excision repair. Acta Naturae 6: 23-34

Pfalz J, Liere K, Kandlbinder A, Dietz KJ, Oelmuller R (2006) PTAC2,-6, and -12 are components of the transcriptionally active plastid chromosome that are required for plastid gene expression. The Plant Cell 18: 176-197

Prakash L (1976) Effect of genes controlling radiation sensitivity on chemically induced mutations in *Saccharomyces cerevisiae*. Genetics 83: 285-301

Qiu Y, Li M, Pasoreck EK, Long L, Shi Y, Galvao RM, Chou CL, Wang H, Sun AY, Zhang YC, Jiang A, Chen M (2015) HEMERA couples the proteolysis and transcriptional activity of PHYTOCHROME INTERACTING FACTORs in Arabidopsis photomorphogenesis. The Plant Cell 27: 1409-1427

Rastogi RP, Richa AK, Tyagi MB, Sinha RP (2010) Molecular mechanisms of ultraviolet radiation-induced DNA damage and repair. Journal of Nucleic Acids 2010

Reed SH (2005) Nucleotide excision repair in chromatin: the shape of things to come. DNA Repair 4: 909-918

Ries G, Heller W, Puchta H, Sandermann H, Seidlitz HK, Hohn B (2000) Elevated UV-B radiation reduces genome stability in plants. Nature 406: 98-101

Risseeuw EP, Daskalchuk TE, Banks TW, Liu E, Cotelesage J, Hellmann H, Estelle M, Somers DE, Crosby WL (2003) Protein interaction analysis of SCF ubiquitin E3 ligase subunits from Arabidopsis. The Plant Journal 34: 753-767

Roy S, Choudhury SR, Singh SK, Das KP (2011) AtPolλ, a homologue of mammalian DNA polymerase λ in *Arabidopsis thaliana*, is involved in the repair of UV-B induced DNA damage through the dark repair pathway. Plant and Cell Physiology 52: 448-467

Rüthemann P, Pogliano CB, Naegeli H (2016) Global-genome Nucleotide Excision Repair controlled by ubiquitin/sumo modifiers. Frontiers in Genetics 7: 68

Saijo M (2013) The role of Cockayne syndrome group A (CSA) protein in transcription-coupled nucleotide excision repair. Mechanisms of Ageing and Development 134: 196-201

Samson F, Brunaud Vr, Balzergue S, Dubreucq B, Lepiniec L, Pelletier G, Caboche M, Lecharny A (2002) FLAGdb/FST: a database of mapped flanking insertion sites (FSTs) of *Arabidopsis thaliana* T-DNA transformants. Nucleic Acids Research 30: 94-97

Sancar A (1994) Structure and function of DNA photolyase. Biochemistry 33: 2-9

Sancar A (1996) DNA excision repair. Annual Review of Biochemistry 65: 43-81

Sarangi P, Bartosova Z, Altmannova V, Holland C, Chavdarova M, Lee SE, Krejci L, Zhao X (2014) Sumoylation of the Rad1 nuclease promotes DNA repair and regulates its DNA association. Nucleic Acids Research 42: 6393-6404

Schalk C, Drevensek S, Kramdi A, Kassam M, Ahmed I, Cognat V, Graindorge S, Bergdoll M, Baumberger N, Heintz D, Bowler C, Genschika P, Barneche F, Colot V, Molinier J (2016) DNA DAMAGE BINDING PROTEIN2 shapes the DNA methylation landscape. The Plant Cell 28: 2043–2059

Schalk C, Molinier J (2016) Global Genome Repair factors control DNA methylation patterns in Arabidopsis. Plant Signaling and Behavior 11: e1253648

Schmid M, Davison TS, Henz SR, Pape UJ, Demar M, Vingron M, Schölkopf B, Weigel D, Lohmann JU (2005) A gene expression map of *Arabidopsis thaliana* development. Nature Genetics 37: 501-506

Schroeder DF, Gahrtz M, Maxwell BB, Cook RK, Kan JM, Alonso JM, Ecker JR, Chory J (2002) De-etiolated 1 and damaged DNA binding protein 1 interact to regulate Arabidopsis photomorphogenesis. Current Biology 12: 1462-1472

Schultz TF, Quatrano RS (1997) Characterization and expression of a rice *RAD23* gene. Plant Molecular Biology 34: 557-562

Schwertman P, Vermeulen W, Marteijn J (2013) UVSSA and USP7, a new couple in transcription-coupled DNA repair. Chromosoma 122: 275-284

Scrima A, Fischer ES, Lingaraju G, Böhm K, Cavadini S, Thomä NH (2011) Detecting UV-lesions in the genome: The modular CRL4 ubiquitin ligase does it best! FEBS Letters 585: 2818-2825

Seki M, Narusaka M, Kamiya A, Ishida J, Satou M, Sakurai T, Nakajima M, Enju A, Akiyama K, Oono Y (2002) Functional annotation of a full-length Arabidopsis cDNA collection. Science 296: 141-145

Shaked H, Avivi-Ragolsky N, Levy AA (2006) Involvement of the Arabidopsis SWI2/SNF2 chromatin remodeling gene family in DNA damage response and recombination. Genetics 173: 985-994

Sharma B, Joshi D, Yadav PK, Gupta AK, Bhatt TK (2016) Role of ubiquitin-mediated degradation system in plant biology. Frontiers in Plant Science 7: 806

Shimanouchi K, Takata K-i, Yamaguchi M, Murakami S, Ishikawa G, Takeuchi R, Kanai Y, Ruike T, Nakamura R, Abe Y (2006) Drosophila damaged DNA binding protein 1 contributes to genome stability in somatic cells. Journal of Biochemistry 139: 51-58

Shultz RW, Tatineni VM, Hanley-Bowdoin L, Thompson WF (2007) Genome-wide analysis of the core DNA replication machinery in the higher plants Arabidopsis and rice. Plant Physiology 144: 1697-1714

Sideri T, Rallis C, Bitton DA, Lages BM, Suo F, Rodríguez-López M, Du L-L, Bähler J (2015) Parallel profiling of fission yeast deletion mutants for proliferation and for lifespan during long-term quiescence. G3: Genes| Genomes| Genetics 5: 145-155

Sievers F, Wilm A, Dineen D, Gibson TJ, Karplus K, Li W, Lopez R, McWilliam H, Remmert M, Soding J, Thompson J, Higgins D (2011) Fast, scalable generation of high-quality protein multiple sequence alignments using Clustal Omega. Molecular Systems Biology 7: 539

Skowyra D, Craig KL, Tyers M, Elledge SJ, Harper JW (1997) F-box proteins are receptors that recruit phosphorylated substrates to the SCF ubiquitin-ligase complex. Cell 91: 209-219

Solimando L, Luijsterburg MS, Vecchio L, Vermeulen W, van Driel R, Fakan S (2009) Spatial organization of nucleotide excision repair proteins after UV-induced DNA damage in the human cell nucleus. Journal of Cell Science 122: 83-91

Spivak G (2005) UV-sensitive syndrome. Mutation Research/Fundamental and Molecular Mechanisms of Mutagenesis 577: 162-169

Spivak G (2015) Nucleotide excision repair in humans. DNA Repair 36: 13-18

Sturm A, Lienhard S (1998) Two isoforms of plant RAD23 complement a UV-sensitive *rad23* mutant in yeast. The Plant Journal 13: 815-821

Sugasawa K (2010) Regulation of damage recognition in mammalian global genomic nucleotide excision repair. Mutation Research/Fundamental and Molecular Mechanisms of Mutagenesis 685: 29-37
Sugasawa K (2011) Multiple DNA damage recognition factors involved in mammalian nucleotide excision repair. Biochemistry (Moscow) 76: 16-23
Sugasawa K (2016) Molecular mechanisms of DNA damage recognition for mammalian nucleotide excision repair. DNA Repair 44: 110-117
Sugasawa K, Akagi J, Nishi R, Iwai S, Hanaoka F (2009) Two-step recognition of DNA damage for mammalian nucleotide excision repair: Directional binding of the XPC complex and DNA strand scanning. Molecular Cell 36: 642-653
Sugasawa K, Ng JM, Masutani C, Iwai S, van der Spek P, Eker AP, Hanaoka F, Bootsma D, Hoeijmakers JH (1998) Xeroderma pigmentosum group C protein complex is the initiator of global genome nucleotide excision repair. Molecular Cell 2: 223-232
Sugasawa K, Okuda Y, Saijo M, Nishi R, Matsuda N, Chu G, Mori T, Iwai S, Tanaka K (2005) UV-induced ubiquitylation of XPC protein mediated by UV-DDB-ubiquitin ligase complex. Cell 121: 387-400
Sugitani N, Sivley R, Perry K, Capra J, Chazin W (2016) XPA: A key scaffold for human nucleotide excision repair. DNA Repair 44: 123-135
Sun N-K, Sun C-L, Lin C-H, Pai L-M, Chao CCK (2010) Damaged DNA-binding protein 2 (DDB2) protects against UV irradiation in human cells and Drosophila. Journal of Biomedical Science 17: 27
Swofford DL (2002) PAUP*: phylogenetic analysis using parsimony (* and other methods). Sunderland, MA. Sinauer Associates
Takashi Y, Kobayashi Y, Tanaka K, Tamura K (2009) Arabidopsis replication protein A 70a is required for DNA damage response and telomere length homeostasis. Plant and Cell Physiology 50: 1965-1976
Tang J, Chu G (2002) Xeroderma pigmentosum complementation group E and UV-damaged DNA-binding protein. DNA Repair 1: 601-616
Tanz SK, Castleden I, Hooper CM, Vacher M, Small I, Millar HA (2013) SUBA3: a database for integrating experimentation and prediction to define the SUB cellular location of proteins in Arabidopsis. Nucleic Acids Research 41: D1185-D1191
Tkach JM, Yimit A, Lee AY, Riffle M, Costanzo M, Jaschob D, Hendry JA, Ou J, Moffat J, Boone C (2012) Dissecting DNA damage response pathways by analysing protein localization and abundance changes during DNA replication stress. Nature Cell Biology 14: 966-976
Treiber DK, Chen Z, Essigmann JM (1992) An ultraviolet light-damaged DNA recognition protein absent in xeroderma pigmentosum group E cells binds selectively to pyrimidine (6-4) pyrimidone photoproducts. Nucleic Acids Research 20: 5805-5810
Tuteja N, Ahmad P, Panda BB, Tuteja R (2009) Genotoxic stress in plants: shedding light on DNA damage, repair and DNA repair helicases. Mutation Research/Reviews in Mutation Research 681: 134-149
Uchida A, Sugasawa K, Masutani C, Dohmae N, Araki M, Yokoi M, Ohkuma Y, Hanaoka F (2002) The carboxy-terminal domain of the XPC protein plays a crucial role in nucleotide excision repair through interactions with transcription factor IIH. DNA Repair 1: 449-461
Van Buskirk EK, Decker PV, Chen M (2012) Photobodies in light signaling. Plant Physiology 158: 52-60

Van Der Spek PJ, Eker A, Rademakers S, Visser C, Sugasawa K, Masutani C, Hanaoka F, Bootsma D, Hoeijmakers JH (1996) XPC and human homologs of RAD23: intracellular localization and relationship to other nucleotide excision repair complexes. Nucleic Acids Research 24: 2551-2559

Vannier J-B, Depeiges A, White C, Gallego ME (2009) ERCC1/XPF protects short telomeres from homologous recombination in *Arabidopsis thaliana*. PLoS Genetics 5: e1000380

Verhage R, Zeeman A-M, de Groot N, Gleig F, Bang DD, Van de Putte P, Brouwer J (1994) The *RAD7* and *RAD16* genes, which are essential for pyrimidine dimer removal from the silent mating type loci, are also required for repair of the nontranscribed strand of an active gene in *Saccharomyces cerevisiae*. Molecular and Cellular Biology 14: 6135-6142

Vonarx EJ, Tabone EK, Osmond MJ, Anderson HJ, Kunz BA (2006) Arabidopsis homologue of human transcription factor IIH/nucleotide excision repair factor p44 can function in transcription and DNA repair and interacts with AtXPD. The Plant Journal 46: 512-521

Wang Z, Wei S, Reed SH, Wu X, Svejstrup JQ, Feaver WJ, Kornberg RD, Friedberg EC (1997) The *RAD7, RAD16,* and *RAD23* genes of *Saccharomyces cerevisiae*: requirement for transcription-independent nucleotide excision repair in vitro and interactions between the gene products. Molecular and Cellular Biology 17: 635-643

Warde-Farley D, Donaldson SL, Comes O, Zuberi K, Badrawi R, Chao P, Franz M, Grouios C, Kazi F, Lopes CT (2010) The GeneMANIA prediction server: biological network integration for gene prioritization and predicting gene function. Nucleic Acids Research 38: W214-W220

Waters R, Evans K, Bennett M, Yu S, Reed S (2012) Nucleotide excision repair in cellular chromatin: studies with yeast from nucleotide to gene to genome. International Journal of Molecular Sciences 13: 11141-11164

Waters R, van Eijk P, Reed S (2015) Histone modification and chromatin remodeling during NER. DNA Repair 36: 105-113

Weber H, Bernhardt A, Dieterle M, Hano P, Mutlu Al, Estelle M, Genschik P, Hellmann H (2005) Arabidopsis AtCUL3a and AtCUL3b form complexes with members of the BTB/POZ-MATH protein family. Plant Physiology 137: 83-93

Weigel D, Glazebrook J (2002) Arabidopsis. A Laboratory Manual 165

Wood RD (1997) Nucleotide excision repair in mammalian cells. Journal of Biological Chemistry 272: 23465-23468

Xiao W, Jang J-C (2000) F-box proteins in Arabidopsis. Trends in Plant Science 5: 454-457

Xie Z, Liu S, Zhang Y, Wang Z (2004) Roles of Rad23 protein in yeast nucleotide excision repair. Nucleic Acids Research 32: 5981-5990

Xue C, Liang K, Liu Z, Wen R, Xiao W (2015) Similarities and differences between Arabidopsis PCNA1 and PCNA2 in complementing the yeast DNA damage tolerance defect. DNA Repair 28: 28-36

Yoo O, Yoon H, Baek K, Jeon C, Miyamoto K, Ueno A, Agarwal K (1991) Cloning, expression and characterization of the human transcription elongation factor, TFIIS. Nucleic Acids Research 19: 1073-1079

Zamore PD, Tuschl T, Sharp PA, Bartel DP (2000) RNAi: double-stranded RNA directs the ATP-dependent cleavage of mRNA at 21 to 23 nucleotide intervals. Cell 101: 25-33

Zhang C, Guo H, Zhang J, Guo G, Schumaker KS, Guo Y (2010) Arabidopsis cockayne syndrome A-like proteins 1A and 1B form a complex with CULLIN4 and damage DNA binding protein 1A and regulate the response to UV irradiation. The Plant Cell 22: 2353-2369

Zhang L, Gong F (2016) The emerging role of deubiquitination in nucleotide excision repair. DNA Repair 44: 118-122

Zhang X, Horibata K, Saijo M, Ishigami C, Ukai A, Kanno S-i, Tahara H, Neilan EG, Honma M, Nohmi T (2012) Mutations in UVSSA cause UV-sensitive syndrome and destabilize ERCC6 in transcription-coupled DNA repair. Nature Genetics 44: 593-597

Zhang Y, Feng S, Chen F, Chen H, Wang J, McCall C, Xiong Y, Deng XW (2008) Arabidopsis DDB1-CUL4 ASSOCIATED FACTOR1 forms a nuclear E3 ubiquitin ligase with DDB1 and CUL4 that is involved in multiple plant developmental processes. The Plant Cell 20: 1437-1455